Functional characterization of bacterial sRNAs involved in stress responses and quorum sensing of bacterial pathogens

Dissertation

Zur Erlangung des Doktorgrades

der Naturwissenschaften

(Dr. rer. nat.)

der Fakultät für Biologie

der Ludwig-Maximilians-Universität München

vorgelegt von

Nikolai Benedikt Johannes Peschek

aus München

Martinsried, März 2020

Diese Dissertation wurde angefertigt

unter der Leitung von Prof. Dr. Kai Papenfort

im Bereich von Department Biologie I

an der Ludwig-Maximilians-Universität München

Gutachter:

1. Prof. Dr. Kai Papenfort
2. Prof. Dr. Kirsten Jung

Datum der Abgabe: 19.03.2020

Tag der mündlichen Prüfung: 16.07.2020

Eidesstattliche Erklärung

Ich versichere hiermit an Eides statt, dass die vorgelegte Dissertation von mir selbstständig und ohne unerlaubte Hilfe angefertigt wurde. Des Weiteren erkläre ich, dass ich nicht anderweitig ohne Erfolg versucht habe, eine Dissertation einzureichen oder mich der Doktorprüfung zu unterziehen. Die folgende Dissertation liegt weder ganz, noch in wesentlichen Teilen einer anderen Prüfungskommission vor.

Nikolai Peschek, München, den 18.03.2020

Statutory Declaration

I declare that I have authored this thesis independently, that I have not used other than the declared sources/resources. As well I declare, that I have not submitted a dissertation without success and not passed the oral exam. The present dissertation (neither the entire dissertation nor parts) has not been presented to another examination board.

Nikolai Peschek, Munich, 18.03.2020

Contents

Nomenclature

Gene deletions are marked by "Δ" (Example: Δ*micV*).
Genes expressed from plasmids are marked with "p" (Example: pMicV).
Promoters are indicated by "P" (Example: P*micV*).
Nucleotide sequence positions are provided with respect to the transcriptional start sites in the case of sRNAs, or with respect to the AUG start codon in the case of mRNAs (Example: +3, indicates AU**G**).
Single nucleotide mutations are indicated by a "*", followed by the respective nucleotide positions (Example: VqmR* (C133G)).
Multi-nucleotide mutations of an sRNA are marked by "M#" (Example: MicV M1), and multi-nucleotide mutations of an mRNA are marked by "M#*" (Example: *ompT* M1*).

Abbreviations

(v/v)	volume per volume
(w/v)	weight per volume
[^{32}P]	phosphorus-32
A	adenosine
A.U.	arbitrary units
A-22	*S*-(3,4-dichlorobenzyl) isothiourea
AI-2	autoinducer-2
Amp	ampicillin
AMP	antimicrobial peptide
ANOVA	analysis of variance
BAM	ß-barrel assembly machinery
bp	base-pair
C	cytosine
CAI-1	cholera autoinducer-1
c-di-GMP	cyclic diguanylate
cDNA	complementary DNA
CDS	coding sequence
Cef	cephalexin
CFU	colony forming units
Cm	chloramphenicol
Co-IP	co-immunoprecipication
conc.	concentration
CPM	counts per million
crRNA	CRISPR RNA
CTX	cholera toxin
Da	Dalton
DNA	deoxyribonucleic acid
DNase	deoxyribonuclease
DPO	3,5-dimethylpyrazin-2-ol
dRNA-seq	differential RNA sequencing
DTT	dithiothreitol
ECF	extracytoplasmic function σ factor
EDTA	ethylene diamine tetraacetic acid
ESR	envelope stress response
EtOH	ethanol
FDR	false discovery rate
fMet	N-formylmethionine
g	gravitational force equivalent
G	guanosine
GFP	green fluorescent protein
GO	gene ontology
HCD	high cell density
IGR	intergenic region
Kan	kanamycin
kb	kilobase-pairs
LB	lysogeny broth
LCD	low cell density
LNA	locked nucleic acid

log_2	binary logarithm
LPS	lipopolysaccharide
M	marker
M.U.	miller units
miRNA	micro RNA
mRNA	messenger RNA
n	number of replicates
N	any nucleotide
nt	nucleotide
n.a.	not available
OD_{600}	optical density at 600 nanometer
OMP	outer membrane protein
ONPG	O-nitrophenyl-ß-D-galactopyranoside
PBS	phosphate buffered saline
PCR	polymerase chain reaction
PenG	penicillin G
qRT-PCR	quantitative real time PCR
QS	quorum sensing
R	purine nucleotide
RBS	ribosome binding site
Rcs	regulator of capsule synthesis
RIL-seq	RNA interaction by ligation and sequencing
RNA	ribonucleic acid
RNAPα	alpha subunit of RNA polymerase
RNase	ribonuclease
rpm	revolutions per minute
rRNA	ribosomal RNA
SD	standard deviation, Shine-Dalgarno
SDS-PAGE	sodium dodecyl sulfate polyacrylamide gel electrophoresis
SE	standard error
sfGFP	superfolder GFP
sRNA	small regulatory RNA
T	thymidine
TIER-seq	Transiently inactivating an endoribonuclease followed by RNA-seq
TCP	toxin-co-regulated pilus
TCS	two component system
TEX	terminator exonuclease
Tris-HCl	tris(hydroxymethyl)aminomethane-hydrochloride
tRNA	transfer RNA
TSS	transcriptional start site
U	uridine, unit
UTR	untranslated region
VPS	*Vibrio* polysaccharide
WT	wild-type
X-gal	5-bromo-4-chloro-3-indolyl-β-D-galactopyranoside

List of publications

Publications and Manuscripts presented in this thesis

Chapter 2:

Peschek N, Hoyos M, Herzog R, Förstner KU, Papenfort K, A conserved RNA seed-pairing domain directs small RNA-mediated stress resistance in enterobacteria. ***EMBO J***, Volume 38, Issue 16, 15 August 2019, doi: 10.15252/embj.2019101650

Chapter 3:

Herzog R*****, Peschek N*, Singh PK, Fröhlich KS, Schröger L, Meyer F, Bramkamp M, Drescher K, Papenfort K, RNA-mediated control of cell shape modulates antibiotic resistance in *Vibrio cholerae*. **Manuscript**

Chapter 4:

Herzog R, Peschek N, Fröhlich KS, Schumacher K, Papenfort K, Three autoinducer molecules act in concert to control virulence gene expression in *Vibrio cholerae*. ***Nucleic Acids Res.***, Volume 47, Issue 6, 08 April 2019, doi: 10.1093/nar/gky1320

Publications and Manuscripts not presented in this thesis

Do H, Makthal N, VanderWal AR, Rettel M, Savitski MM, Peschek N, Papenfort K, Olsen RJ, Musser JM, Kumaraswami M, Leaderless secreted peptide signaling molecule alters global gene expression and increases virulence of a human bacterial pathogen, ***PNAS***, Epub 2017 Sep 18, doi: 10.1073/pnas.1705972114

* Authors contributed equally

Contributions to publications and manuscripts presented in this thesis

Chapter 2:

NP and KP initiated and conceptualized the study. KUF contributed by analyzing the transcriptional start sites identified in (46) for sigma factor binding motifs. NP constructed the majority of plasmids and strains and performed the majority of experiments and data analyses (Fig. 1, Fig. 2, Fig. 3, Fig. 4A; B; D, Fig 5A, Fig. 6D, Fig. 7, Fig. EV1A; B, C; E, Fig. EV2, Fig. EV4D, Appendix Fig. S1B; C, Appendix Fig. S2, Appendix Fig. S3). RH contributed by measuring P*micV* promoter activity in *E. coli* and performing analyses of OMP composition in *V. cholerae* and *E. coli* cells carrying sRNA overexpression plasmids (Fig. 4C, Fig. EV1F, Fig. Appendix Fig. S1A). MH constructed and validated the synthetic sRNA library, MH and NP performed the selection experiments and analyzed the resulting sequencing data (MH: Fig. 5B; C, Fig. EV4A; B; C; Fig. EV5A; B, MH and NP: Fig. EV3, Fig. EV5A; B). NP and MH identified and validated OmpA as the key target for ethanol resistance (NP: Fig. 6D, Fig. EV5C; D; E, MD: Fig. 6C, Fig. EV4A, NP and MH: Fig. 6A; B). NP constructed the figures, KP, NP, MH, and RH wrote the manuscript. NP was assisted by the research students: Roman Herzog and Raphaela Götz.

…….. ……..

Nikolai Peschek Prof. Dr. Kai Papenfort

Chapter 3:

NP and KP initiated and NP, RH, and KP conceptualized the study. NP performed experiments to characterize gene expression of the *vadR* sRNA (Fig. 1C). NP performed screens to identify the transcription factor driving *vadR* expression and validation experiments (Fig. 1D, Fig. S1D-F). RH and LS characterized the transcription factor binding sites in the *vadR* promotor region (Fig. S1H) and RH reanalyzed publicly available ChIP-seq data for VxrB (Fig. S1G). KSF performed structure probing experiments (Fig. S1A; B) and RH tested half-life of VadR in presence or absence of *hfq* (Fig. S1C). NP globally identified VadR targets using RNA-seq (Fig. 2A-C, Table S1), validated the results using qRT-PCRs (Fig. S2A), and NP and LS validated base-pairing of VadR and targets using a GFP-based reporter system (Fig. 3, Fig. S3A). LS and NP validated expression of VadR mutants using Northern blot analyses (Fig. S3B). RH performed Western blot analysis of the biofilm related protein RbmA (Fig. S2B). PKS designed and performed experiments to characterize effects of VadR on biofilm formation (Fig. 2D-I, Fig. 6A-C). RH and NP analyzed CrvA protein levels using Western blots (Fig. 4A). RH performed all phase-contrast microscopy experiments to test for VadR and sRNA candidate effects on cell curvature (Fig. 1A, Fig 4B, C, Fig. S4). FM performed initial microscopy experiments and set up the analysis pipeline to test for cell curvature and other cell shape parameters. NP tested the effect of A-22 on P*vadR* promotor activity (Fig. S5A) and RH validated the effect of penicillin G on *vadR* expression (Fig. 5A, B). NP performed experiments to test effects of penicillin G treatment in *vadR* and *crvA* mutants on cell survival (Fig. 5C, Fig. S5D). RH tested *crvA* mRNA levels in *vadR* and *crvA* mutants (Fig. S5C), and the effect of *crvA* overexpression on cell survival after PenG treatment (Fig. S5B). NP and RH performed statistical analyses and created the figures. NP wrote an initial draft for the manuscript, and KP wrote the final version, with the help of all authors. NP was assisted by the research students: Elena Evertz and Alexandra Eklund.

We hereby confirm the above statements:

….. …..

Nikolai Peschek Roman Herzog

…..

Prof. Dr. Kai Papenfort

Chapter 4:

RH and KP initiated and designed the study. RH constructed most strains and plasmids and performed a majority of experiments (Figs. 1; 2; 3; 4; 5, Figs. S1; S2; S4; S5; S6). KS contributed by assisting RH with experiments and strain construction. KSF performed ribosome-profiling experiments (Fig. S3). NP initially identified *aphA* as a target of VqmR and analyzed the RNA-sequencing data (Table 1, RH and NP: Fig. 6, Table S1, Fig. S7). RH constructed the figures and RH and KP wrote the manuscript.

….....	….....
Nikolai Peschek	Prof. Dr. Kai Papenfort

Summary

Pathogenic bacteria such as *Vibrio cholerae*, the causative agent of cholera disease, thrive in host and non-host environments. This lifestyle requires constant monitoring of environmental signals to mediate adaptation through changes in gene expression. Furthermore, *V. cholerae* employs quorum sensing systems to synchronize group behaviors, such as biofilm formation and virulence gene expression. Both processes frequently involve regulation of gene expression by small regulatory RNAs (sRNAs). Bacterial sRNAs base-pair to *trans* encoded target mRNAs to alter their stability or translation. Recent studies in *V. cholerae* identified 107 putative sRNAs with yet undescribed functions. The present work aimed to characterize candidate sRNAs with respect to their involvement in stress responses and quorum sensing.

Specifically, a bioinformatical approach aiming to identify binding sites of the envelope stress related, alternative sigma factor σ^E, identified the MicV sRNA as a member of the σ^E regulon. The σ^E stress response of *V. cholerae* involves regulation by another sRNA, VrrA. Expression of both sRNAs is activated under high cell density conditions or by treatment with membrane damaging agents. Global transcriptome analyses revealed that both sRNAs act together to control outer membrane protein expression, and to maintain envelope homeostasis under membrane damaging conditions. We pinpoint collective functions of both sRNAs to the presence of a conserved base-pairing domain in both sRNAs. Finally, laboratory selection experiments employing a library of synthetic sRNAs revealed that regulation of a single porin is sufficient to mediate stress relief.

The third sRNA studied in this thesis, VadR, was identified using a genetic screen to assess sRNAs affecting cell curvature of *V. cholerae.* Analyses of the *vadR* promoter revealed that *vadR* expression is activated in response to cell wall damage by the VxrAB two component system. Transcriptome analyses revealed that VadR regulates a large gene cluster responsible for synthesis of the biofilm matrix, and biofilm formation was inhibited in cells overexpressing *vadR*. Additionally, we found that VadR regulates cell curvature by inhibiting translation of *crvA*, encoding the major curvature determinant of *V. cholerae*. Finally, we pinpoint regulation of *crvA* by VadR to be critical to mediate resistance to cell wall damage.

Expression of the fourth sRNA analyzed in this study, VqmR, is controlled by quorum sensing system, involving the autoinducer DPO. Analyses aiming to identify additional mRNA targets for the VqmR sRNA found five additional targets, including the low cell density master regulator *aphA*. VqmR base-pairs to *aphA* using an unusual site located in the rho-independent terminator of the sRNA. Regulation of *aphA* by VqmR resulted in reduced virulence gene expression. Finally, the present work found that the interplay of all three quorum sensing systems is required to achieve a full quorum sensing response.

Zusammenfassung

Bakterielle Pathogene wie *Vibrio cholerae*, der Erreger der Cholera, finden sich in der Umwelt und in Wirtsorganismen. Dieser Lebenszyklus setzt ein konstantes Überwachen von Umweltsignalen voraus, um sich durch entsprechende Genexpression anzupassen. Zudem verwendet *V. cholerae* bakterielle Kommunikationssysteme um Gruppenverhalten, wie das Bilden von Biofilmen und die Expression von Virulenzgenen, in der Population zu synchronisieren. Diese beiden Prozesse beinhalten häufig die Regulation der Genexpression durch kleine regulatorische RNAs (sRNAs). Bakterielle sRNAs interagieren über Basenpaarungen mit *trans*-kodierten mRNAs, um deren Stabilität oder Translation zu regulieren. Jüngste Studien haben 107 potenzielle sRNAs, mit bisher ungeklärten Funktionen, in *V. cholerae* identifiziert. Ziel der vorliegenden Arbeit war es diese sRNAs, unter Berücksichtigung ihrer Beteiligung an Stressantworten und bakterieller Kommunikation, zu charakterisieren.

Im Einzelnen wurde ein bioinformatischer Ansatz verwendet, um die Bindestellen des Membranstress-Sigmafaktors σ^E zu finden und dabei wurde die sRNA MicV als Teil des σ^E-Regulons identifiziert. Die σ^E Stressantwort in *V. cholerae* beinhaltet Regulation durch eine weitere sRNA, VrrA. Die Expression beider sRNAs wird bei hohen Zelldichten, oder durch Behandlung mit membranschädigenden Substanzen, aktiviert. Transkriptomanalysen zeigten das beide sRNAs gemeinsam die Expression von Proteinen der äußeren Membran regulieren, um die Membranhomeostase unter Membranstressbedingungen zu gewährleisten. Die überlappenden Funktionen beider sRNAs begründen sich durch das Vorhandensein einer konservierten Domäne zur Basenpaarung. Abschließend zeigten wir durch Selektionsexperimente mit einer Sammlung von synthetischen sRNAs, dass die Regulation eines einzigen Porins ausreicht, um Membranstress zu lindern.

Die dritte sRNA in dieser Studie, VadR, wurde durch einen genetischen Screen für sRNAs die die Zellkrümmung von *V. cholerae* beeinflussen gefunden. Analysen des *vadR* Promotors zeigten das die Expression von *vadR* bei Zellwandstress durch das VxrAB Zweikomponentensystem aktiviert wird. Transkriptomanalysen zeigten das VadR ein großes Gencluster, verantwortlich für die Synthese der Biofilm Matrix, reguliert. Demzufolge war die Bildung von Biofilmen in Zellen die *vadR* überexprimieren inhibiert. Zusätzlich regulierte VadR durch Inhibieren der Translation der *crvA* mRNA, welche für eine wichtige Zellkrümmungsdeterminante kodiert, die Zellkrümmung. Letztendlich zeigten wir das die Regulation von *crvA* durch VadR entscheidend für die Resistenz gegen Zellwandstress ist.

Die Expression der vierten sRNA in dieser Studie, VqmR, wird durch ein bakterielles Kommunikationssystem und den Autoinducer DPO reguliert. Durch Analysen, die darauf abzielten neue Ziel-mRNAs der VqmR sRNA zu identifizieren, konnten fünf weitere Ziel-mRNAs identifiziert werden, welche unter anderem, für den Hauptregulator bei niedriger Zelldichte, AphA, kodieren. Die Basenpaarung zwischen VqmR und *aphA* ist ungewöhnlich, und benötigte eine Region im Rho-unabhängigen Terminator der sRNA. Die Regulation von *aphA* durch VqmR resultierte in einer Reduktion der Virulenzgenexpression. Schlussendlich konnte die vorliegende Arbeit zudem zeigen das drei bakterielle Kommunikationssysteme zusammenwirken, um ihre volle Wirkung zu entfalten.

Chapter 1: Introduction

1.1 *Vibrio cholerae*, a model pathogen

Cholera is a widespread and serious infectious disease, affecting an estimated 2.86 million patients in 69 endemic countries annually, of which 95,000 infections are fatal (1). The Gram-negative bacterium *Vibrio cholerae* was identified as the causative agent of cholera disease in 1854 (2).

Today, the literature groups *V. cholerae* into more than 200 serotypes, based on O-antigen structure (3). Interestingly, only the O1 and O139 serotypes are reported to cause pandemic outbreaks (4–6). The O1 group is further divided into the distinct biotypes: “classical” and “El Tor”, and into three sub-serovars: Ogawa, Inaba, and Hikojima (7). The strain used in this thesis is *V. cholerae* C6706 and was collected by the Center for Disease Control and Prevention (CDC) during a pandemic outbreak in Peru in 1991, and is classified as O1 El Tor Inaba (8, 9). Due to their interesting life cycle, *V. cholerae* strains are frequently used as model organisms to study bacterial pathogenesis, disease transmission and gene regulation (10).

1.1.1 The life cycle of *Vibrio cholerae*

V. cholerae species are considered environmental pathogens and their life cycle can be described in three stages: the presence in aquatic environments, the entry into the human host, and the exit from the host and re-release into the aquatic environment (Fig. 1.1). *V. cholerae* spends the majority of its life cycle as an autochthonous inhabitant of aquatic environments, such as brackish and estuarial waters (11, 12). Here, *V. cholerae* is predominantly found in microbial communities called biofilms (13), that are commonly associated with chitinous surfaces on zoo- and phytoplankton (14, 15). Cholera infections occur through the uptake of contaminated food or water by the human host. *V. cholerae* utilizes a competent acid tolerance response to survive passage through the low pH environment of the stomach (16, 17). Of note, increased survival of *V. cholerae* in the stomach was reported, if the infection occurs through ingestion of biofilms (18). Having progressed to the small intestine, *V. cholerae* is able to attach to and penetrate the mucus barrier, a thick coat of complex glycoproteins, protecting the intestinal surface (19–21). Subsequently, *V. cholerae* uses the key virulence factor TCP (toxin-coregulated pilus) to attach to epithelial cells and initiates the production of cholera toxin (CTX) (8, 22). CTX is an oligomeric protein complex, consisting of one A subunit and five B subunits (23). The CTXB subunits specifically bind membrane receptors to mediate uptake of the toxin complex. Intracellular CTXA subunits stimulate adenylate cyclase activity, which activates chloride efflux channels, and subsequently causes severe watery diarrhea - the hallmark

symptom of cholera disease (24). During late-stage infections, *V. cholerae* initiates a genetic program, called the mucosal escape response, to exit the small intestine and disseminate in high numbers (25). *V. choleraes'* persistence in these complex environments is largely attributable to adjustable genetic tools, that allow adaptation through changes in gene expression (26). These mechanisms are discussed in the following sections.

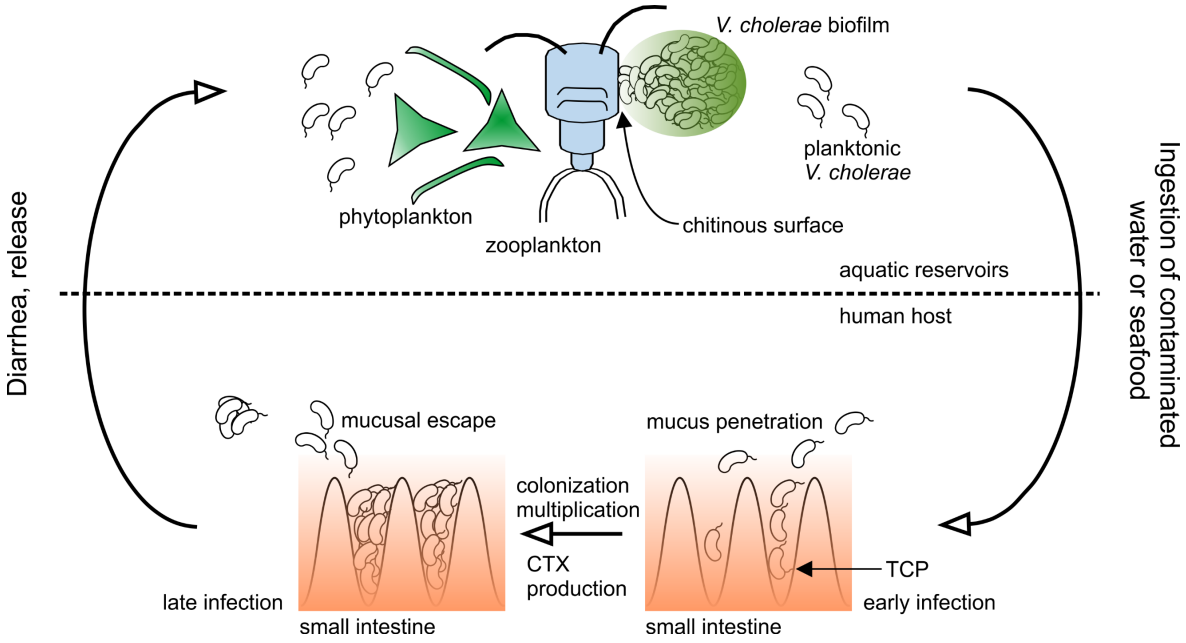

Figure 1.1: Overview of the life cycle of *V. cholerae*: *V. cholerae* mainly inhabits aquatic reservoirs as free swimming planktonic cells, or in biofilms associated to chitinous surfaces on phyto- and zooplankton. Infection occurs through uptake by a human host. *V. cholerae* invades the small intestine, penetrates the mucus barrier, and attaches to epithelial cells via the TCP. *V. cholerae* initiates production of CTX, and multiplies in the small intestine. During late-stage infections, *V. cholerae* escapes the mucus barrier and disseminates from the human host through CTX-induced diarrhea.

1.2 The role of non-coding RNA in regulating bacterial gene expression

Bacteria must sense and respond to a variety of environmental signals, requiring efficient adaptation of gene expression. Bacteria respond to environmental stimuli, such as heat stress, nitrogen limitation, iron limitation, stationary phase growth conditions and envelope stress by activation of alternative sigma factors (27). These regulatory proteins associate with the RNA-polymerase core enzyme and direct transcriptional control towards specific promoters. Importantly, this mode of action restricts sigma factors to act as direct transcriptional activators (28). Likewise, a plethora of transcription factors sense an equally diverse amount of input signals and respond by activating or repressing transcription from specific promoter sequences (29–31).

Since early models predicted control of gene expression to occur entirely through modulating transcription, the regulatory potential of non-coding RNA was initially overlooked. Non-coding RNA molecules in bacteria were thought to mainly include the

abundant class of ribosomal RNAs (rRNA), transfer RNAs (tRNA) and other RNAs involved in house-keeping functions (32). While these RNAs comprise up to 95% of all transcripts in a bacterial cell (33), research in the past decades has unveiled an unexpected complexity of RNA molecules that modulate gene expression, employing a wide repertoire of distinct mechanisms (34).

Several analyses of 5' untranslated regions (5'UTR) revealed the presence of riboswitches, and RNA thermometers, that modulate translation of their associated coding sequences, by responding to metabolites or temperature shifts, respectively (35, 36). For example, in *V. cholerae* the transcription factor ToxT activates expression of the virulence factor genes *tcp* and *ctx* (37). Translation of *toxT* mRNA is under control of a structured RNA element within its 5'UTR. At low temperature, intramolecular base-pairing interactions occlude the Shine-Dalgarno (SD) sequence within a double-stranded RNA stem-loop, thus preventing 30S ribosome access and resulting in low basal translation activity. At high temperatures, as present in the human intestine, the structure unfolds, releasing the SD sequence to allow ribosome access and translation of *toxT* (38).

The most prominent class of regulatory RNAs in bacteria are the so called small regulatory RNAs (sRNA). These sRNAs exert their regulatory function by base-pairing with cognate mRNAs, thus forming sRNA-mRNA duplexes. We distinguish two types of regulators: *cis*-acting and *trans*-acting sRNAs (discussed in the next section).

Cis-acting sRNAs derive from the same genomic locus as their mRNA targets - but in the antisense orientation - and control target gene expression by formation of RNA duplexes, with perfect complementarity (39). Double-stranded RNA duplexes of about 20 base-pairs (bp), provide substrates for endoribonucleolytic cleavage by RNAse III, resulting in RNA duplex degradation (40, 41). The first *cis*-acting sRNA was discovered as part of the replication machinery of the plasmid ColE1 (42), and to date most *cis*-acting sRNAs have been associated with plasmids, phages, and transposons (43). Nonetheless, *cis*-acting sRNA are also found in bacterial chromosomes. In *V. cholerae*, translation of the mannitol-specific transporter *mtlA* mRNA is controlled by the *cis*-acting sRNA, MtlS. In the presence of sugars other than mannitol, MtlS forms a 71nt long RNA duplex with the *mtlA* mRNA, occluding the SD sequence to prevent translation of the mannitol-specific permease MtlA (44, 45). Due to the direct proximity of the *cis*-acting sRNA and the mRNA target on opposing strands, RNA duplex formation in this, and most other cases does not require protein cofactors, such as Hfq (discussed below) (39, 44). Importantly, the influence of *cis*-acting antisense sRNAs on bacterial gene regulation might be underestimated. This is, for instance, illustrated by a recent study that found that 47% of all transcriptional start sites (TSS) in *V. cholerae* initiated transcription in the antisense orientation (46).

1.2.1 Regulation of gene expression by *trans*-acting small RNAs

The largest class of sRNAs are *trans*-acting sRNAs. These regulators derive from a wide range of genomic *loci*, including: 5'UTRs, intergenic regions (IGR) or, 3'UTRs via internal promoters within coding sequences (CDS), or released via endoribonucleolytic cleavage (34) (Fig.1.2 A-D). In contrast to *cis*-acting sRNAs, *trans*-acting sRNAs base-pair to mRNA targets irrespective of genomic proximity. This process is in most cases aided by the action of auxiliary proteins, such as Hfq (discussed below). A prototypical sRNA contains an RNA stem-loop on its 3'end that is followed by a stretch of Uridines (poly(U)-stretch), to facilitate Rho-independent transcription termination. Rho-independent terminators provide binding sites for the RNA chaperone Hfq and protect sRNAs against 3' exonuclease-mediated decay (47, 48). Additionally, sRNAs often contain conserved, single-stranded regions to initiate base-pairing to target mRNAs. Due to the analogous function with their eukaryotic microRNA counterparts these regions are called "seed-regions" (49).

Trans-acting sRNAs use a wide variety of mechanisms to regulate their cognate mRNA targets (Fig. 1.2 E). The most common mechanism is negative regulation by translational repression. Here, base-pairing by an sRNA occludes the ribosome binding site of the mRNA target, thereby blocking accessibility to the 30S ribosomal subunit and inhibiting translation initiation (34). 30S ribosomal subunits have been reported to occupy a region of -35 to +19 nucleotides, with respect to the AUG start codon (50, 51). In general, this region has been reported to contain unstructured, single-stranded RNA elements (52) and is thus accessible for base-pairing interactions. While this mechanism of translation repression is sufficient to reduce protein levels, some sRNAs recruit the major endoribonuclease RNase E to initiate transcript degradation (53). RNase E is composed of an N-terminal catalytic domain and a flexible C-terminal scaffolding domain. Auxiliary proteins associate with the C-terminal domain of RNaseE to form a protein complex called the RNA degradosome (54). Interestingly, Hfq has been reported to associate with the C-terminal domain of RNase E, suggesting the formation of a ribonucleoprotein complex, involving sRNAs, Hfq, and RNase E (55). In *E. coli*, the SgrS and RyhB sRNAs have been reported to recruit an Hfq-RNase E complex towards their cognate mRNA targets *ptsG* and *sodB* to initiate rapid ribonucleolytic decay (55). As shown for the RyhB-*sodB* interaction, this decay is not limited to the mRNA target, but degrades the regulator, RyhB, as well – a concept referred to as coupled degradation (56, 57). Importantly, this mechanism ensures robust regulation and restricts sRNAs to act stoichiometrically (56). Due to the rapid turnover of sRNA and cognate mRNA target, regulation via a coupled degradation mechanism reduces leaky expression of target genes and is important to maintain homeostatic gene expression (58).

Importantly, *trans*-acting sRNAs are not restricted to interact within the tight region

around the start codon for efficient regulation. In *S. typhimurium*, the GcvB sRNA base-pairs to a translational enhancer element within the *gltI* mRNA, that is located -57 to -47 nucleotides from the start codon (59). Likewise, sRNAs can also regulate by base-pairing deep in the CDS. For instance, the MicC sRNA regulates *ompD* mRNA by base-pairing to a region +67 to +78 nucleotides from the start codon. Here, regulation of *ompD* mRNA is achieved by recruitment of RNase E, instead of translational repression (60).

Furthermore, *trans*-acting sRNAs are also not limited to negatively regulate their cognate mRNA targets. There is a wide variety of mechanisms described in which base-pairing of an sRNA results in an activation of gene expression, in many cases involving an "anti-antisense" base-pairing mechanism (61, 62) (Fig. 1.2 F). For instance, in *V. cholerae* the *vca0939* mRNA, encoding a diguanylate cyclase, contains an RNA stem-loop close to the SD sequence, which prevents 30S ribosomal access, and therefore causes low translation activity. The stem-loop is disrupted by base-pairing of four homologous sRNAs, Qrr1-4, resulting in upregulated Vca0939 protein levels (63). Interestingly, the Qrr1-4 sRNAs employ the same seed-sequence, to downregulate *hapR* mRNA (64), indicating that sRNA seed-sequences do not determine positive or negative target regulation.

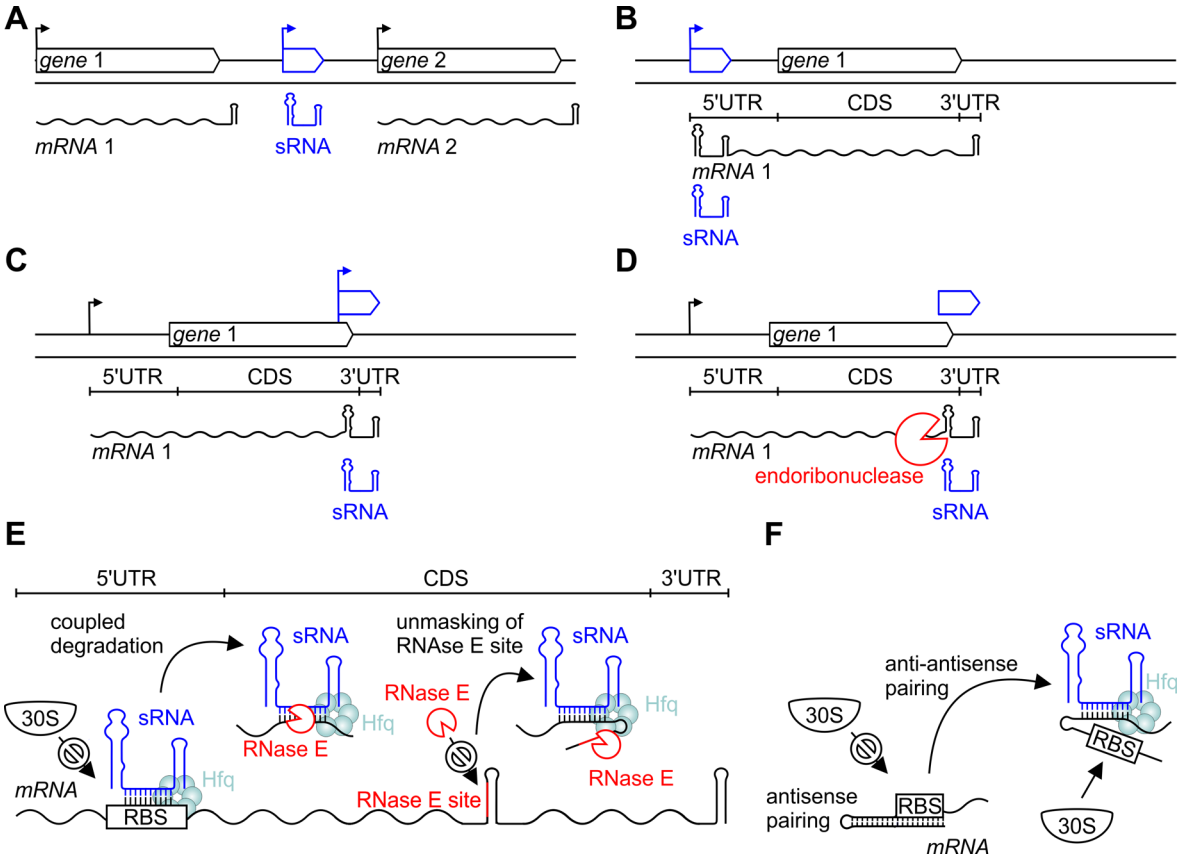

Figure 1.2: Overview of sRNA localization and common regulatory mechanisms: (A-D) sRNAs are encoded in intergenic regions **(A)**, part of the 5'UTR of associated mRNAs **(B)**, derived from independent promoters in an overlapping gene **(C)**, or generated through endoribonucleolytic cleavage of an associated mRNA **(D)**. **(E)** Negative regulation by an sRNA is commonly enacted by Hfq-mediated base-pairing to ribosome binding sites (RBS), or by recruiting RNaseE to the corresponding mRNA target. **(F)** Hairpin structures within the 5'UTR can occlude the RBS, preventing efficient translation. Anti-antisense pairing by an sRNA can relieve this inhibition, by unmasking the RBS.

1.2.2 The role of RNA chaperones for trans-acting sRNAs

In most bacteria the process of base-pairing between sRNAs and mRNAs is controlled by auxiliary proteins - in the majority of cases by the Hfq protein. Initially, Hfq was described in *E. coli* as an essential host factor required for bacteriophage Qß RNA replication (65). In Bacteria, Hfq is largely conserved, and found in ~50% of bacterial species (66). Hfq controls large and complex post-transcriptional networks, which is reflected by strong pleiotropic phenotypes if *hfq* is deleted (67). For instance, in *V. cholerae hfq* mutants displayed strongly attenuated virulence in a suckling mouse infection model (68).

Hfq belongs to the family of Sm-like (LSm) proteins, which perform essential tasks in the RNA biology of all domains of life (69). In eukaryotes, LSm family proteins control several processes, including: precursor mRNA splicing (70), mRNA decapping and decay (71), and RNA metabolism (72). In prokaryotes, the LSm family protein Hfq was reported to stabilize sRNAs (73), to accelerate sRNA-mRNA target annealing (74–76), and to unfold inhibitory RNA structures - a “classic” chaperone function (77). For instance, Hfq has been reported to unfold an intramolecular, double-stranded RNA structure in the OxyS sRNA, required for base-pairing to the *rpoS* mRNA (78, 79). Likewise, the interaction of the OmrA/B sRNAs with the *dgcM* mRNA requires Hfq to unfold a stem-loop in the *dgcM* mRNA, that prevents OmrA/B binding (80).

Hfq monomers assemble a homohexameric structure, resembling a characteristic donut-shape, that distinguish it from the heteroheptameric complexes formed by other LSm protein members (69, 81, 82). This distinctive architecture exposes four sites to the surrounding environment: (i) the proximal face (ii) the distal face (iii) the lateral face (the rim) (iv) and the C-terminal tail of variable size, which is missing in several species (83). These regions contain unique architectures and electrostatic surfaces, allowing them to discriminate between different RNA species (84–86). The proximal face preferentially interacts with poly(U) (Uridine) sequences, as found in Rho-independent transcription terminators, and ubiquitous in Hfq binding sRNAs (87–89). The preferential binding to transcription terminator structures is illustrated by the frequently observed enrichment of mRNA 3’UTRs in Hfq co-immunoprecipitation experiments (90, 91). The distal face of Hfq preferentially binds to A (Adenosine)-rich sequences in both sRNAs and mRNAs, often containing a canonical A-R-N (where R represents a purine (A or G (Guanosine) and N represents any nucleotide) motif (92–95). The lateral face contains secondary binding sites for UA-rich sequences and is required for several interactions of both sRNAs and mRNAs (94). Due to its intrinsically disordered nature, the C-terminal tail of Hfq was not resolved in initial Hfq crystal structures and its function remained unclear. But recent studies propose that the C-terminal tail displaces weakly bound sRNAs, thus achieving selective binding (96–98). According to these observations, Hfq-interacting sRNAs can be classified by two

different modes of interaction with Hfq. Class I sRNAs, bind to the proximal face of Hfq, and base pair with cognate, distal-face-binding mRNA targets. Class II sRNAs, can bind both the proximal and distal face of Hfq, and base-pair to lateral face-binding mRNAs (86, 94). According to the different binding sites on Hfq, Class I sRNAs have been reported to turn-over rapidly, while Class II sRNAs have been reported to be more stable (94).

1.2.3 Identification and characterization of small RNAs in bacteria

In 1984, Mizuno *et al.* identified the first sRNA-mRNA pair by chance, while characterizing *ompC* promoter fragments. The researchers observed a strong downregulation of OmpF protein levels, when a 300 bp DNA fragment - encoding the MicF sRNA - was introduced into *E. coli,* on a plasmid (99). This observation motivated a series of follow-up studies, aiming at the identification of novel sRNAs on a genome-wide scale. In *E. coli,* a screen predicting promoter and terminator locations with limited space separation, and taking phylogenetic conservation into account, yielded 14 novel sRNAs derived from IGRs (100). One drawback of these computational sRNA studies was the limited transferability to less well-characterized species, for example, due to missing promotor consensus motifs (101). This emphasized the need for unbiased approaches to experimentally identify bacterial sRNAs (102). For example, the usage of high-density tilling microarrays was adapted from the usage in *E. coli* (103) to distantly related bacteria (104, 105). Modern methods for sRNA identification employ high-throughput sequencing to a large extent. For example, deep-sequencing approaches have been used to identify the global sRNA ligands bound to the RNA chaperone Hfq in *S. typhimurium* (90, 106). Furthermore, the use of differential RNA-seq (dRNA-seq), a method that allows to distinguish between primary and processed transcriptomes has been developed as an elegant method to map transcriptional start sites (TSS), by selective sequencing of primary transcripts. To achieve this, total RNA samples are split into pairs, and treated with terminator exonuclease (TEX), or left untreated. TEX treatment selectively depletes processed, 5'-monophosphate (5'-P) carrying transcripts from the sample, so that primary transcripts, carrying a 5'-triphosphate (5'-PPP), become enriched. Subsequently, complementary-DNA (cDNA) libraries are generated from the samples and subjected to high-throughput sequencing. Primary transcripts and sRNAs are then identified through the enrichment in TEX treated samples. *Vice versa*, processed sRNAs are detected through the depletion in TEX treated samples (107). While initially applied to *Helicobacter pylori* (108), the method has been broadly adapted to numerous bacterial species (109). In *V. cholerae*, the application of dRNA-seq identified 7,240 TSS and 107 novel sRNAs (46).

While the listed approaches can successfully identify novel sRNAs, they don't necessarily inform about their physiological roles. Since sRNA gene deletion approaches

rarely yield strong phenotypes, a straightforward way to gain insight into their biological roles is the identification of their respective mRNA targets (110, 111). Numerous approaches exist to achieve this goal. First, state-of the art computational approaches, that account for complementarity, phylogenetically conserved interactions, and necessarily accessible interaction sites, have successfully identified mRNA targets (112, 113). Nonetheless, these *in silico* approaches can suffer high false-positive rates (114). Second, scoring changes in global transcript abundance by RNA-seq after induction of a short burst of sRNA overexpression - referred to as pulse-induction - has successfully captured mRNA targets, since rapid transcript degradation is often a consequence of translational inhibition by sRNAs (111). For instance, a pulse-induction approach unveiled a whole network of sRNA-mRNA interactions for the RybB sRNA, downregulating multiple mRNAs encoding outer membrane proteins (115). Third, recent developments in the field of eukaryotic microRNA (miRNA), have employed ligation of miRNA-mRNA pairs bound to the RNA-binding Argonaut protein (116–118). This inspired several approaches to transform this methodology to RNA-binding proteins in bacteria (119). To name one such approach, the application of RNA interaction by ligation and sequencing (RIL-seq), has unveiled 2,800 putative sRNA-mRNA interactions occurring on *E. coli* Hfq (120). An important limitation of RIL-seq approaches is the strict requirement for an RNA binding protein (121). While a breadth of approaches listed here allow the analysis of bacterial sRNA interactomes in a top-down manner, they still require validation experiments. Further analysis of sRNA expression and identification of the involved transcription factors is needed to deduce physiological roles.

1.3 Involvement of sRNAs in bacterial stress responses

During their life cycle, *V. cholerae* and related bacteria encounter diverse environmental stress signals, such as: temperature fluctuations, salinity shifts, nutrient availability, protozoan grazing, phages, pH shifts, reactive oxygen species, bile salts and antimicrobial peptides (122).

In many cases, the first interaction site between bacteria and these environmental signals is the bacterial cell envelope. The envelope allows bacteria to selectively transport small molecules, such as nutrients or autoinducers (discussed below), while excluding toxic molecules, such as antibiotics (123, 124). In Gram-negative bacteria the envelope is composed of the outer membrane, the periplasm, a layer of peptidoglycan and the inner membrane (125). Maintaining the integrity of the envelope is critical for cell survival and is therefore tightly controlled. Enterobacteria have evolved adequate stress response systems, that monitor insults to the envelope and mitigate stress by adapting gene expression accordingly (126). There are five stress response systems described, that

respond to various stressors to the Gram-negative cell envelope: (i) the Psp (phage shock protein) stress response, activated by disruption of the proton motive force in the inner membrane (ii) the Bae (bacterial adaptive response) stress response, activated by exposure to toxic molecules (iii) the Rcs (regulator of capsule synthesis) stress response, responding to peptidoglycan and lipopolysaccharide damage (iv) the Cpx (conjugative plasmid expression) stress response, responding to misfolded or delocalized inner membrane proteins (v) and the σ^E-dependent stress response, activated in response to misfolded outer membrane proteins (OMPs) (127). Importantly, the downstream reactions facilitated by these major stress responses often involve regulation by one or more sRNAs to rapidly alleviate stress (128).

One of the best studied examples is the σ^E-dependent stress response of *E. coli* and related enterobacteria (Fig. 1.3). In the absence of outer membrane damage (e.g. during exponential phase growth conditions), the alternative sigma factor σ^E is kept inactive by direct interaction with its corresponding, inner-membrane associated, anti-sigma factor RseA (129, 130). Accumulation of toxic, misfolded OMPs (e.g. during stationary phase growth conditions) in the periplasm activates the inner-membrane associated protease DegS, inducing a conformational change to enable cleavage of the periplasmic domain of RseA (131). To ensure specific σ^E activation under inducing conditions, the periplasmic domain of RseA is additionally protected from proteolysis by interaction with RseB (132). While the exact molecular mechanism remains elusive, the RseA-RseB interaction is likely disrupted by interaction with off-pathway lipopolysaccharides (133) or misfolded OMPs (132), under inducing conditions. Cleavage of the periplasmic domain of RseA, renders the protein accessible for proteolytic attack by a second protease, RseP, subsequently cleaving its transmembrane domain (134, 135). The remaining cytoplasmic fragments of RseA are cleaved by the cytoplasmic protease ClpXP and the released σ^E recruits RNA polymerase core enzyme to activate its regulon (136). The σ^E regulon comprises protein chaperones to assist with OMP folding, proteins involved in the insertion of OMPs into the outer membrane, and proteases to degrade misfolded OMPs (137). Additionally, σ^E activates expression of three sRNAs, MicA (138), RybB (115), and MicL (139). MicL specifically downregulates expression of a single mRNA, *lpp*, encoding the most abundant protein of *E. coli* (139). In contrast, MicA and RybB control large regulons to stop *de novo* synthesis of major OMPs upon σ^E induction, thereby allowing the restoration of envelope homeostasis (140, 141). While the protein components of the σ^E stress response are largely conserved, *V. cholerae* encodes no direct homologous of the MicA, RybB and MicL sRNAs (142, 143). Instead, an evolutionary unrelated σ^E-dependent sRNA, VrrA, has been reported to control expression of the major porins OmpA, OmpT, the ribosome hibernation protein Vrp, and the biofilm matrix protein RbmC (142, 144–146). Interestingly, the interaction of VrrA with *ompA* mRNA

has been reported to be independent of the RNA chaperone Hfq, but *ompA* mRNA levels were increased in *hfq* mutants (142). Furthermore, the σ^E-response and several additional porins are deregulated in *V. cholerae hfq* and *rpoE* mutants (68), together suggesting potential regulation by a yet undescribed σ^E-dependent sRNA. The present work addresses this hypothesis by functional characterization of the sRNA arm of the σ^E-response of *V. cholerae* in Chapter 2.

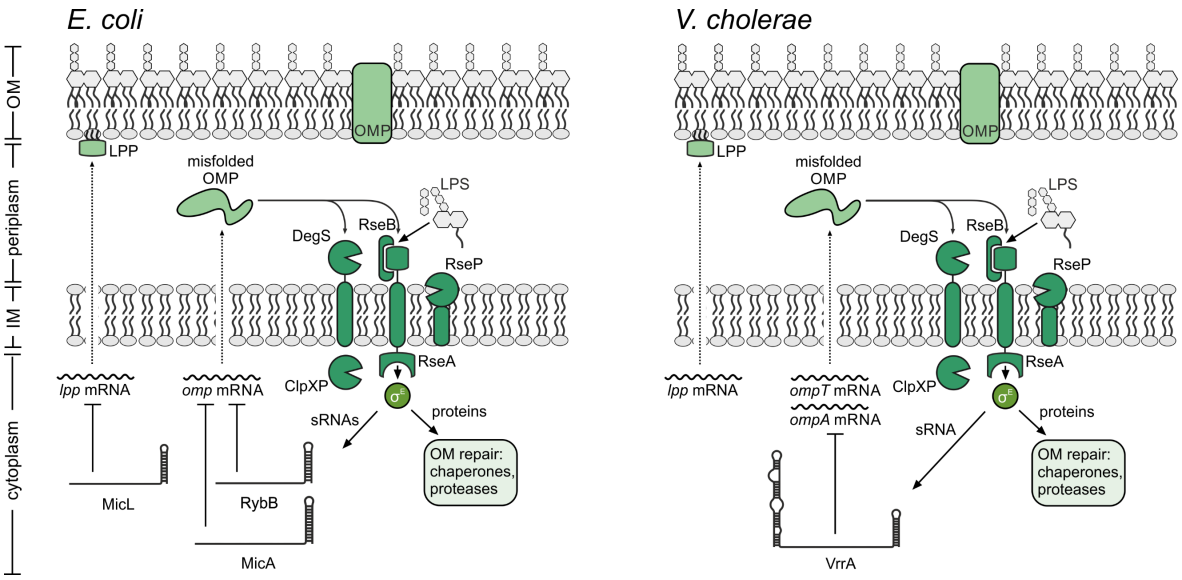

Figure 1.3: Overview of the σ^E mediated envelope stress response of *E. coli* and *V. cholerae*: The σ^E-response is activated by accumulation of misfolded OMPs in the periplasm, and off-pathway LPS, which induce a proteolytic cascade in the inner membrane. Consecutive cleavage of the DegS, RseP, and ClpXP proteases cleaves the anti-sigma factor RseA, resulting in the release of σ^E. Free σ^E activates expression of a protein arm for outer membrane repair and an sRNA arm to rapidly halt OMP *de novo* synthesis. In *E. coli*, the sRNAs RybB and MicA inhibit the expression of large regulons, comprising all major OMPs and several related targets. The MicL sRNA specifically downregulates *lpp* expression. In *V. cholerae*, the functionally homologous sRNA VrrA inhibits translation of the *ompT* and *ompA* mRNAs. The figure was adapted and modified from: (128, 147)

Another key system to maintain envelope homeostasis, the Rcs stress response, is activated by damage to the peptidoglycan layer or LPS, for instance upon encountering cell wall acting antibiotics or cationic antimicrobial peptides (148, 149). The Rcs system is reported to control production of exopolysaccharide biosynthesis, biofilm formation, and motility in *E. coli* (150–152). In addition, the Rcs system activates expression of the RprA sRNA (153). Subsequently, RprA activates translation of *rpoS* through an anti-antisense pairing mechanism (154). The *rpoS* gene encodes the stationary phase sigma factor σ^S, that controls the general stress response, and provides cross-protection from several stresses (155). For instance, the Rcs system has been shown to be critical for recovery of cell shape, if the cell-wall has been artificially removed by lysozyme treatment (156).

Interestingly, *V. cholerae* is remarkably tolerant to similar treatments, and fails to lyse under beta-lactam induced cell wall damage, although no homologs of the Rcs response related proteins exist in *V. cholerae* (157). Instead of the Rcs system, recovery from cell wall damaging conditions is mediated by the VxrAB (a.k.a. WigKR) two component

system. The VxrAB regulon is activated by penicillin G treatment and activates expression of cell wall biosynthesis genes (158), controls host colonization and Type VI secretion (159), and biofilm formation (160). Although sRNA-based regulation plays a key role in related stress response systems and it has been speculated that each bacterial regulon contains at least one sRNA (161), no homolog of RprA is known in *V. cholerae*, and no sRNA has been associated to the VxrAB regulon. The present work addresses the involvement of sRNA-based regulation in the VxrAB response in Chapter 3.

1.4 Involvement of sRNAs in bacterial communication systems

In addition to the above mentioned responses, bacteria use a process called quorum sensing (QS) to efficiently interact with the environment as a group (162). QS allows bacteria to distinguish and count members of their own species apart from others, through the synthesis, export, and subsequent detection of small molecules, called autoinducers (163). In *V. cholerae*, QS directly controls synchronization of group behaviors, such as biofilm formation and virulence gene expression (18, 164, 165).

The canonical QS system of *V. cholerae* involves production of the autoinducers CAI-1 and AI-2 by the synthases, CqsA and LuxS, respectively (166, 167) (Fig 1.4). Under low cell density conditions, when autoinducer concentrations in the environment are low, the autoinducer receptor proteins CqsS and LuxPQ phosphorylate the LuxU protein. The phosphate signal is transferred to the transcription factor LuxO, which, in complex with the alternative sigma factor σ^N, activates the expression of four homologous sRNAs, called Qrr1-4 (Quorum regulatory RNA) (64). The Qrr1-4 sRNAs have been reported to collectively control expression of 20 mRNAs (168). Importantly, the Qrr1-4 sRNAs use an “anti-antisense” base-pairing mechanism to unfold an inhibitory RNA stem-loop in the 5’UTR of *aphA*, thereby activating *aphA* translation (169). The *aphA* mRNA, encodes the master regulator of low cell density functions AphA, that has been reported to control expression of 300 genes, involved in virulence and biofilm formation (170). Conversely, the Qrr1-4 sRNAs inhibit *hapR* translation by base-pairing to a region close to the Shine-Dalgarno sequence (64). The *hapR* mRNA, encodes the master regulator of high cell density functions HapR, that has been reported to control expression of 100 genes, for example involved in chemotaxis and motility (25, 171). Importantly, HapR activates expression of the Hap protease, required for host escape (172). In summary, the Qrr1-4 sRNAs function at the center of the QS system to tune expression of the key regulators AphA and HapR, controlling virulence gene expression and host escape functions (170). Under high cell density conditions, autoinducer-binding to CqsS and LuxPQ induces a conformational change, converting the receptors to phosphatases. In turn, CqsS and LuxPQ dephosphorylate LuxU, resulting in a de-repression of *hapR* and thus inhibiting virulence

gene expression and biofilm formation (173).

Recently, a third quorum sensing circuit has been established in *V. cholerae*. Here, the Tdh enzyme catalyzes synthesis of the autoinducer DPO (Fig. 1.4). DPO is sensed by the transcriptional regulator VqmA, which subsequently activates expression of the VqmR sRNA (174). The regulon for the VqmR sRNA has been established, and involves, among other mRNA targets, the *vpsT* mRNA, encoding the key regulator of biofilm matrix production (46, 175). Importantly, the initial transcriptome analysis to identify the VqmR regulon was conducted under high cell density conditions using microarrays (46). Considering the limited dynamic range of microarrays (176), and that VqmR has been shown to be expressed in exponential phase of bacterial growth (174), we aimed to identify additional targets for the VqmR sRNA in Chapter 4. To this end, we performed transcriptome analysis under low cell density conditions using RNA-seq.

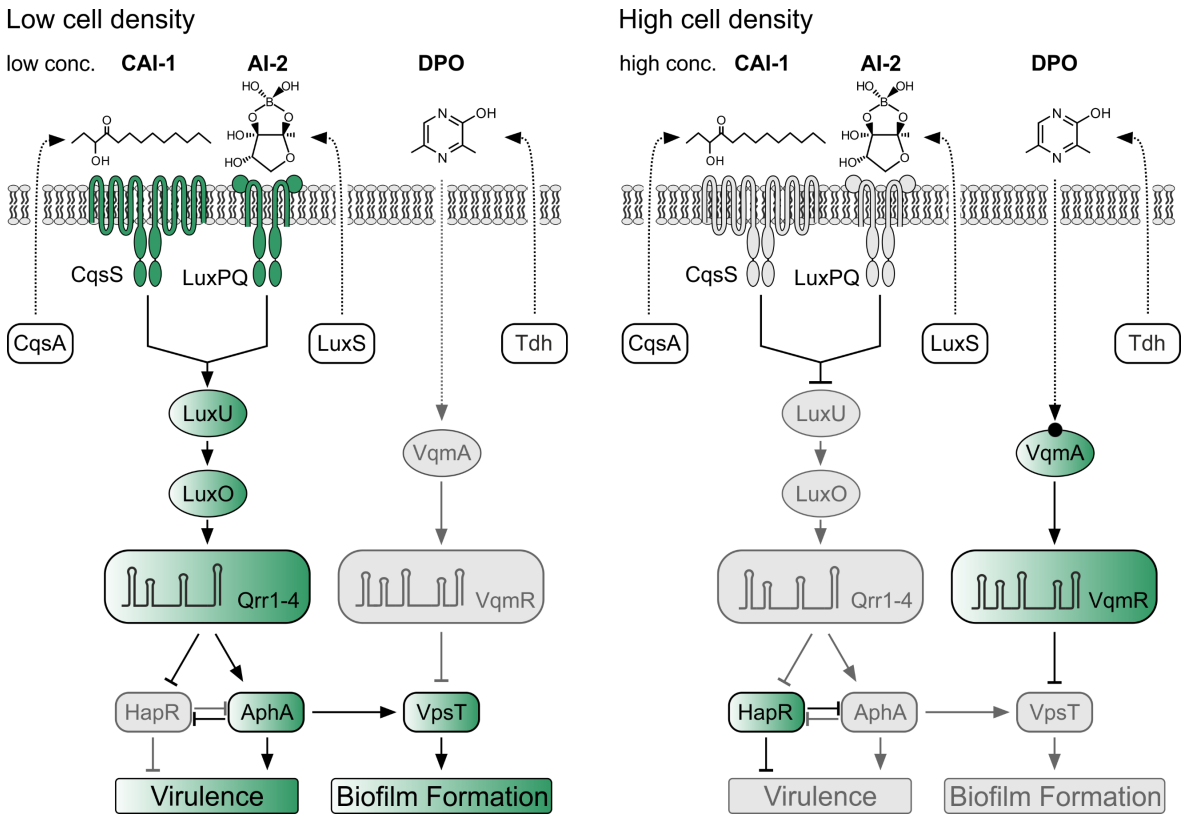

Figure 1.4: Overview of the quorum-sensing systems of *V. cholerae*: Quorum sensing in *V. cholerae* involves the synthesis, detection, and response to the three autoinducers CAI-1, AI-2, and DPO. CAI-1 and AI-2 are synthesized by CqsA and LuxS, respectively. DPO is synthesized by Tdh. Under low cell-density conditions, CqsS and LuxPQ channel phosphate through LuxU to LuxO. Phosphorylated LuxO activates expression of the Qrr1-4 sRNAs. The Qrr1-4 sRNAs collectively activate expression of *aphA*, while inhibiting translation of *hapR*. AphA activates expression of virulence gene expression and biofilm formation through VpsT. Presence of autoinducers under high cell density conditions, converts CqsS and LuxPQ to phosphatases, resulting in dephosphorylation of LuxU. This leads to de-repression of *hapR* expression and reduced virulence gene expression. DPO is sensed by its cognate receptor VqmA. VqmA activates expression of the VqmR sRNA, which inhibits translation of the *vpsT* mRNA. The figure has been adapted and modified from: (177)

1.5 Aim of the study

The key objective of this thesis was the identification and functional characterization of regulatory small RNAs involved in stress responses and quorum sensing in the human pathogen *V. cholerae.* While sRNAs and their cognate regulons have been extensively studied in model organisms such as *E. coli* and *S. typhimurium*, only few studies in distantly related pathogens exist (178). Importantly, the evolution of sRNAs is thought to occur rapidly and often prevents identification of sRNA homologs between species (161). Direct transfer of the obtained knowledge from model species to other bacteria is thus challenging, and further complicated by the observation that homologous sRNAs frequently show different expression patterns and control different regulons (179, 180). For instance, while both *V. cholerae* and *S. typhimurium* encode homologs of the GcvB sRNA, their expression patterns differ. In *S. typhimurium*, GcvB shows high expression in exponential growth phase, and low expression in stationary growth phase (59). In *V. cholerae* this trend is inversed (46). Furthermore, while both *E. coli* and *V. cholerae* encode significantly similar (identical at 31 of 34 nucleotides in the core region) copies of the RyhB sRNA, their regulons are different (181). Although some examples of homologous sRNAs between *E. coli* and *V. cholerae* exist, the majority of *V. cholerae* sRNAs remain uncharacterized.

A recent dRNA-seq approach identified 107 novel sRNA candidates in *V. cholerae* (46). The key aim of this thesis was to investigate these candidate sRNAs with respect to their transcriptional regulation, their regulons, and their physiological roles. We addressed these questions in the following chapters:

In Chapter 2, a screen for sigma factor binding sites in the promotor regions of the 107 candidate sRNAs should be used to investigate potential involvement in *V. cholerae* envelope stress response. Identified candidates should be investigated with respect to their regulons and physiological roles under membrane stress conditions.

In Chapter 3, a plasmid library, overexpressing candidate sRNAs, should be used to identify candidate that affect *V. cholerae* cell shape. Identified candidates should be investigated concerning their physiological roles, transcriptional control, and mRNA targets, and their potential involvement in bacterial stress responses.

In Chapter 4, the VqmR sRNA should be investigated for additional mRNA targets. Since previous approaches aimed to identify mRNA targets under high-cell density (46), the conditions should be altered by probing low-cell density conditions.

Chapter 2: A conserved RNA seed-pairing domain directs small RNA-mediated stress resistance in enterobacteria

Peschek N, Hoyos M, Herzog R, Förstner KU, Papenfort K, A conserved RNA seed-pairing domain directs small RNA-mediated stress resistance in enterobacteria. ***EMBO J***, Volume 38, Issue 16, 15 August 2019, doi: 10.15252/embj.2019101650

The full-text article is available online at:
https://www.embopress.org/doi/10.15252/embj.2019101650

The supplementary material is available online at:
https://www.embopress.org/action/downloadSupplement?doi=10.15252%2Fembj.2019101650&file=embj2019101650-sup-0001-Appendix.pdf

The corresponding source data files are available online at:
https://www.embopress.org/doi/10.15252/embj.2019101650

Chapter 3: RNA-mediated control of cell shape modulates antibiotic resistance in *Vibrio cholerae*

Herzog R*****, Peschek N*, Singh PK, Fröhlich KS, Schröger L, Meyer F, Bramkamp M, Drescher K, Papenfort K, RNA-mediated control of cell shape modulates antibiotic resistance in *Vibrio cholerae*. **Manuscript**

* authors contributed equally

RNA-mediated control of cell shape modulates antibiotic resistance in *Vibrio cholerae*

Roman Herzog[1,2*], Nikolai Peschek[1,2*], Praveen K. Singh[3], Kathrin S. Fröhlich[1,2], Luise Schröger[1,2], Fabian Meyer[1,4], Marc Bramkamp[1,4], Knut Drescher[3,5], and Kai Papenfort[1,2,6#]

[1] Friedrich Schiller University, Institute of Microbiology, 07745 Jena, Germany

[2] Faculty of Biology I, Ludwig-Maximilians-University of Munich, 82152 Martinsried, Germany

[3] Max Planck Institute for Terrestrial Microbiology, 35043 Marburg, Germany

[4] Institute for General Microbiology, Christian-Albrechts-University, Kiel, Germany,

[5] Department of Physics, Philipps-Universität Marburg, 35032 Marburg, Germany

[6] Microverse Cluster, Friedrich Schiller University Jena, 07743 Jena, Germany.

* These authors contributed equally

Corresponding author:

Kai Papenfort

E-mail: kai.papenfort@uni-jena.de

Phone: +49-3641-939-5753

Friedrich Schiller University of Jena

Institute of Microbiology

General Microbiology

Winzerlaer Straße 2

07745 Jena, Germany

Key words: *Vibrio cholerae*, small RNA, cell shape, biofilm formation, CrvAB

Abstract

Bacteria employ remarkably sophisticated mechanisms to control their cell shape and size. *Vibrio cholerae*, the causative agent of cholera disease, exhibits a characteristic curved rod morphology, which promotes infectivity and motility in dense hydrogels. The periplasmic protein CrvA determines cell curvature in *V. cholerae*, yet the regulatory factors controlling CrvA are currently unknown. In this study, we discovered the VadR small RNA (sRNA) as a post-transcriptional inhibitor of the *crvA* mRNA. Mutation of *vadR* increases cell curvature, whereas over-expression has the inverse effect. We show that transcription of *vadR* is activated by the VxrAB two-component system and triggered by cell-wall-targeting antibiotics, such as penicillin G. *V. cholerae* cells failing to repress *crvA* by VadR display strongly decreased survival upon challenge with penicillin G indicating that cell shape maintenance by the sRNA is critical for antibiotic resistance. VadR also blocks the expression of various key biofilm matrix genes and thereby inhibits biofilm formation in *V. cholerae*. Thus, VadR is an important regulator for synchronizing peptidoglycan integrity, cell shape, and biofilm formation in *V. cholerae*. To our knowledge, VadR is the first sRNA required for resistance towards ß-lactam antibiotics and the first sRNA regulator controlling cell shape in bacteria.

MAIN TEXT

Bacterial cell shape is highly diverse and tightly conserved at the species level. Certain cell morphologies have been associated with distinct physiological functions such as optimized nutrient uptake, efficient surface adherence, and increased evasion from protist grazing[1]. Cell shape is determined by the geometry of the cell-wall, which can be affected by filamentous protein factors that change or interfere with peptidoglycan insertion[2-4]. For example, the cytoskeleton-like filament, crescentin (CreS), controls cell curvature in the model bacterium *Caulobacter crescentus*[5]. In *Vibrio cholerae*, CrvA protein polymerizes in the periplasmic space to promote cell bending[6,7]. *V. cholerae* cells lacking the *crvA* gene display attenuated colonization in animal infection models and it has been reported that cell curvature of *V. cholerae* increases in a cell-density dependent manner[6]. These findings indicate that CrvA levels is continuously adjusted during growth, however, the necessary regulatory factors are currently unknown.

Recently, post-transcriptional control by small regulatory RNAs (sRNAs) in *V. cholerae* was shown to be key for modulating spatiotemporal processes such as virulence, biofilm formation, secondary messenger production, and stress resistance[8-11]. The largest class of sRNAs associates with the RNA chaperone Hfq and typically regulate the expression of target mRNAs by base-pairing *via* short stretches of imperfect complementarity[12,13]. The network regulated by a single sRNA frequently involves dozens of targets and therefore sRNAs can rival transcription factors with respect to their regulatory scope and biological importance[14]. For example sRNAs are crucial for iron, membrane, and sugar homeostasis, as well as motility, biofilm formation, and virulence[15,16], however, no sRNA has been yet reported to control cell shape.

Here, we employed the curved rod-shaped bacterium *V. cholerae* as a model system to study the impact of sRNAs on cell curvature. To this end, we used a forward genetic screen and quantified the effect of 21 previously uncharacterized Hfq-dependent sRNAs on cell shape in *V. cholerae*. We discovered that production of the VadR (VxrB activated small RNA, see below) sRNA efficiently reduced cell curvature in *V. cholerae* by inhibiting the expression of the *crvAB* mRNA at the post-transcriptional level. VadR also controls several main genes required for biofilm assembly, including *rbmA*[17]. Consequently, we show that VadR also inhibits biofilm formation in *V. cholerae*. We further show that transcription of VadR is controlled by the VxrAB two-component system (a.k.a. WigKR[18,19]) and is activated by ß-lactam antibiotics. *V. cholerae* mutants deleted for *vadR* display increased sensitivity towards penicillin and we pinpoint this phenotype to VadR-mediated repression of *crvAB*. Our results reveal how a non-coding RNA involved regulates a cytoskeleton-like filament in bacteria and establishes a link between cell shape, biofilm formation, and antibiotic resistance in *V. cholerae*.

RESULTS

To identify sRNAs regulating cell curvature in *V. cholerae*, we performed a microscopy-based forward genetic screen. We selected 21 uncharacterized sRNAs candidates from a pool of recently identified Hfq-dependent sRNAs[20] and cloned their respective genes onto multi-copy plasmids. We transferred these plasmids into *V. cholerae* and assayed the resulting strains for centerline curvature using phase contrast microscopy. In line with a previous report[6], we found that curvature decreased ~3-fold in *crvA* deficient cells, when compared to wild-type *V. cholerae* (Fig. 1a). Over-expression of 20 sRNAs did not render curvature significantly, however, cells overexpressing one sRNA, which we term VadR (a.k.a. Vcr090[20], see below), displayed ~2-fold reduced curvature (Fig. 1a).

The *vadR* gene is located on the plus strand of the smaller *V. cholerae* chromosome between the *vca0002* and *vca0003* genes[20]. The sRNA is present in numerous other *Vibrios* and carries a highly conserved 5' end (Fig. 1b) frequently involved in RNA duplex formation with *trans*-encoded target mRNAs[8,21]. Structure probing experiments confirmed that this region is unstructured and therefore available for base-pairing with other transcripts (Figs. S1a-b). Northern blot analysis revealed that VadR accumulates as a ~85 nt transcript and is most highly expressed at low cell densities (Fig. 1c). Stability of VadR was ~3 min in *V. cholerae* wild-type cells and ~4-fold reduced in cells lacking the *hfq* gene (Fig. S1c). Together, we conclude that VadR is a Hfq-dependent sRNA that is likely to act by base-pairing other transcripts.

Alignment of *vadR* promoter sequences revealed three conserved elements upstream the -10 box (Fig. 1b). While we were unable to directly assign a transcriptional regulator to these elements, we discovered that a *vadR* transcriptional reporter was ~150-fold more active in *V. cholerae* when compared to *Escherichia coli* (Fig. S1d). These results suggested that *vadR* expression depended on a *V. cholerae*-specific factor, which allowed us to perform another genetic screen. Here, we employed a plasmid library expressing ~2.5 kb *V. cholerae* genomic fragments, which we co-transformed with a P*vadR*::*lacZ* transcriptional reporter into *E. coli*. We assayed ~23,000 colonies for ß-galactosidase activity on plates containing X-gal and isolated seven blue colonies. Sequence analysis of the respective plasmids revealed that all mapped to the *vxrABCDE* (*vca0565-0569*) locus; five plasmids contained sequences of *vxrAB* and two plasmids contained sequences of *vxrABCDE* (Fig. S1e). To corroborate these results, we monitored *vadR* production in wild-type and Δ*vxrABCDE V. cholerae* by means of (i) promoter activity measurements and (ii) Northern blot analysis. Indeed, promoter activity was ~50-fold reduced in the *vxrABCDE* mutant (Fig. S1f) and VadR was no longer detectable on Northern blots (Fig. 1d). Successive complementation of the *vxrABCDE* genes from a plasmid revealed that *vxrAB* (constituting the histidine kinase and response regulator of the two component system,

respectively) restored VadR expression, while *vxrCDE* were dispensable for regulation (Fig. 1d). Finally, to pinpoint direct regulation of *vadR* by VxrB, we reanalyzed previously reported ChIP-Seq data[22] for binding of VxrB at the *vadR* promoter. Indeed, we discovered a pronounced, VxrB-specific peak upstream of the *vadR* gene (Fig. S1g). These analyses also revealed a putative VxrB binding motif (TTGACAAAA-N2-TTGAC), which matched the three conserved sequence elements in the *vadR* promoter (Fig. 1b). Deletion of each of these sites efficiently reduced *vadR* promoter activity with sites 2 and 3 being most critical for transcription activation (Fig. S1h). Together, we conclude that VadR is a VxrAB-activated sRNA that modulates cell shape in *V. cholerae*.

To explore the molecular mechanism of VadR-mediated inhibition of cell bending, we next aimed to identify base-pairing partners of VadR *in vivo*. We used RNA-seq analyses to assess changes in global transcriptome levels following transient (15 min) overexpression of *vadR* in a Δ*vadR V. cholerae* strain. In total, 28 mRNAs, including *crvA*, displayed significant changes following VadR expression (Fig. 2a and Table S1). We validated regulation of all targets, except *ibpA*, using quantitative real-time PCR (by testing all monocistronic genes and the first gene of all regulated operons; Fig. S2a). The majority of repressed targets (15) corresponded to a single biofilm gene cluster (*vc0916-vc0939*) required for the production of the VPS biofilm exopolysaccharide, as well as genes producing the auxiliary biofilm components, RbmA-F[23] (Fig. 2b). Gene ontology (GO) analyses revealed a significant overrepresentation of GO terms associated with polysaccharide synthesis in the downregulated targets (Fig. 2c). Indeed, using the wrinkly colony morphology phenotype of *V. cholerae* Δ*hapR* cells as a read-out for biofilm formation[20], we discovered that VadR over-expression resulted in strongly decreased biofilm formation (Fig. 2d). This phenotype was further corroborated by quantitative measurements of biofilm formation in microfluidic flow chambers, analyzed by confocal microscopy (Figs. 2e-h). Detailed analysis of the respective microscopic images revealed that VadR expression resulted in a phenotype mimicking *V. cholerae* cells lacking the *rbmA* gene (Figs. 2e-i). RbmA is required to form higher order structures in *V. cholerae* biofilms and depletion of the protein from the biofilm results in decreased biofilm density[17,24,25]. Indeed, we observed a significant reduction in local biofilm density in cells over-expressing VadR (Figs. 2f, i), which is consistent with reduced RbmA levels determined by quantitative Western blots (Fig. S2b). These results show that in addition to controlling cell shape, VadR also regulates biofilm formation in *V. cholerae*.

To investigate the molecular underpinnings of VadR-mediated gene control in *V. cholerae*, we cloned the 5' UTR (untranslated region) and the TIR (translation initiation region) of the 14 potential VadR targets into a GFP-based reporter plasmid designed to score post-transcriptional control[26]. Co-transformation of these plasmids with a VadR over-

expression vector or a control plasmid in *E. coli* confirmed post-transcriptional repression of nine targets (*crvA*, *irpA*, *rbmA*, *rbmD*, *vpsL*, *vpsU*, *vc2352*, *vca0075*, and *vca0864*), while we were unable to validate direct regulation of *bapI*, *rbmC*, *rbmF*, *rbsD*, and *vca0043* (Figs. 3a and S3a). Using the RNA hybrid algorithm[27], we predicted RNA duplex formations of VadR with *crvA*, *rbmA*, *vpsU*, and *vpsL* (Figs. 3b-e). In all four cases, pairing involved the target's TIR and sequence elements located in the first 30 nucleotides of VadR. Using compensatory base-pair exchange experiments (creating mutants M1, M2, and M3 in *vadR*, see Figs. S1a and S3), we validated binding at the predicted positions (Figs. 3f-i). To bolster these results at the phenotypic level, we tested biofilm formation of Δ*vadR* cells expressing a mutated VadR variant (VadRΔR1, see Figs. S1a and S3b) unable to repress three of the four target genes. In contrast to wild-type VadR (Figs. 2d, f), VadRΔR1 did not affect biofilm formation and architecture in *V. cholerae* (Fig. 2d, g, i).

Given that we confirmed VadR as a direct repressor of *crvA* (Figs. 3b, f), we next aimed to study the role of VadR in cell curvature in *V. cholerae*. Western blot analysis showed CrvA levels were ~1.5-fold elevated in Δ*vadR* cells, whereas VadR over-expression led to a ~2-fold reduction in CrvA production (Fig. 4a). We correlated these results with microscopic curvature analyses of single cells and discovered that *vadR*-deficient mutants displayed increased curvature, whereas plasmid-borne VadR production had the reverse effect (Figs. 4b top and 4c). This effect was further amplified when cells were treated with sub-inhibitory concentrations of cefalexin forcing filamentation in *V. cholerae* (Fig. 4b, bottom). Importantly, neither *vadR* deletion, nor its over-expression affected cell length or volume of *V. cholerae* (Figs. S4a-b), indicating that VadR specifically modulates cell curvature by inhibiting *crvA* expression.

CrvA regulates cell curvature by spatially modulating peptidoglycan insertion in *V. cholerae*[6] and the VxrAB regulon is induced by peptidoglycan-targeting antibiotics such as penicillin G[19]. Consequently, we tested the effect of penicillin G on VadR expression. Indeed, Northern blot analysis showed ~7-fold increased VadR levels in *V. cholerae* wild-type cells following treatment with penicillin G (Fig. 5a) and we observed ~25-fold induction when we tested *vadR* promoter activity using a transcriptional reporter (Fig. 5b). In both cases, penicillin G-dependent activation of *vadR* was abrogated in the Δ*vxrABCDE* strain (Figs. 5a-b). Expression of *vadR* was also activated by the MreB-targeting antibiotic A22[28], albeit to a lower extent when compared to penicillin G (Fig. S5a).

Based on these results, we speculated that resistance towards cell-wall damaging antibiotics requires the remodeling of cell shape-determining components by VxrAB and VadR. Following this hypothesis, we first determined the relationship between CrvA production and penicillin G resistance. To this end, we cloned the inducible pBAD promoter upstream of the chromosomal *crvAB* gene in *V. cholerae* and activated expression for 1.5h

using various concentrations of L-arabinose. Next, we added penicillin G and continued incubation for additional 3 h when we determined survival by counting colony-forming units on agar plates. Indeed, we obtained ~2-fold fewer colony counts at low L-arabinose concentrations (0.0125% final conc.) and up to ~3.5-fold reduced colonies when the promoter was strongly induced (0.05% final conc.) (Fig. S5b). These data indicated that elevated CrvA levels impair penicillin G resistance in *V. cholerae*. In accordance with this observation, we also discovered reduced penicillin G survival rates for *vadR*-deficient *V. cholerae* cells and we were able to complement this phenotype using plasmid-borne VadR production (Fig. 5C). To pinpoint this effect to VadR-mediated repression of *crvA* in the presence of penicillin G, we introduced mutation M1* (Fig. 3b) at the chromosomal *crvA* locus. This mutation keeps *crvA* production intact (Fig. S5c), but renders the transcript immune towards post-transcriptional repression by VadR. This strain phenocopied the effect of a *vadR* mutant. We obtained almost identical results when we introduced the corresponding mutation (M1, Figs. 3b and S1a) at the chromosomal *vadR* gene (Fig. 5C). Combination of the two mutant alleles resulted in a partial restoration of penicillin G resistance (Fig. 5C), supporting our initial hypothesis that VadR is required to mitigate the detrimental effect of CrvA under antibiotic pressure. Notably, neither mutation nor over-expression of *vadR* affected survival of *V. cholerae* under standard growth conditions (Fig. S5d).

To connect the roles of VadR in cell curvature regulation and biofilm formation in *V. cholerae*, we monitored VadR expression (using a P*vadR*::mRuby2 transcriptional reporter) in growing biofilms employing single-cell confocal microscopy analysis[29]. When normalized for sfGFP production driven from the constitutive P_{tac} promoter, we discovered that the *vadR* promoter is most active during the initial phases of biofilm formation, while expression is switched off in mature biofilms (Fig. 6a). In parallel, we also determined cell curvature of individual cells during biofilm development (Fig. 6b). Comparison of the two datasets showed that VadR expression and cell curvature are negatively correlated (Fig. 6c), suggesting that VadR expression results in straighter cells during early phases of biofilm development, whereas mature biofilms are more likely to contain a higher proportion of curved cells.

Given that VadR also controls the production of several mRNAs encoding important biofilm factors such as VPS, RbmA, RbmC and Bap1 (Fig. S2a), it seems possible that VadR also limits the expression of these components in early biofilms (Fig. 6d). Transcription of *vadR* is controlled by the VxrAB system (Fig. 1d), which has been reported to control cell-wall synthesis and repair, biofilm formation, type 6 secretion, and iron homeostasis in *V. cholerae*[18,19,22,30]. In closely related *Vibrio parahaemolyticus*, the VxrAB system (here called VbrKR) has been reported to respond to ß-lactam antibiotics *via* direct

interaction with the histidine kinase, VbrK[31]. Our results support activation of the system by ß-lactam antibiotics, *i.e.* penicillin G (Figs. 5a-b), however, since we also discovered *vadR* activation in the presence of A22 (Fig. S5a) it is likely that additional cues also trigger the system.

Indeed, VadR is readily detectable under standard growth conditions (Fig. 1c) suggesting a regulatory role for the system under non-stress conditions. Here, VadR might take the role of adjusting cell growth with the production of CrvA and biofilm-forming factors (Fig. 6d). CrvA is an abundant periplasmic protein[6] and biofilm components require transport across two membranes to reach their final destination[23]. Uncoordinated export of proteins and polysaccharides can clog the cellular transport machineries and compromise the permeability barrier or structural integrity of the cell[32,33]. It is therefore vital for the cell to synchronize these functions with cell growth and sRNAs have previously been implicated in this process[34]. For example, sRNAs activated by the alternative sigma-factor E promote envelope homeostasis by tuning the levels of newly synthesis outer membrane proteins in response to misfolded proteins in the periplasm[8,21,35,36]. VadR could take an analogous position in the VxrAB stress response system and given the relatively short half-life of VadR (~3min, Fig. S1c), sRNA-based regulation might provide regulatory dynamics that are superior over canonical protein-based regulation[14]. This hypothesis is supported by our finding that VadR directly base-pairs with the mRNAs of the multiple biofilm components (Fig. 3a), rather than acting through a higher-level transcriptional regulator such as VpsT. VpsT activates the transcription of the genes encoding biofilm components in *V. cholerae*[37] and is repressed by the VqmR sRNA, which blocks biofilm formation[20,38]. Therefore, over-expression of VadR or VqmR has similar consequences for biofilm formation in *V. cholerae*, however, the underlying molecular mechanisms differ. Deciphering these differences will allow important conclusions about the biological roles of these sRNAs and their associated pathway, but could also provide a deeper understanding of how sRNAs evolve and select their targets[39].

Our data further showed that besides repressing biofilm formation and cell curvature, VadR also inhibits the expression of *vc2352* (encoding a NupC-type nucleoside transporter[40]), *irpA* (encoding an iron-regulated membrane protein carrying a peptidase domain[41]), *vca0864* (encoding a methyl-accepting chemotaxis protein[42]), and *vca0075*, which has unknown functions[43] (Figs. 3a and 6d). We do not yet understand how these genes fit into the VadR regulon, however, *vca0075* is co-repressed with *cdgA*[20], a diguanylate cyclase gene with documented functions in biofilm formation[44]. In addition, Vca0864 has been reported to inhibit chemotaxis towards N-acetylglucosamine, which is a key component of peptidoglycan[45]. Simultaneous repression of biofilm formation and Vca0864 by VadR could promote cell motility towards N-acetylglucosamine and thereby

replenish the necessary building blocks for peptidoglycan remodeling under conditions of cell-wall stress.

How CrvA affects peptidoglycan remodeling in *V. cholerae* is currently not fully understood. Previous reports revealed that filament-like proteins such as CrvA and CreS render the activity of enzymes involved in cell-wall synthesis and thereby reduce the rate of peptidoglycan insertion at one site of the cell[6,46]. This process results in asymmetric growth and cell curvature, but might also create an "Achilles heel" in the presence of ß-lactam antibiotics or other cell-wall damaging agents. VadR-mediated repression of *crvA* mRNA could help to mitigate this effect by reducing the de-novo production of CrvA protein.

METHODS

Bacterial strains and growth conditions

Bacterial strains used in this study are listed in Supplementary Table S2. Details for strain construction are provided in the Supplementary Material and Methods section. *V. cholerae* and *E. coli* cells were grown under aerobic conditions (200rpm, 37°C) in LB (Lenox). Where appropriate, media were supplemented with antibiotics at the following concentrations: 100 µg / ml ampicillin; 20 µg / ml chloramphenicol; 50 µg / ml kanamycin; 50 U / ml polymyxin B; 5 mg / ml streptomycin, 5 µg / ml cefalexin.

Plasmids and DNA oligonucleotides

All plasmids and DNA oligonucleotides used in this study are listed in Supplementary Tables S3 and S4, respectively. Cloning details are provided in the Supplementary Material and Methods section.

RNA isolation and Northern blot analysis

Total RNA was prepared and blotted as described previously[47]. Membranes (GE Healthcare Amersham) were hybridized with [^{32}P] labelled DNA oligonucleotides at 42°C. Signals were visualized using a Typhoon phosphorimager (GE Healthcare) and quantified using Gelquant software (biochemlabsolutions).

Microscopy analysis

Samples for microscopy analyses were prepared by growing the respective *V. cholerae* strains in LB to OD_{600} of 0.4. Cells were pelleted, washed in 1xPBS, and finally resuspended in 2.5% paraformaldehyde in 1xPBS. Phase contrast imaging was performed on a Zeiss Axio Imager M1 microscope equipped with EC Plan Neofluar 100x/ 1.3 Oil Ph3 objective (Zeiss). For additional magnification a 2.5 x optovar was used. Image acquisition was conducted with the AxioVision software-package (Zeiss). For further analysis, e.g. measurements of cell center line curvature, cell length and cell are, the FIJI-plugin MicrobeJ was used[48,49].

Flow chamber biofilms and confocal imaging

The strains were grown in LB medium supplemented with 50 µg/mL kanamycin, to mid-exponential growth phase, before introducing into microfluidic flow chambers. Flow chambers were constructed from poly(dimethylsiloxane) bonded to glass coverslips using an oxygen plasma. The microfluidic channels measured 500 µm in width, 100 µm in height and 7 mm in length. After the cultures were introduced into the channels, the channels were incubated at 24°C for 1 h without any flow, to allow cells to attach to the bottom glass surface of the channels. The flow was then set to 0.3 µl/min for approximately 18 h before images were acquired. Cells were stained with green fluorescent nucleic acid stain dye, SYTO 9 (Thermo Fisher Scientific), by exchanging the syringes containing LB with SYTO 9 for 30 min. Flow rates were controlled using a high-precision syringe pump (Pico Plus, Harvard Apparatus). To acquire the spatiotemporal information of individual cells in a growing biofilm, time lapse confocal microscopy was performed as described previously[50]. To reduce photobleaching and phototoxicity during time-lapse imaging, a live feedback between image acquisition, image analysis and microscope control was used to automatically detect the biofilm height to avoid imaging of empty space on top of the biofilms. Images were acquired with an Olympus 100x objective with numerical aperture of 1.35, using a Yokogawa spinning disk confocal scanner and laser excitation at 488 nm. Images were acquired at spatial resolution of 63 nm in the xy plane and 400 nm along the z direction. To detect all single cells, measure cell curvature of each cell, and quantify the relative *vadR* promoter-reporter strength from biofilm grown in flow chambers, biofilm images were analysed with the BiofilmQ software available from the Drescher Lab[51]. Kymograph heatmaps showing the strength of *vadR* promoter and cell curvature during biofilm growth were generated with BiofilmQ. 3-D cell rendering was done using BiofilmQ-analysed biofilm data using the ParaView software[52]. Biofilm images were prepared with the NIS-Elements AR Analysis software (Nikon) by cropping a fixed z-plane with xy and yz projections.

RNA-seq analysis

Biological triplicates of *V. cholerae* Δ*vadR* strains harboring pBAD-Ctr or pBAD-*vadR* plasmids were grown to exponential phase (OD_{600} of 0.2) in LB media. sRNA expression was induced by addition of L-arabinose (0.2% final conc.). After 10 min of induction, cells were harvested by addition of 0.2 volumes of stop mix (95% ethanol, 5% (v/v) phenol) and snap-frozen in liquid nitrogen. Total RNA was isolated and digested with Turbo DNase (Thermo Fischer Scientific). Ribosomal RNA was depleted using Ribo-Zero kits (Epicentre) for Gram-negative bacteria, and RNA integrity was confirmed using a Bioanalyzer (Agilent). Directional cDNA libraries were prepared using the NEBNext Ultra II Directional RNA Library Prep Kit for Illumina (NEB, #E7760). The libraries were sequenced using a HiSeq

1500 system in single-read mode for 100 cycles. The read files in FASTQ format were imported into CLC Genomics Workbench v11 (Qiagen) and trimmed for quality and 3' adaptors. Reads were mapped to the *V. cholerae* reference genome (NCBI accession numbers: NC_002505.1 and NC_002506.1) using the "RNA-Seq Analysis" tool with default parameters. Reads mapping to annotated coding sequences were counted, normalized (CPM) and transformed (log_2). Differential expression between the conditions was tested using the "Empirical Analysis of DGE" command. Genes with a fold change ≥ 1.75 and an FDR adjusted p-value ≤ 1E-3 were defined as differentially expressed.

Fluorescence measurements

Fluorescence assays to measure GFP expression were performed as described previously[26]. *E. coli* strains expressing translational GFP-based reporter fusions were grown for 16h in LB medium and resuspended in 1xPBS. Fluorescence intensity was quantified using a Spark 10M plate reader (Tecan). *V. cholerae* and *E. coli* strains carrying mKate2 transcriptional reporters were grown in LB medium, resuspended in 1xPBS, samples were collected at the indicated time points and mKate2 fluorescence was measured using a Spark 10M plate reader (Tecan). Control samples not expressing fluorescent proteins were used to subtract background fluorescence.

Western blot analysis

Experiments were performed as previously described[47]. If not stated otherwise, 0.075 OD / lane were separated using SDS-PAGE and transferred to PVDF membranes for Western blot analysis. 3xFLAG-tagged fusions were detected using anti-FLAG antibody (Sigma, #F1804). RnaPα served as a loading control and was detected using anti-RnaPα antibody (BioLegend, #WP003). Signals were visualized using a Fusion FX EDGE imager (Vilber) and band intensities were quantified using BIO-1D software tools (Vilber).

ß-galactosidase reporter assays

A plasmid library, expressing *V. cholerae* genomic fragments[53], was screened for activation of *vadR* promotor (P*vadR*) activity. To this end, *lacZ*-deficient *E. coli* BW25113 strains, harboring pNP-122, were transformed with pZach library plasmids. Transformants were selected on LB plates, containing the respective antibiotics and 20 µg / ml 5-Brom-4-chlor-3-indoxyl-β-D-galactopyranosid (X-gal). 23,000 colonies (representing ~11-fold coverage) were monitored for ß-galactosidase activity. Obtained hits were validated for ß-galactosidase activity as described previously, with modifications[54]. Briefly, *E. coli* BW25113 strains harboring the pZ genomic fragment expression plasmids and pNP-122 were grown to OD_{600} of 1.5 in LB. Cells were resuspended in Z-buffer to yield 1.0 OD_{600} / ml. Cells were lysed by addition of 75 µl chloroform and 50 µl 0.1 % SDS and vortexing. Lysates were centrifuged (16.000 x g, 5 min) and the resulting supernatant treated with O-Nitrophenyl-β-

D-galactopyranoside (ONPG). The reactions were stopped by addition of sodium carbonate (Na_2CO_3). The specific activities were obtained by measuring absorbance at OD_{420}, OD_{550}, and OD_{600} using a Spark 10M plate reader (Tecan). ß-galactosidase activity was deduced from the values by calculating Miller units.

Sequence alignments

VadR and its promoter sequences among various *Vibrio* species were aligned using the MultAlin webtool[55]. Vch: *Vibrio cholerae* (NCBI:txid243277), Vmi: *Vibrio mimicus* (NCBI:txid1267896), Van: *Vibrio anguillarum* (NCBI:txid55601), Vqi: *Vibrio qinghaiensis* (NCBI:txid2025808), Vfu: *Vibrio furnissii* (NCBI:txid29494), Vfl: *Vibrio fluvialis* (NCBI:txid676), Vme: *Vibrio mediterranei* (NCBI:txid689), Vvu: *Vibrio vulnificus* (NCBI:txid672), Val: *Vibrio alginolyticus* (NCBI:txid663), Vpa: *Vibrio parahaemolyticus* (NCBI:txid670).

Statistical analyses

Statistical parameters for the respective experiment are indicated in the corresponding figure legends. *n* represents the number of biological replicates. Details for the performed statistical tests are provided in the supporting information. Statistical analyses of CFUs were performed as follows: The data were log10-transformed and tested for normality and equal variance using Kolmogorov–Smirnov and Brown–Forsythe tests, respectively. The data were tested for significant differences using one-way ANOVA and post hoc Holm-Sidak tests. Significance levels are reported in the in the supporting information. Statistical analysis was performed using SigmaPlot v14 (Systat). No blinding or randomization was used in the experiments. No estimation of statistical power was used before performing the experiments, and no data were excluded from analysis.

DATA AVAILABILITY

The raw data of the transcriptome analyses are available at the National Center for Biotechnology Information Gene Expression Omnibus (GEO) under the accession number GSE145764.

CODE AVAILABILITY

The biofilm image analysis software tool BiofilmQ[51] is available online (https://drescherlab.org/data/biofilmQ/).

ACKNOWLEDGMENTS

We thank Helmut Blum for help with the RNA sequencing experiments and Andreas Starick, Hannah Jeckel, and Konstantin Neuhaus for excellent technical support. We thank Gisela Storz, Zemer Gitai, and Jörg Vogel for comments on the manuscript and all members of the Papenfort lab for insightful discussions and suggestions. This work was supported by the

DFG (TRR174/P5 and P15 and EXC2051- ID390713860), the Human Frontier Science Program (CDA00024/2016-C), and the European Research Council (StG-758212 and StG-716734) and the Max Planck Society. RH acknowledges support by the Joachim Herz Foundation.

AUTHOR CONTRIBUTIONS

RH, NP, KSF, PKS, MB, KD, and KP designed the experiments; RH, NP, PKS, LS, and KSF performed the experiments; RH, NP, PKS, KSF, FM, KD and K.P. analyzed data; and KP wrote the manuscript with the help of all authors.

COMPETING INTERESTS

The authors declare no competing financial interests.

REFERENCES

1. Taylor, J.A., Sichel, S.R. & Salama, N.R. Bent Bacteria: A Comparison of Cell Shape Mechanisms in Proteobacteria. *Annu Rev Microbiol* **73**, 457-480 (2019).
2. Cabeen, M.T. & Jacobs-Wagner, C. The bacterial cytoskeleton. *Annu Rev Genet* **44**, 365-92 (2010).
3. Wagstaff, J. & Lowe, J. Prokaryotic cytoskeletons: protein filaments organizing small cells. *Nat Rev Microbiol* **16**, 187-201 (2018).
4. Govindarajan, S. & Amster-Choder, O. Where are things inside a bacterial cell? *Curr Opin Microbiol* **33**, 83-90 (2016).
5. Ausmees, N., Kuhn, J.R. & Jacobs-Wagner, C. The Bacterial Cytoskeleton: An Intermediate Filament-Like Function in Cell Shape. *Cell* **115**, 705-713 (2003).
6. Bartlett, T.M. et al. A Periplasmic Polymer Curves Vibrio cholerae and Promotes Pathogenesis. *Cell* **168**, 172-185.e15 (2017).
7. Altinoglu, I., Merrifield, C.J. & Yamaichi, Y. Single molecule super-resolution imaging of bacterial cell pole proteins with high-throughput quantitative analysis pipeline. *Sci Rep* **9**, 6680 (2019).
8. Peschek, N., Hoyos, M., Herzog, R., Forstner, K.U. & Papenfort, K. A conserved RNA seed-pairing domain directs small RNA-mediated stress resistance in enterobacteria. *EMBO J* **38**, e101650 (2019).
9. Herzog, R., Peschek, N., Frohlich, K.S., Schumacher, K. & Papenfort, K. Three autoinducer molecules act in concert to control virulence gene expression in Vibrio cholerae. *Nucleic Acids Res* **47**, 3171-3183 (2019).
10. Davies, B.W., Bogard, R.W., Young, T.S. & Mekalanos, J.J. Coordinated regulation of accessory genetic elements produces cyclic di-nucleotides for V. cholerae virulence. *Cell* **149**, 358-70 (2012).
11. Bradley, E.S., Bodi, K., Ismail, A.M. & Camilli, A. A genome-wide approach to discovery of small RNAs involved in regulation of virulence in Vibrio cholerae. *PLoS Pathog* **7**, e1002126 (2011).
12. Kavita, K., de Mets, F. & Gottesman, S. New aspects of RNA-based regulation by Hfq and its partner sRNAs. *Curr Opin Microbiol* **42**, 53-61 (2018).
13. Gorski, S.A., Vogel, J. & Doudna, J.A. RNA-based recognition and targeting: sowing the seeds of specificity. *Nat Rev Mol Cell Biol* **18**, 215-228 (2017).
14. Hor, J., Gorski, S.A. & Vogel, J. Bacterial RNA Biology on a Genome Scale. *Mol Cell* **70**, 785-799 (2018).
15. Waters, L.S. & Storz, G. Regulatory RNAs in bacteria. *Cell* **136**, 615-28 (2009).
16. Wagner, E.G.H. & Romby, P. Small RNAs in bacteria and archaea: who they are, what they do, and how they do it. *Adv Genet* **90**, 133-208 (2015).

17. Fong, J.C. et al. Structural dynamics of RbmA governs plasticity of Vibrio cholerae biofilms. *Elife* **6**(2017).
18. Cheng, A.T., Ottemann, K.M. & Yildiz, F.H. Vibrio cholerae Response Regulator VxrB Controls Colonization and Regulates the Type VI Secretion System. *PLoS Pathog* **11**, e1004933 (2015).
19. Dörr, T. et al. A cell wall damage response mediated by a sensor kinase/response regulator pair enables beta-lactam tolerance. *Proceedings of the National Academy of Sciences of the United States of America* **113**, 404-409 (2016).
20. Papenfort, K., Forstner, K.U., Cong, J.P., Sharma, C.M. & Bassler, B.L. Differential RNA-seq of Vibrio cholerae identifies the VqmR small RNA as a regulator of biofilm formation. *Proc Natl Acad Sci U S A* **112**, E766-75 (2015).
21. Papenfort, K., Bouvier, M., Mika, F., Sharma, C.M. & Vogel, J. Evidence for an autonomous 5' target recognition domain in an Hfq-associated small RNA. *Proc Natl Acad Sci U S A* **107**, 20435-40 (2010).
22. Shin, J.-H. et al. A multifaceted cellular damage repair and prevention pathway promotes high level tolerance to β-lactam antibiotics. *bioRxiv*, 777375 (2019).
23. Teschler, J.K. et al. Living in the matrix: assembly and control of Vibrio cholerae biofilms. *Nat Rev Microbiol* **13**, 255-68 (2015).
24. Drescher, K. et al. Architectural transitions in Vibrio cholerae biofilms at single-cell resolution. *Proceedings of the National Academy of Sciences of the United States of America* **113**, E2066-E2072 (2016).
25. Yan, J., Sharo, A.G., Stone, H.A., Wingreen, N.S. & Bassler, B.L. Vibrio cholerae biofilm growth program and architecture revealed by single-cell live imaging. *Proc Natl Acad Sci U S A* **113**, E5337-43 (2016).
26. Corcoran, C.P. et al. Superfolder GFP reporters validate diverse new mRNA targets of the classic porin regulator, MicF RNA. *Mol Microbiol* **84**, 428-45 (2012).
27. Rehmsmeier, M., Steffen, P., Hochsmann, M. & Giegerich, R. Fast and effective prediction of microRNA/target duplexes. *RNA* **10**, 1507-17 (2004).
28. Gitai, Z., Dye, N.A., Reisenauer, A., Wachi, M. & Shapiro, L. MreB actin-mediated segregation of a specific region of a bacterial chromosome. *Cell* **120**, 329-41 (2005).
29. Hartmann, R. et al. Emergence of three-dimensional order and structure in growing biofilms. *Nat Phys* **15**, 251-256 (2019).
30. Teschler, J.K., Cheng, A.T. & Yildiz, F.H. The Two-Component Signal Transduction System VxrAB Positively Regulates Vibrio cholerae Biofilm Formation. *Journal of Bacteriology* **199**, 1-16 (2017).
31. Li, L. et al. Sensor histidine kinase is a beta-lactam receptor and induces resistance to beta-lactam antibiotics. *Proc Natl Acad Sci U S A* **113**, 1648-53 (2016).
32. Typas, A., Banzhaf, M., Gross, C.A. & Vollmer, W. From the regulation of peptidoglycan synthesis to bacterial growth and morphology. *Nat Rev Microbiol* **10**, 123-36 (2011).
33. Mitchell, A.M. & Silhavy, T.J. Envelope stress responses: balancing damage repair and toxicity. *Nat Rev Microbiol* **17**, 417-428 (2019).
34. Papenfort, K., Espinosa, E., Casadesus, J. & Vogel, J. Small RNA-based feedforward loop with AND-gate logic regulates extrachromosomal DNA transfer in Salmonella. *Proc Natl Acad Sci U S A* **112**, E4772-81 (2015).
35. Gogol, E.B., Rhodius, V.A., Papenfort, K., Vogel, J. & Gross, C.A. Small RNAs endow a transcriptional activator with essential repressor functions for single-tier control of a global stress regulon. *Proc Natl Acad Sci U S A* **108**, 12875-80 (2011).
36. Thompson, K.M., Rhodius, V.A. & Gottesman, S. SigmaE regulates and is regulated by a small RNA in Escherichia coli. *J Bacteriol* **189**, 4243-56 (2007).
37. Casper-Lindley, C. & Yildiz, F.H. VpsT is a transcriptional regulator required for expression of vps biosynthesis genes and the development of rugose colonial morphology in Vibrio cholerae O1 El Tor. *J Bacteriol* **186**, 1574-8 (2004).

38. Papenfort, K. et al. A Vibrio cholerae autoinducer-receptor pair that controls biofilm formation. *Nat Chem Biol* **13**, 551-557 (2017).
39. Updegrove, T.B., Shabalina, S.A. & Storz, G. How do base-pairing small RNAs evolve? *FEMS Microbiol Rev* **39**, 379-91 (2015).
40. Gumpenberger, T. et al. Nucleoside uptake in Vibrio cholerae and its role in the transition fitness from host to environment. *Mol Microbiol* **99**, 470-83 (2016).
41. Davies, B.W., Bogard, R.W. & Mekalanos, J.J. Mapping the regulon of Vibrio cholerae ferric uptake regulator expands its known network of gene regulation. *Proc Natl Acad Sci U S A* **108**, 12467-72 (2011).
42. Boin, M.A., Austin, M.J. & Häse, C.C. Chemotaxis in Vibrio cholerae. *FEMS Microbiology Letters* **239**, 1-8 (2004).
43. Heidelberg, J.F. et al. DNA sequence of both chromosomes of the cholera pathogen Vibrio cholerae. *Nature* **406**, 477-83 (2000).
44. Lim, B., Beyhan, S., Meir, J. & Yildiz, F.H. Cyclic-diGMP signal transduction systems in Vibrio cholerae: modulation of rugosity and biofilm formation. *Mol Microbiol* **60**, 331-48 (2006).
45. Minato, Y. et al. Roles of the sodium-translocating NADH:quinone oxidoreductase (Na+-NQR) on vibrio cholerae metabolism, motility and osmotic stress resistance. *PLoS One* **9**, e97083 (2014).
46. Cabeen, M.T. et al. Bacterial cell curvature through mechanical control of cell growth. *EMBO J* **28**, 1208-19 (2009).
47. Frohlich, K.S., Haneke, K., Papenfort, K. & Vogel, J. The target spectrum of SdsR small RNA in Salmonella. *Nucleic Acids Res* **44**, 10406-10422 (2016).
48. Schindelin, J. et al. Fiji: an open-source platform for biological-image analysis. *Nat Methods* **9**, 676-82 (2012).
49. Ducret, A., Quardokus, E.M. & Brun, Y.V. MicrobeJ, a tool for high throughput bacterial cell detection and quantitative analysis. *Nat Microbiol* **1**, 16077 (2016).
50. Singh, P.K. et al. Vibrio cholerae Combines Individual and Collective Sensing to Trigger Biofilm Dispersal. *Curr Biol* **27**, 3359-3366 e7 (2017).
51. Hartmann, R. et al. BiofilmQ, a software tool for quantitative image analysis of microbial biofilm communities. 735423 (2019).
52. Ayachit, U. *The ParaView Guide: A Parallel Visualization Application*, (Kitware, Inc., 2015).
53. Donnell, Z. Regulation of cqsA and cqsS in Vibrio cholerae. (Princeton, NJ : Princeton University, 2015).
54. Frohlich, K.S., Papenfort, K., Berger, A.A. & Vogel, J. A conserved RpoS-dependent small RNA controls the synthesis of major porin OmpD. *Nucleic Acids Res* **40**, 3623-40 (2012).
55. Corpet, F. Multiple sequence alignment with hierarchical clustering. *Nucleic Acids Res* **16**, 10881-90 (1988).
56. Ashburner, M. et al. Gene ontology: tool for the unification of biology. The Gene Ontology Consortium. *Nat Genet* **25**, 25-9 (2000).

FIGURES

Figure 1

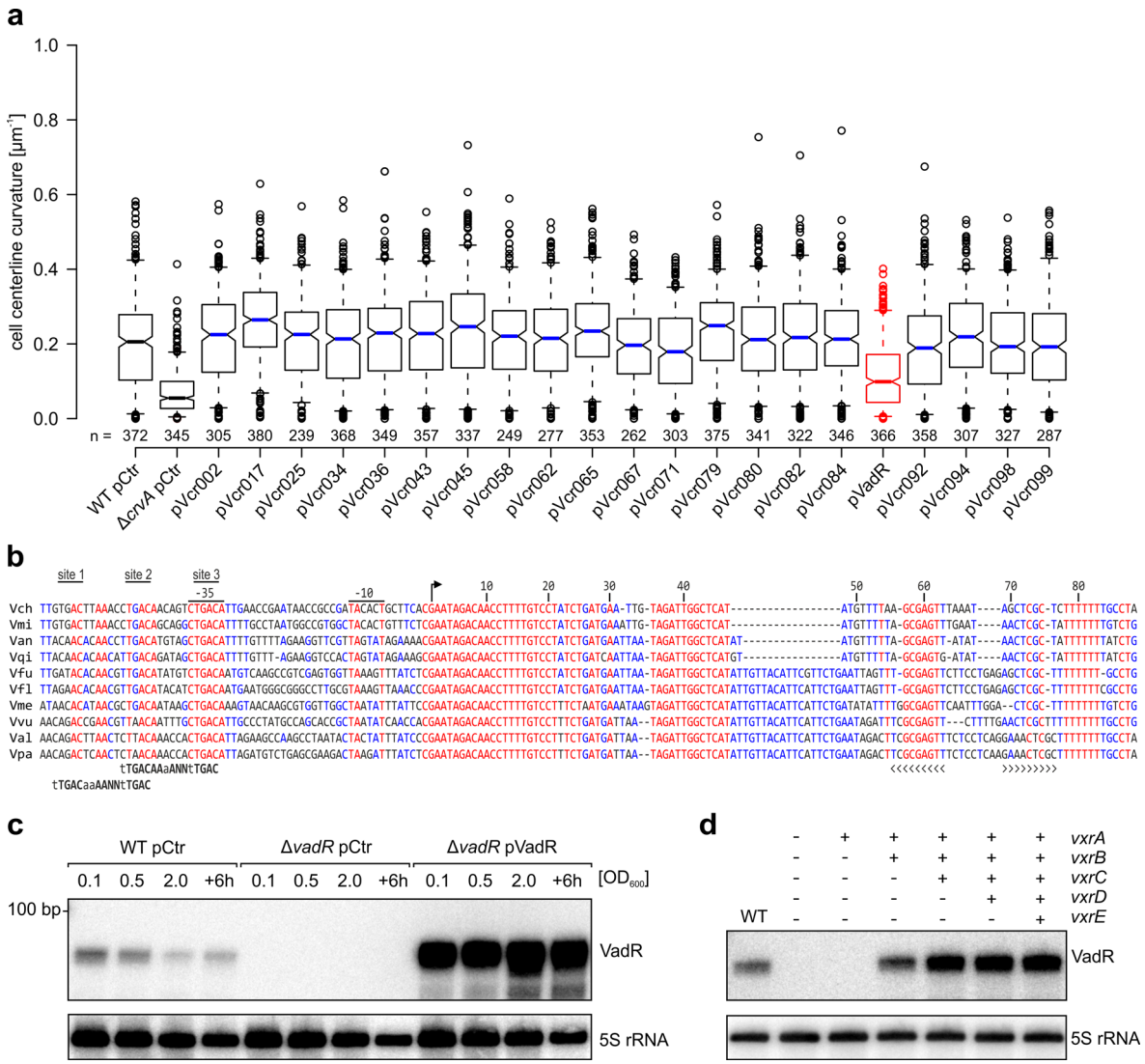

Figure 1: The VadR sRNA alters *V. cholerae* cell shape and is transcribed by VxrB
(a) Centerline curvature of *V. cholerae* cells expressing the indicated sRNAs (x-axis). The blue line indicates the median, boxes represent 25th and 75th percentiles, whiskers represent 5th and 95th percentiles and notches indicate 95% confidence intervals for each median. *n* of each set is listed above the x-axis. **(b)** Alignment of *vadR* and its promoter sequence from various *Vibrio* species. The -35 box, -10 box, TSS (arrow) and the Rho-independent terminator (brackets) are indicated. Putative VxrB binding sites and binding motifs (bold) are illustrated. **(c)** VadR expression throughout bacterial growth was tracked on Northern blots. *V. cholerae* wild-type or *vadR* mutant cells carrying either a control plasmid (pCtr) or a constitutive *vadR* overexpression plasmid (pVadR) were tested. **(d)** *V. cholerae* Δ*vxrABCDE* cells were complemented with various cistrons of the *vxrABCDE* operon and tested for VadR expression on Northern blots. Expression of the *vxrABCDE* fragments was driven by the inducible pBAD promoter (0.02 % L-arabinose final conc.) and exponentially growing cells were harvested (OD_{600} of 0.2). A *V. cholerae* strain wild-type harboring an empty vector served as control. The experiment was performed with three independent biological replicates (*n* = 3).

Figure 2

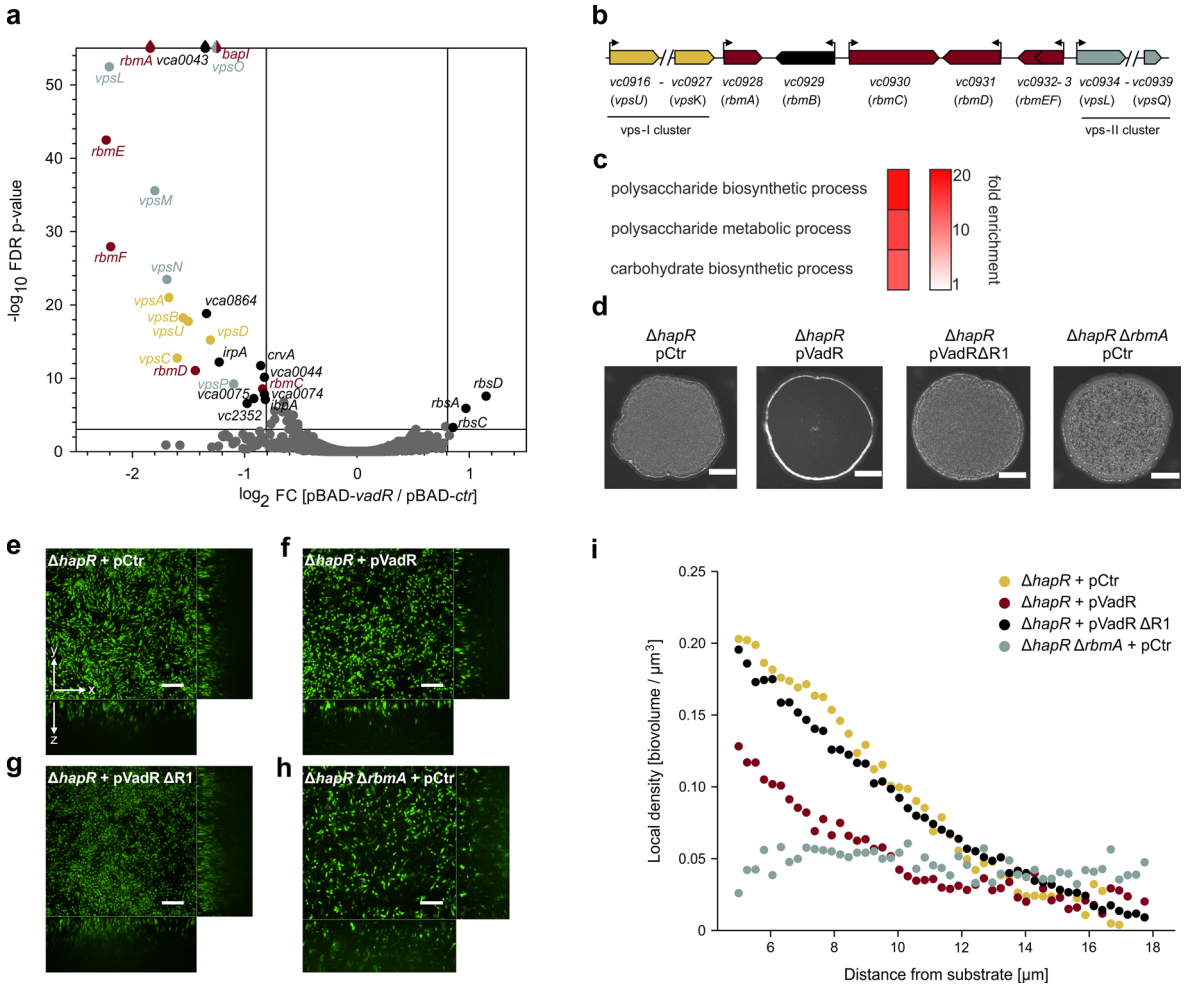

Figure 2: Target spectrum of VadR and its role in biofilm formation

(a) Volcano plot analysis showing differentially regulated genes after pulse induction of VadR. Genes with absolute fold changes ≥ 1.75 and an FDR corrected p-value of ≤ 0.001 were considered significantly expressed and are indicated. **(b)** Genomic context of the major biofilm cluster in *V. cholerae*. **(c)** Gene enrichment analysis of the differentially expressed genes shown in (a) using [56]. **(d)** Colony biofilm images of *V. cholerae* Δ*hapR* cells carrying the indicated plasmids. 5 µl of each strain were spotted on a LB agar plates and incubated for 24h at room temperature before imaging. **(e-h)** Confocal Spin Disk Microscope images of biofilms (grown for 18 h) formed by *V. cholerae* Δ*hapR* cells carrying the following plasmids: (e) control plasmid, (f) *vadR* overexpression, (g) *vadR* ΔR1 overexpression. (h) A Δ*hapR*/Δ*rbmA* mutant harboring a control plasmid was used for comparison. The central images show bottom-up views, and the flanking images show vertical optical sections. Scale bars = 10 µm. (i) Local cell density as a function of distance from the substratum was plotted for each of the indicated strains using the BiofilmQ software[51].

Figure 3

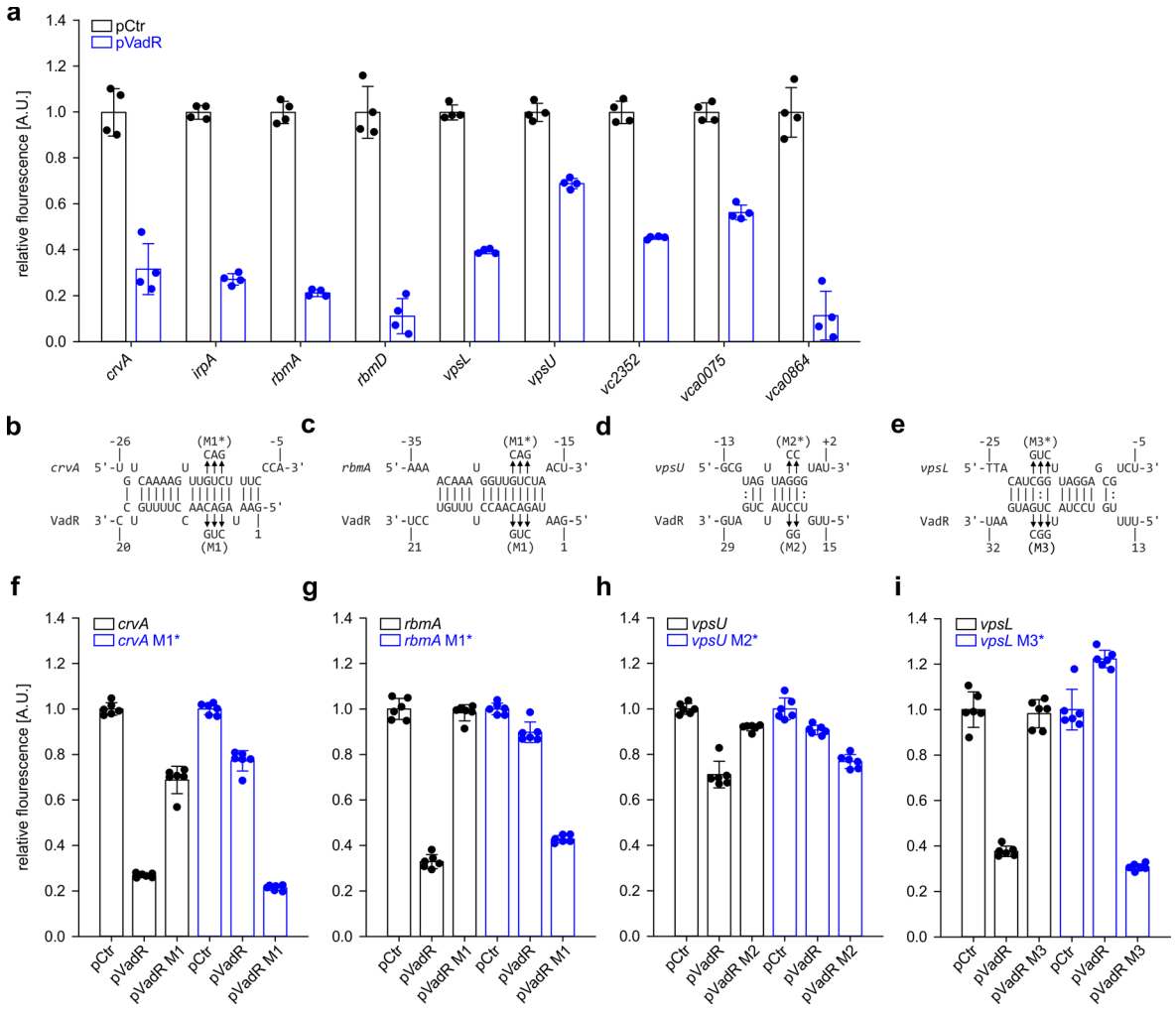

Figure 3: VadR is a direct inhibitor of *crvA* and key biofilm transcripts
(a) Genes post-transcriptionally regulated by VadR. Fluorescence intensities of *E. coli* strains carrying the gene-specific reporters and the control plasmid (pCtr) were set to 1. Bars show mean of biological replicates ± SD, *n* = 4. **(b-e)** Prediction of RNA duplex formation between selected mRNAs and VadR. Numbers indicate the distances from the TSS for VadR and the start codons of the target mRNA sequences, respectively. Arrows indicate the mutations tested in (f-i). **(f-i)** Validation of the predicted mRNA-sRNA duplexes shown in (b-e) using compensatory base-pair mutations. Fluorescence levels of *E. coli* strains harboring an empty vector control (pCtr) were set to 1. Bars show mean of biological replicates ± SD, *n* = 6.

Figure 4

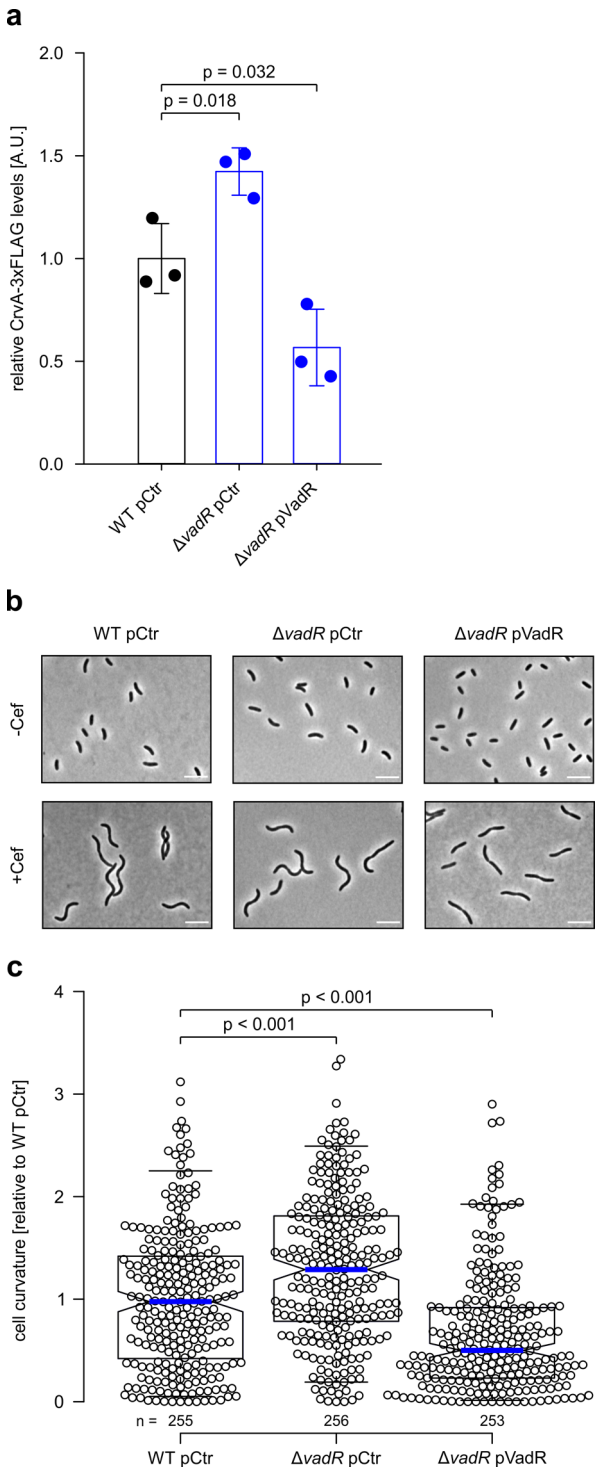

Figure 4: VadR modulates *V. cholerae* curvature by repressing CrvA

(a) Quantification of CrvA-3xFLAG protein levels in *V. cholerae* wild-type and *vadR*-deficient cells. Total protein samples of the indicated strains were harvested (OD_{600} of 0.5) and tested by Western blot analysis. CrvA-3xFLAG protein levels detected in the wild-type cells were set to 1. Bars show mean of biological replicates ± SD, *n* = 3. Statistical significance was determined using one-way ANOVA and post-hoc Holm-Sidak test. **(b)** Microscopy of cells used in (a; –Cef). A second set of cells was treated with cefalexin for 1h (+Cef) after reaching an OD_{600} of 0.5. Shown are representative fields of vision. Scale bars = 5 µm. **(c)** Analysis of cell centerline curvature in –Cef samples of (b). The curvature mean of wild-type cells was set to 1. A blue line indicates the median, boxes represent 25th and 75th percentiles, whiskers represent 5th and 95th percentiles and notches indicate 95%

confidence intervals for each median. *n* of each set is listed above the x-axis. Statistical significance was determined using Kruskal-Wallis test and post-hoc Dunn's test.

Figure 5

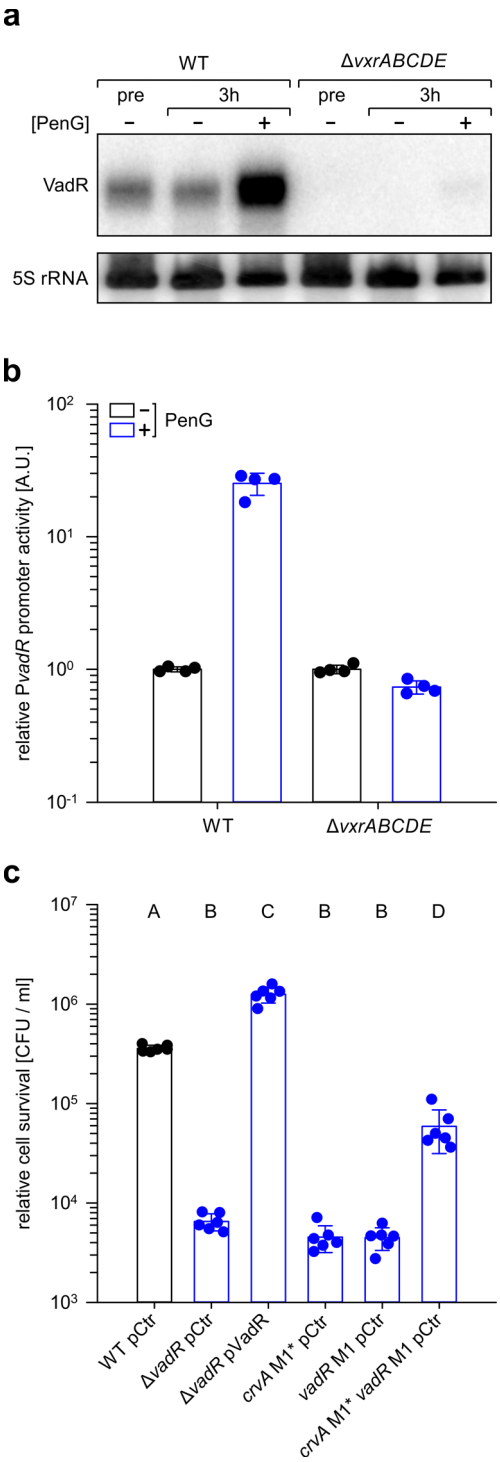

Figure 5: VadR mediates ß-lactam resistance through repression of CrvA
(a) *V. cholerae* wild-type and *vxrABCDE* mutant strains were grown to OD = 0.2 (pre) and split into two sets. One set was treated with penicillin G, while the other set received a mock treatment. After 3h, RNA was isolated and VadR expression was monitored by Northern analysis. **(b)** VadR promoter activity was tested under the same conditions as in (a) using a fluorescent transcriptional reporter. Promoter activities of mock-treated strains were set to 1. Bars represent mean of biological replicates ± SD, *n* = 4. **(c)** The indicated *V. cholerae* strains (x-axis) were grown to OD_{600} = 0.4 and treated with Penicillin G for 3h. Survival after treatment was determined by counting colony forming units (CFUs). Bars represent mean of biological replicates ± SD, *n* = 6. Statistical significance was determined

using one-way ANOVA and post-hoc Holm-Sidak test. Significantly different groups ($p < 0.01$) are labelled with corresponding letters.

Figure 6

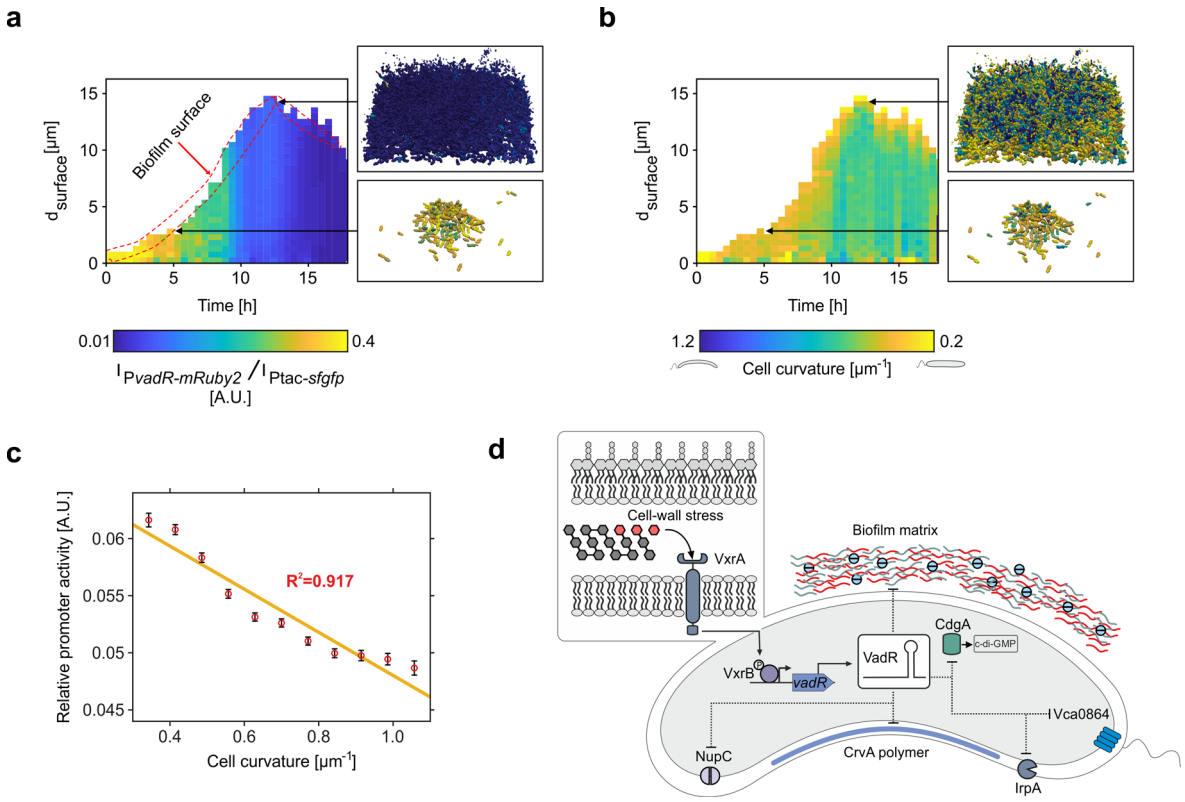

Figure 6: VadR controls cell curvature during biofilm development

(a) Relative activity of the *vadR* promoter during biofilm growth of *V. cholerae*. In each cell the fluorescence of mRuby2, expressed from the *vadR* promoter was normalized by the signal of the constitutive Ptac-promoter-driven sfGFP-fluorescence signal. Heatmap shows *vadR* promoter activity at both spatial (distance from surface of biofilm representing height of the biofilm) and temporal (time of biofilm growth) resolution. Subset of images show the cells from two time points and separate locations of the biofilm. These cells were rendered by ParaView[51] after final segmentation and analysis using BiofilmQ[51]. The color of each cell represents the activity of the *vadR* promoter. **(b)** Spatio-temporal heatmap showing cell curvature of each cell for *V. cholerae* biofilms. Cell curvature was calculated as cell convexity parameter from BiofilmQ. Lower cell convexity (0.5) reflects highly curved cells and higher cell convexity (1) indicates straight cells. To show the cell curvature of individual cell inside the biofilms, similar positions of the biofilm as in (a) subset of images were selected for rendering. In these subsets of images, the color represents the cell curvature of each cell. **(c)** A correlation graph was plotted for *vadR* promoter activity as function of cell curvature. Calculation of *vadR* promoter activity and cell curvature was done for *V. cholerae* wild-type biofilms grown in flow chambers. Each point represents >1000 cells for given time point in a biofilm. The error bars for each point correspond to the standard error. **(d)** Model showing the regulatory functions of the VadR sRNA in *V. cholerae*. Expression of *vadR* sRNA is controlled by the VxrAB two-component system. The sRNA regulates multiple biological processes, including cell shape and biofilm formation.

Chapter 4: Three autoinducer molecules act in concert to control virulence gene expression in *Vibrio cholerae*

Herzog R, Peschek N, Fröhlich KS, Schumacher K, Papenfort K, Three autoinducer molecules act in concert to control virulence gene expression in *Vibrio cholerae*. ***Nucleic Acids Res.***, Volume 47, Issue 6, 08 April 2019, doi: 10.1093/nar/gky1320

The full-text article is available online at:
https://academic.oup.com/nar/article/47/6/3171/5289484

The supplementary material is available online at:
https://academic.oup.com/nar/article/47/6/3171/5289484#supplementary-data

Chapter 5: Concluding discussion

Parts of this chapter have been adapted from:

Chapter 2: Peschek N, Hoyos M, Herzog R, Förstner KU, Papenfort K, A conserved RNA seed-pairing domain directs small RNA-mediated stress resistance in enterobacteria. ***EMBO J***, Volume 38, Issue 16, 15 August 2019, doi: 10.15252/embj.2019101650

Chapter 3: Herzog R*, Peschek N*, Singh PK, Fröhlich KS, Schröger L, Meyer F, Bramkamp M, Drescher K, Papenfort K, RNA-mediated control of cell shape modulates antibiotic resistance in *Vibrio cholerae*. **Manuscript**

Chapter 4: Herzog R, Peschek N, Fröhlich KS, Schumacher K, Papenfort K, Three autoinducer molecules act in concert to control virulence gene expression in *Vibrio cholerae*. ***Nucleic Acids Res.***, Volume 47, Issue 6, 08 April 2019, doi: 10.1093/nar/gky1320

* authors contributed equally

5.1 Functional characterization of sRNAs in *V. cholerae*

Bacteria thrive in a plethora of different habitats, due to their ability to quickly adjust to their surrounding environments. To this end, bacteria need to sense environmental cues and initiate adequate responses to rapidly adapt their gene expression profiles (122). Gene expression is controlled by a wide variety of transcription factors, regulating transcription initiation, and sRNAs, acting at the post-transcriptional level (Chapter 1.2). In *S. typhimurium* and *E. coli,* sRNA-mediated regulation of gene expression is wide-spread, and more than 100 sRNAs are expressed in these model organisms (90, 178). While initial screens estimated the presence of more than 500 sRNAs in *V. cholerae* (182), a recent dRNA-seq approach identified 107 putative sRNA candidates and verified the expression 32 sRNAs (46). Despite of this abundance of post-transcriptional regulators in *V. cholerae*, only few of them have been experimentally studied (Fig. 5.1, Table 5.1).

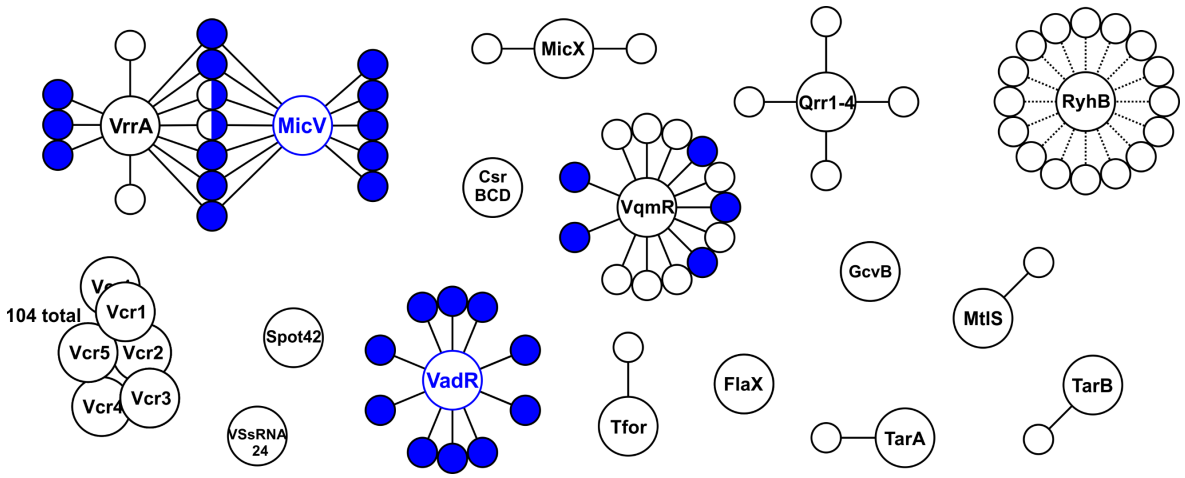

Figure 5.1: Overview of the sRNA regulatory landscape of *V. cholerae*: Depicted are all described sRNAs and experimentally validated sRNA-mRNA interactions of *V. cholerae*. Contributions made in the present work are highlighted in blue. Previously identified sRNAs and sRNA-mRNA interactions have been adapted from: (44, 45, 183–192, 46, 193–196, 64, 142, 144–146, 168, 169).

The present work substantially contributed to a better understanding of the sRNA regulatory landscape in *V. cholerae* (Fig. 5.1). First, we identified the MicV (formerly Vcr089) sRNA, as a new member of the σ^E-regulon in *V. cholerae* (Chapter 2, Appendix Table S1, Figs. 1, EV1). Furthermore, RNA-seq analyses combined with post-transcriptional reporter assays and mutational analyses, revealed that MicV controls expression of 28 genes, organized in 13 transcriptional units. Additionally, the present work expanded the known regulon of the related VrrA sRNA, by identifying 9 new mRNA targets (Chapter 2, Appendix Table S2, Appendix Figs. S2, Fig. 2). Second, we found that the VadR (formerly Vcr090) sRNA is activated by the VxrAB two-component system (Chapter 3, Figs. 1D, S1) and

controls the expression of 10 mRNA targets (Chapter 3, Figs. 2A, 3, S2A). Third, we identified 5 additional targets for the VqmR (formerly Vcr107) sRNA, including *aphA*, encoding the master regulator of low-cell density functions (Chapter 4, Table 1, Fig. 2).

Furthermore, the sRNA-mRNA interactions identified in this work allow us to propose likely mechanisms of mRNA target regulation by sRNAs in *V. cholerae*. Predictions of sRNA-mRNA duplex formation (Chapters 2-4) allows us to propose that the majority of sRNAs in *V. cholerae* base-pair to a region within -35 to +19 nucleotides from the AUG start codon (49 out of 58 described interactions) (Table 5.1, (50, 51, 197)). These data indicate that regulation of a majority of mRNA targets is achieved by ribosomal occlusion (34, 53) and potentially coupled degradation of sRNA-mRNA duplexes (56). In contrast to that, sRNA interactions within the 5'UTR, but outside the RBS window, are rare (3 out of 58 described interactions) (Table 5.1). While base-pairing of the Qrr1-4 sRNAs within the 5'UTR of *aphA* has been described to result in activation of *aphA* translation by an anti-antisense mechanism (168, 169), we observed negative regulation for the MicV-*btuB* (Chapter 2, Fig. 2D) and VqmR-*ndk* interactions (Chapter 4, Fig. 2B). Interestingly, those interactions occur within a few nts of the RBS window (Table 5.1, Chapter 2, Appendix Fig. S3), and it would be interesting to use toeprinting analyses to test whether these interactions result in ribosomal occlusion (197), or if another mechanism is involved. For instance, in *S. typhimurium* the GcvB sRNA inhibits translation of the *gltI* mRNA, by base-pairing to a translational enhancer element, located -57 to -47 nts from the start codon (59). Intriguingly, the present work identified the first interactions of sRNAs deep within the CDS of target mRNAs in *V. cholerae* (6 out of 58 described interactions) (Table 5.1, Chapter 2, Appendix Fig. S3). While it is currently unclear how target regulation is achieved in those cases, the MicC sRNA has been reported to regulate expression of the *ompD* mRNA in *S. typhimurium* by base-pairing to a region deep in the CDS (+67 to +78 nts from the start codon). In this case, regulation of *ompD* is not achieved by inhibiting translation initiation, but by accelerating RNase E-mediated transcript decay (60). Such a mechanism would require the presence of RNase E-sites in the corresponding region of the transcripts, but it is currently unclear if RNase E-sites are associated to those transcripts. However, recent approaches employing TIER-seq (Transiently inactivating an endoribonuclease followed by RNA-seq), have successfully mapped RNAse E-sites on a transcriptome scale in *S. typhimurium* (198). It would be interesting to use a similar approach in *V. cholerae* to test for the presence of RNase E-sites, located close to the predicted base-pairing regions, and to confirm the predicted mechanism of target regulation.

Table 5.1: Overview of sRNA-mRNA interactions in *V. cholerae*: Depicted are validated sRNA-mRNA interactions with predicted or validated base-pairing interactions. Nucleotide positions of sRNAs involved in base-pairing are depicted with respect to the corresponding TSSs, and nucleotide positions of mRNAs are depicted with respect to the AUG start codons. The interaction regions have been classified with respect to the region occluded by the 30S ribosomal subunit: -35 - +19 nt from the AUG start codon (50, 51, 197). n.a. = not available.

sRNA	mRNA	sRNA region	mRNA region	classification	seed-region	reference
MicV	*ompT*	2 - 17	-7 - -22	RBS	R1	Chapter 2
MicV	*vca0951*	10 - 18	-5 - -13	RBS	R1	Chapter 2
MicV	*rpoE*	5 - 19	-41 - -29	RBS	R1	Chapter 2
MicV	*vc1563*	1 - 9	+48 - +58	CDS	R1	Chapter 2
MicV	*dsbD*	1 - 10	+59 - +72	CDS	R1	Chapter 2
MicV	*vc1485*	1 - 16	-19 - -5	RBS	R1	Chapter 2
MicV	*ompA*	1 - 14	+2 - +16	RBS	R1	Chapter 2
MicV	*bamD*	1 - 18	-3 - +10	RBS	R1	Chapter 2
MicV	*prvT*	1 - 9	-11 - -1	RBS	R1	Chapter 2
MicV	*btuB*	1 - 8	-47 - -34	5'UTR	R1	Chapter 2
MicV	*ushA*	1 - 10	-34 - -19	RBS	R1	Chapter 2
MicV	*ompU*	1 - 8	+67 - +73	CDS	R1	Chapter 2
MicV	*oppA*	1 - 9	+48 - +55	CDS	R1	Chapter 2
MicX	*vc0620*	259 - 293	-18 - +4	RBS	n.a.	(192)
MtlS	*mtlA*	1 - 70	-75 - -5	RBS	n.a.	(44, 45)
Qrr1-4	*hapR*	diff. in Qrr1-4	-35 - -5	RBS	n.a.	(64)
Qrr1-4	*aphA*	diff. in Qrr1-4	-147 - -120	5‘UTR	n.a.	(168, 169)
Qrr1-4	*luxO*	diff. in Qrr1-4	-23 - -3	RBS	n.a.	(169)
Qrr1-4	*vc0939*	diff. in Qrr1-4	-23 - 38	RBS	n.a.	(185)
TarA	*ptsG*	9 - 28	-3- +24	RBS	n.a.	(187)
TarB	*tcpF*	12 - 43	-22 - +8	RBS	n.a.	(188)
TfoR	*tfoX*	2 - 59	-51 - -2	RBS	n.a.	(189–191)
VadR	*vpsU*	18 - 26	-10 - -2	RBS	R2	Chapter 3
VadR	*rbmA*	4 - 18	-32 - -18	RBS	R1	Chapter 3
VadR	*rbmD*	1 - 23	-33 - -15	RBS	R1	Chapter 3
VadR	*vpsL*	16 - 29	-22 - -2	RBS	R1	Chapter 3
VadR	*crvA*	1 - 19	-25 - -2	RBS	R1	Chapter 3
VadR	*vca0864*	1 - 15	-11 - +13	RBS	R1	Chapter 3
VadR	*irpA*	1 - 21	-10 - +18	RBS	R1	Chapter 3
VadR	*vc2352*	24 - 36	-1 - +14	RBS	R2	Chapter 3
VadR	*vca0075*	15 - 25	-24 - -13	RBS	R1	Chapter 3
VqmR	*vca0068*	76 - 91	-15 - +3	RBS	R2	(46)
VqmR	*vc0200*	76 - 91	-16 - +3	RBS	R2	(46)
VqmR	*vc1063*	54 - 67	-14 - +5	RBS	R1	(46)
VqmR	*vpsT*	74 - 99	-22 - +5	RBS	R2	(46)
VqmR	*vc1865*	93 - 113	-9 - +11	RBS	R2	(46)
VqmR	*vc1449*	75 - 95	-24 - +3	RBS	R1	(46)
VqmR	*vca0917*	84 - 99	-17 - -8	RBS	R2	(46)
VqmR	*vca0591*	76 - 90	-11 - +3	RBS	R2	(46)
VqmR	*ulaA*	93 - 104	+8 - +20	RBS	R2	Chapter 4
VqmR	*vc0865*	80 - 102	-27 - -2	RBS	R2	Chapter 4

sRNA	mRNA	sRNA region	mRNA region	classification	seed-region	reference
VqmR	*ndk*	62 - 72	-57 - -33	5'UTR	R1	Chapter 4
VqmR	*vc0789*	58 - 71	-19 - -2	RBS	R1	Chapter 4
VqmR	*aphA*	131 - 143	-13 - -1	RBS	R3	Chapter 4
VrrA	*ompT*	69 - 83	-21 - -2	RBS	R1	Chapter 2, (144)
VrrA	*vca0951*	57 - 83	-11 - +13	RBS	R1	Chapter 2
VrrA	*rpoE*	71 - 80	-38 - -23	RBS	R1	Chapter 2
VrrA	*vc1563*	64 - 75	+48 - +57	CDS	R1	Chapter 2
VrrA	*dsbD*	61 - 72	+60 - +72	CDS	R1	Chapter 2
VrrA	*vc1485*	69 - 82	-19 - -5	RBS	R1	Chapter 2
VrrA	*ompA*	64 - 86	-14 - +21	RBS	R1	Chapter 2, (142)
VrrA	*bamD*	72 - 79	+3 - +10	RBS	R1	Chapter 2
VrrA	*pal*	93 - 102	-11 - -2	RBS	R2	Chapter 2
VrrA	*lpp*	90 - 107	-21 - -5	RBS	R2	Chapter 2
VrrA	*acfA*	91 - 106	-25 - -6	RBS	R2	Chapter 2
VrrA	*tcpA*	70 - 106	-25 - +19	RBS	R2	(142)
VrrA	*rbmC*	91- 106	-25 - -8	RBS	R2	(146)
VrrA	*vrp*	72 - 84	-15 - -3	RBS	R1	(145)

5.2 Bacterial stress response systems are a hotspot for sRNA-mediated regulation

5.2.1 The MicV and VrrA sRNAs act as the non-coding arm of the σ^E-stress response in *V. cholerae*

An interesting feature of sRNAs are their dynamic expression profiles, observed even during batch culture conditions in the laboratory. In many cases, sRNA expression profiles correlated with corresponding binding to the RNA-Chaperone Hfq (90). Intriguingly, in *E. coli* a majority of sRNAs have been described to show highest expression levels in stationary phase of bacterial growth (100, 103), and Hfq levels have been reported to increase by two-fold under stationary phase conditions (199). Entry into stationary phase growth conditions presents a drastic change in environmental conditions, for instance due to nutrient limitation and accumulation of metabolic waste products. Consequently, adaptation to stationary phase growth conditions includes the activation of several stress response systems and changes in gene expression to embark on strategies for persistence in harsh environments (155). Interestingly, the induction of sRNA expression in stationary phase correlates with the observed changes in gene expression, indicating the potential activation of sRNA expression by alternative sigma factors or stress response systems (100). Similar observations have been made in *V. cholerae*. For instance, Papenfort *et al*. probed the expression patterns of putative sRNAs and found increased expression levels

in stationary phase for 23 out of 32 sRNAs (46).

Intriguingly, the MicV and VrrA sRNAs have been reported to be expressed specifically in stationary phase of bacterial growth (46, 142), which was confirmed in the present study (Chapter 2, Fig. EV1). Additionally, the present study provides evidence that the *micV* and *vrrA* promoters are strongly activated in stationary phase (Chapter to, Figs. 1, EV1). Entry into stationary phase of bacterial growth has been reported previously as an inducing condition to activate the σ^E-stress response (200), and indeed the present work showed direct activation of both sRNA promoters by the alternative sigma factor σ^E (Chapter 2, Appendix Table S1, Figs. 1, EV1). Furthermore, the *micV* promoter responded dynamically to ectopic *rpoE* overexpression (Chapter 2, Fig. EV1F). Together, these data suggested high expression levels of both sRNAs under σ^E-inducing conditions. Similar observations have been made for the σ^E-dependent promoters of *E. coli*. Mutalik *et al*., performed genome wide, *in vivo* analyses of σ^E-dependent promoters in *E. coli* and found that the promoters driving expression of the σ^E-dependent sRNAs RybB and MicA are ranked among the strongest in the σ^E-regulon (201). Consequently, the conservation of σ^E-dependent sRNAs in Enterobacteria (141) (Chapter 2, Fig. 1A, Fig. EV1A), and high expression levels during envelope stress conditions point to a crucial role in the σ^E-regulon. Indeed, the present study showed reduced cell survival of *V. cholerae* under envelope stress conditions in absence of σ^E-dependent sRNAs (Chapter 2, Fig. 1F) and increased survival of strains lacking *rpoE* and overexpressing the σ^E-dependent sRNAs (Chapter 2, Fig. 4C). Increased protection from lysis during σ^E shutoff was also previously reported for the RybB and MicA sRNAs (140).

The important role of σ^E-dependent sRNA during envelope stress became evident by analyses of their respective target profiles. The σ^E stress response is activated by accumulation of misfolded OMPs, and misfolded OMPs in the periplasm have been reported to insert into the inner membrane, disrupt the proton motif force and potentially cause cell death (127). Rapid downregulation of stable *omp* mRNAs upon σ^E-activation presents an obvious solution to restore envelope homeostasis and has been previously observed in *E. coli* (137). However, sigma factors are restricted to act as transcriptional activators (28). An elegant solution to this problem would be to employ post-transcriptional regulators as indirect, negative regulators in the regulon (140, 202). Indeed, the RybB and MicA sRNAs have been identified to be the responsible for downregulating the expression of all major OMPs in *E. coli*, and related enterobacteria (115, 140, 141). For instance, the half-life of the *ompA* mRNA has been reported to be ~15 min (203), and is reduced to ~5 min upon *rpoE* induction (137), or ~3 min after pulse-induction of *rybB* (115). In the present work, we made similar observations and could show that *ompT*, *ushA*, and *lpp* mRNA levels are rapidly reduced after pulse-induction of *rpoE*. Importantly, the observed reduction of mRNA half-

life was dependent on the presence of the VrrA and MicV sRNAs (Chapter 2, Fig. 3G-I).

The mRNA target profiles of MicA and RybB have been reported to include all major OMPs and several other transcripts of *E. coli,* and related enterobacteria (115, 140). In addition to that, the σ^E-dependent sRNA MicL has been reported to control expression of *lpp* (139). Furthermore, it has been reported that RybB controls expression of 16 mRNA targets, MicA controls expression of 9 mRNA targets, and 6 mRNA targets, including *ompA* and *lamB,* have been reported to be regulated by both sRNAs (140) (Fig. 5.2). Similar to the observed targets of RybB and MicA, we found that the mRNA targets of the MicV and VrrA sRNAs in *V. cholerae* include all major OMPs and the *rpoE-rseABC* operon (Chapter 2. Fig. 2, Appendix Table S2, Appendix Fig. S2). Interestingly, previous studies found increased mRNA levels of the *rpoE-rseABC* operon in *V. cholerae hfq* mutants (68) and a RIL-seq approach in *E. coli* suggested that the MicL sRNA base-pairs to *rpoE-rseABC* mRNA (120), indicating that autorepression of the *rpoE* operon by sRNAs could be a conserved feature to further modulate the envelope stress in many bacteria. Intriguingly, the strongest promoter in the σ^E-regulon of *E. coli* has been reported to be the one driving expression of *rpoE* (201), and we identified a σ^E-motif in the promoter of *rpoE* in *V. cholerae* (Chapter 2, Appendix Table S1). Autorepression of their associated transcription factor by sRNAs has been reported before (202), and in this case might create an important feedback-circuit in which the MicV and VrrA sRNAs can modulate their own expression and the output of the σ^E-stress response. In agreement with this hypothesis, we found increased σ^E-activity in cells lacking the MicV and VrrA sRNAs (Chapter 2, Appendix Fig. S1C). Furthermore, we found that MicV and VrrA down-regulate expression of the *bamD* gene (Chapter 2, Fig. 2). BamD is part of the BAM (ß-barrel assembly machinery) complex, that has been reported to be responsible for integrating OMPs into the outer membrane (204). In *E. coli*, *bamD* is encoded by the *yfiO* gene and depletion of YfiO has been shown to reduce OMP levels (205). Thus, the regulation of BamD synthesis by MicV and VrrA, suggests the presence of another mechanism to relieve envelope stress, by reducing the amount of OMPs that get transported to the outer membrane under envelope stress conditions.

In contrast to RybB and MicA, we found that the majority of mRNA targets are co-regulated by both MicV and VrrA (Fig. 5.2). We identified 5 unique mRNA targets for MicV, 3 unique mRNA targets for VrrA, and 8 transcription units containing 23 genes for both sRNAs, suggesting functional redundancy for the regulation of most targets (Chapter 2, Fig. 2, Appendix Fig. S2).

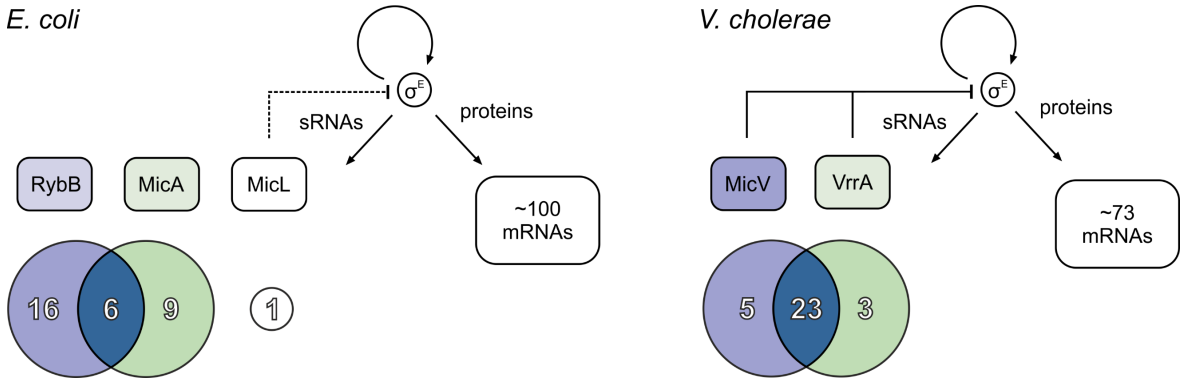

Figure 5.2: Comparison of the non-coding arms of the σ^E-response of *E. coli* and *V. cholerae*: In *E. coli,* σ^E activates the expression of ~100 mRNAs, the three sRNAs RybB, MicA, and MicL, as well as its own expression. RybB and MicA control expression of 31 mRNAs, and collectively regulate the expression 6 mRNAs. MicL controls expression of a single target, *lpp*, and might regulate expression of the *rpoE-rseABC* operon. In *V. cholerae*, the present work predicted σ^E to activate the expression of ~73 mRNAs, the MicV and VrrA sRNAs, as well as its own expression. MicV and VrrA control expression of 31 genes, however the majority of mRNAs are jointly regulated by both sRNAs. Both, MicV and VrrA, directly control expression of the *rpoE-rseABC* operon. The data for *E. coli* has been obtained from: (120, 140) and the data for *V. cholerae* from Chapter 2, respectively.

5.2.2 On the role of sRNA redundancy

Functional redundancy, *i.e.* co-regulation of the expression of a single mRNA by multiple sRNAs, has been observed in numerous studies (180). Recent studies have probed global sRNA-target interactions using RIL-seq and found several mRNAs to interact with multiple sRNAs (120). The most prominent example is presented in the regulation of OMPs by multiple sRNAs (141). For instance, the *ompA* mRNA has been reported to interact with the MicA (73, 115, 138), RybB (115, 140), and RseX (206) sRNAs in *E. coli*. In the present study we found that the MicV and VrrA sRNAs jointly control expression of 8 transcriptional units, encoding several OMPs (Chapter 2, Fig. 2, Appendix Fig. S2, Appendix Table S2). Interestingly, we observed differences in the potency of regulation of several targets by either MicV or VrrA. For instance, MicV appeared to be a stronger repressor of *ompT* and *rpoE*, while VrrA repressed *ompA* and *bamD* more efficiently (Chapter 2, Fig. 2C, Appendix Table S2). A likely explanation for this observation might be differences in sRNA stability (Chapter 2, Fig. EV1D) or different strength of regulation due to energetically more or less favorable base-pairing to the corresponding target (Chapter 2, Appendix Fig. S3).

The reason for the regulation of OMPs by multiple sRNAs is unclear, but it might be important to achieve saturated regulation for very abundant mRNAs (207). Indeed, *omp* mRNAs have been reported to be very stable and highly abundant (203). In line with this observation, we found increased *ompT* mRNA (N. Peschek, unpublished results) and increased OmpT protein levels under stationary phase growth conditions, when compared to exponential phase growth conditions (Chapter 2, Appendix Fig. S2B). Thus, the regulation by multiple sRNAs might be required to achieve rapid shut-off of translation under envelope stress conditions. Interestingly, we observed no difference in the decay of the

ompT mRNA after *rpoE* pulse induction in absence of *micV* or *vrrA* alone. However, the decay was attenuated if both sRNAs were absent (Chapter 2, Fig. 3G). Similar to that, we found a maximal increase of OmpT protein levels in *micV*, *vrrA* double mutants (Chapter 2, Appendix Fig. S1B). Curiously, *vrrA* mutation did not result in changed OmpT protein levels (Chapter 2, Appendix Fig. S1B), and differences in σ^E activity, while the *micV*, *vrrA* double mutants displayed increased σ^E activity (Chapter 2, Appendix Fig. S1C). In contrast to that, we found that only *vrrA* or *vrrA*, *micV* double mutants showed increased survival upon induction of envelope stress by exposure to ethanol (Chapter 2, Fig. 1F). Together these data suggest, that MicV and VrrA serve specialized functions in the envelope stress response, *i.e.* VrrA mediates resistance to ethanol stress conditions, and MicV is the more important regulator under stationary phase growth conditions.

A likely explanation for the observed co-regulation of multiple mRNA targets by MicV and VrrA is the presence of a conserved seed-region in both sRNAs (Chapter 2, Fig. 4A). Indeed, mutation of this conserved seed-region resulted in a loss of *ompT* regulation (Chapter 2, Figs. 3A, 3D), and base-pairing predictions of co-regulated targets with both sRNAs suggested energetically favorable base-pairing to occur with this seed-region (Chapter 2, Appendix Fig. S3). In the same line of thought, base-pairing of MicV to its unique targets involves the 2 nucleotides at the very 5'end, that are not conserved in the *vrrA* sequence (Chapter 2, Figs. 1A, 2A, 3D, E, 4A, Appendix Fig. S3). Indeed, seed-regions have been reported to mediate very selective base-pairing. For instance, the SgrS sRNA in *S. typhimurium* has been reported to discriminate between the *sopD* and the horizontally acquired *sopD2* mRNA through a single nucleotide (208). Likewise, VrrA unique targets are regulated by a second seed-region, that is not present in MicV (Chapter 2, Figs. EV2A, 3C, F, Appendix Fig. S3). Intriguingly, the shared seed-region is also conserved in the functional homologous sRNA RybB of *E. coli* and related bacteria (Chapter 2, Fig. 4A). Furthermore, RybB functionally repressed OmpT protein synthesis in *V. cholerae* (Chapter 2, Fig. 4B), *vice versa* MicV and VrrA reduced OmpC and OmpA levels in *E. coli* (Chapter 2, Fig. 4C), and overexpression of each sRNAs recovered cell survival of *rpoE* deficient *V. cholerae* after ethanol treatment (Chapter 2, Fig. 4D). Together, these data suggest that multiple functionally analogous, σ^E-dependent sRNAs carry conserved seed-regions to mediate OMP repression and mitigate envelope stress in many bacteria.

The present work therefore has important implications for the "core sRNA" concept. "Core sRNAs" are largely conserved in many Enterobacteria and perform similar functions (209). While the overall sequences of the σ^E-dependent sRNAs of *E. coli* and *V. cholerae* are not conserved, we provide evidence that they can functionally classified by their conserved seed sequences and physiological analogous function.

5.2.3 Implications for sRNA evolution

The present work addresses several questions related to how sRNAs evolve in the context of enterobacterial stress responses. Expression of the MicV and VrrA sRNAs is activated by the same sigma factor, and both sRNAs regulate OMP expression (Chapter 2, Figs. 1, 2). These features are conserved with the functionally analogous σ^E-dependent sRNAs of *E. coli* (115, 140). However, albeit the highly conserved seed-region, we observed limited sequence homology between those sRNAs (Fig. 5.3). Furthermore, sRNAs sizes differ between *rybB*, *micA*, *micL*, *vrrA*, and *micV*. Additionally, the chromosomal locations of these sRNAs are not conserved between *E. coli* and *V. cholerae*. The *micV* gene is located in the intergenic region of *vc2640* (encoding a hypothetical protein) and *vc2641* (encoding argininosuccinate lyase) (Chapter 2, Fig. EV1A) and the *vrrA* gene is located in the intergenic region of *vc1741* (encoding a putative TetR family transcriptional regulator) and *vc1743* (encoding a hypothetical protein) (142). In *E. coli*, the *rybB* gene is located in the intergenic region of *rcdA* (encoding a TetR family transcriptional regulator, ~20% amino acid identity to *vc1741*) and *ybjL* (encoding a putative transport protein), the *micA* gene is located in the intergenic region of *luxS* (encoding a S-ribosylhomocysteine lyase) and *gshA* (encoding a glutamate-cysteine ligase), and the *micL* gene is located at the 3' end of the of the *cutC* gene (139), but no sRNA transcription has been associated with the *V. cholerae cutC* homolog, *vc0730* (46). Remarkably, the OMP composition of *V. cholerae* and *E. coli* is also different. In *E. coli* the most abundant OMPs are OmpC and OmpF (210), while in *V. cholerae* OmpT and OmpU are most abundant (211). Despite limited sequence identity (<20%), OmpU/T and OmpF/C have been reported to be functional analogs (212) and are regulated by the functional analogous sRNAs RybB, MicA (140) and MicV, VrrA (Chapter 2, Fig. 2(142)). It is interesting to speculate whether the σ^E-dependent sRNAs of *E. coli* and *V. cholerae* present an example of convergent evolution or derived from a common ancestor sRNA.

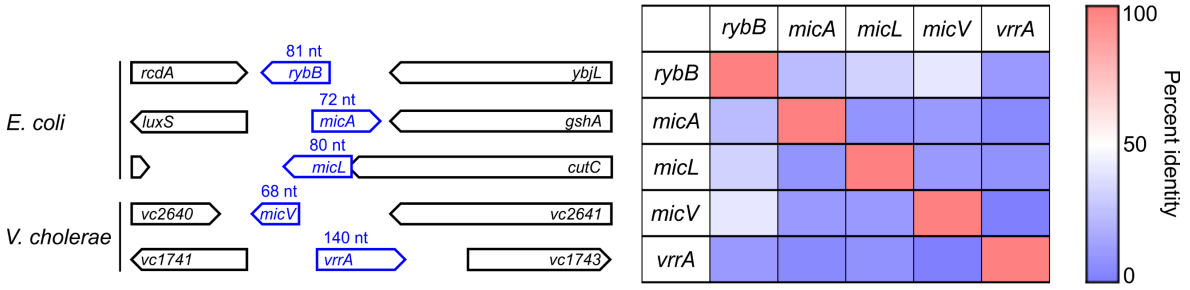

Figure 5.3: Overview of the functionally analogous σ^E-dependent sRNAs of *E. coli* and *V. cholerae*: Comparison of genomic location and size of the *rybB*, *micA*, *micL*, *micV*, and *vrrA* sRNAs (left side) as well as sequence identity scores (right side).

Importantly, the present work provides further evidence on how σ^E-dependent sRNAs base-pairing to target mRNAs evolves in the framework of the envelope stress response. To address this, we employed *E. coli* RybB as a scaffold and randomized the nucleotide sequence of the first nine nucleotides (Chapter 2, Fig. 5A). Deletion of the first nine nucleotides in *rybB* has been reported previously to abolish regulation of all target *omp* mRNAs (49), and also prevented recovery under ethanol stress conditions in *V. cholerae* (Chapter 2, Fig. EV4D). Our laboratory selection experiments revealed successful enrichment of variants, that mediated ethanol resistance (Chapter 2, Fig. 4). Sequence analyses of the 15 most abundant variants revealed an enrichment of GC-rich sequences in the seed regions (Chapter 2, Figs. EV5A, B), which might be required to mediate specific base-pairing (213). Furthermore, we found that the conserved seed-pairing motif of σ^E-dependent sRNAs was recovered in high numbers after consecutive rounds of ethanol treatment (Chapter 2, Fig. 5, Figs EV4, EV5A). Curiously, several other sequence variants were also recovered, and sufficiently mediated ethanol resistance (Chapter 2, Figs. EV4, EV5A, B). Base-pairing to multiple mRNA targets is thought to constrain sRNA evolution (161), and in line with this thought, we expected selection for fewer motifs to accommodate the regulatory capacity for regulation of multiple *omp* mRNAs in the limited size of the seed-region. On the other hand, regulation of a single mRNA target could be established by base-pairing to different sites in the target and thus result in an increased number of successful motifs (Chapter 1.2.1). Interestingly, we found that the 15 most abundant sequence variants all mediated resistance to ethanol treatment by downregulation of a single mRNA - *ompA* (Chapter 2, Fig. 6, Fig. EV5). Furthermore, the 15 variants showed preferential base-pairing to a single stranded region, involving mainly the first six codons, of *ompA* (Chapter 2, Fig. EV5). Intriguingly, we showed that the same region is targeted by the MicV and VrrA sRNAs (Chapter 2, Fig. EV5C, Appendix Fig. S3 (142)). In general, this matches with the observation that sRNA preferentially interact within a window of -35 to +19 nucleotides, with respect to the AUG start codon, in the target mRNA to interfere with 30S ribosome binding (50, 51, 197). Since the *ompA* leader sequence is mostly AU-rich, sRNA-pairing to the more GC-rich coding sequence might have resulted in more robust base-pairing and preferential binding to this region (Chapter 2, Fig. EV5C). Together, these data provide further evidence that evolution of sRNA-mRNA target pairs is dynamic and dependent on the availability of suitable base-pairing regions in target mRNAs.

Intriguingly, while all misfolded OMPs can induce the σ^E-stress response, specific OMPs have been reported to play specialized roles in mediating resistance to different compounds, or vary in strength of induction of the σ^E-stress response (131, 214). For instance, deletion of *ompU* has been reported to suppress the essentiality of σ^E in *V. cholerae* by an unknown mechanism (215). Furthermore, OmpU has been reported to

protect *V. cholerae* from bile salts, *i.e.* deoxycholate, encountered during colonization of the intestine (216–218). A likely explanation for this observation is that OmpU has an inhibitory effect on OmpT, and OmpT likely functions as channel for deoxycholate (212). In the present work, we found that regulation of a single OMP - OmpA - was sufficient to mediate resistance to ethanol stress conditions (Chapter 2, Fig. 6, Fig. EV5). Intriguingly, Zhang *et al*. performed analyses of the outer membrane proteome of *E. coli* cells treated with low amounts of ethanol (~3%), and found that deletion of *ompA* resulted in reduced intracellular ethanol levels, suggesting that OmpA is a channel for the uptake of ethanol (219). Our results support this hypothesis and the function of OmpA as a channel for ethanol might well explain the protective effect of the synthetic RybB variants under ethanol stress (Chapter 2, Figs. 5B, 6, Fig. EV5C-E). It is interesting to speculate what sequence variants and mRNA targets might be selected for under stress conditions induced with different compounds, *i.e.* deoxycholate, combinations of compounds, or in infection models and to test if the necessary regulation of multiple targets would lock a specific seed-region.

5.2.5 The VadR sRNA controls cell shape and biofilm formation in response to cell wall damage

In addition to the above-mentioned alternative sigma factors, bacteria frequently employ two-component systems (TCS) to respond to specific environmental stressors. These regulatory systems consist of a sensor histidine kinase and a cognate response regulator (220). Binding of a specific signal by the sensor kinase induces phosphorylation of the response regulator, which can activate or repress transcription of associated promoters to mediate adaptation (220). *V. cholerae* is predicted to encode 43 sensor histidine kinases and 52 response regulators (159) to monitor the environment for a diversity of signals (221). One of these systems was recently studied in detail and is referred to as VxrAB (159) (a.k.a WigKR (158)). The VxrAB two component system is specific to *Vibrios* and has been reported to respond to treatment with ß-lactam antibiotics, such as penicillins, and to control various processes, including biofilm formation, type VI secretion, virulence, peptidoglycan synthesis, and iron transport (158–160, 222). The related bacterium *Vibrio parahaemolyticus* encodes a *vxrAB* homolog called *vbrKR*, and Li *et al.* showed direct and specific sensing of ß-lactam antibiotics by the VbrK sensor kinase *in vitro* (223). However, it is unclear where in their life-cycle *Vibrios* might encounter ß-lactam antibiotics, since those are predominantly associated to soil-inhabiting microorganisms (224).

In the present work we found that the VxrAB system activates the expression of the VadR sRNA (Chapter 3, Figs. 1D, S1). In agreement with previous reports (158), we validated that *vadR* expression is induced by treatment with the ß-lactam antibiotic penicillin G, in a process that is dependent on the presence of *vxrAB* (Chapter 3, Figs. 5A, B).

However, in contrast to the hypothesis of direct ß-lactam binding by VxrA *in V. cholerae*, we found that treatment with the MreB-inhibitor A-22 also induced *vadR* expression, albeit to a smaller extent when compared to penicillin G (Chapter 3, Fig. S5A). MreB polymers have been reported to form cytoskeletal filaments, that, with the help of linker proteins, direct cell wall synthesis enzymes to insert new peptidoglycan into the cell wall (225). Both, A-22 and penicillin G, have been reported to damage the bacterial cell wall, resulting in a drastic loss of cell shape (157, 226, 227). Furthermore, we found that *vadR* expression is not detectable in *vxrAB* deficient cells, indicating that *vadR* expression is solely controlled by VxrAB (Chapter 3, Fig. 1D). Moreover, *vadR* expression was detectable at all stages of *V. cholerae* cell growth (Chapter 3, Fig. 1C), indicating that the VxrAB system is active in absence of cell wall damaging antibiotics. Together, these data argue against the idea that the VxrAB TCS is a direct ß-lactam sensor in *V. cholerae*. As of now, it is unclear what the exact signal activating the sensor kinase VxrA in *V. cholerae* is, but, for instance, sensing of cell wall intermediates upon induction of cell wall damage has been reported for other systems (228).

A possible answer to the question which specific signal activates VxrA in *V. cholerae* may be found in the genomic neighborhood of the *vxrAB* genes. The *vxrAB* genes are transcribed as a part of the operon *vxrABCDE* (159). Interestingly, we observed that overexpression of *vxrABC* leads to increased *vadR* expression, compared to *vxrAB* overexpression (Chapter 3, Fig. 1D). Furthermore, we found that expression of genomic fragments containing *vxrABC* showed increased induction of the P*vadR* promoter, compared to fragments containing only *vxrAB* (Chapter 3, Fig. S1E and unpublished data). Together, these data suggest a yet unknown regulatory role of *vxrC*. However, the proteins encoded by the *vxrCDE* genes are uncharacterized and feature no described protein domains or characterized homologs outside the *Vibrio* genus.

Intriguingly, we observed that *vadR* expression is highest in exponential growth phase (Chapter 3, Fig. 1C), indicating a potential physiological role of VadR under low cell density conditions. At low cell density, the master regulator AphA is active and induces virulence gene expression and biofilm formation (Chapter 1.4). AphA has been reported to directly activate expression of the biofilm regulator VpsT (229). Subsequently, VpsT activates expression of the gene cluster *vc0916-vc0939* required for synthesis of the vibrio-polysaccharide (VPS) and encoding the biofilm regulatory proteins *rbmA-F* (230). Global transcriptome analyses to identify mRNA targets found that VadR downregulates expression of all genes, except *rbmB*, encoded by the *vc0916-vc0939* gene cluster (Chapter 3, Figs. 2A, 3, S2). Consequently, VadR overexpression resulted in reduced biofilm formation (Chapter 3, Figs. 2D-I). Importantly, VadR is not the first sRNA reported to control biofilm formation in *V. cholerae.* The VqmR sRNA has been reported to control biofilm formation by regulating expression of the upstream regulators *vpsT* (46, 174) and *aphA*

(Chapter 4). However, *vqmR* expression is controlled by a quorum sensing system, and therefore activated at HCD, in the presence of increased autoinducer concentrations (46, 174), indicating that regulation of biofilm formation by both sRNAs might not occur at the same time. Furthermore, it is not clear why regulation of the upstream regulators is preferred by VqmR, while VadR regulates the *vc0916-vc0939* gene cluster directly. A potential explanation might be that direct downregulation of biofilm synthesis genes is faster and might be required to avoid initiation of biofilm formation under cell wall damaging conditions. Initiation of biofilm formation comes at a high metabolic cost (231), and depends on the secretion of VPS, RbmA, BapI, and RbmC (232), which we identified as targets of the VadR sRNA (Chapter 3, Figs. 2A, 3, S2). Furthermore, we found that *vadR* is specifically expressed in early phases of biofilm formation (Chapter 3, Fig. 6). Taken together, we could imagine a model, in which the VxrAB system monitors the cell wall status and activates *vadR* expression to prevent initiation of biofilm formation under unfavorable conditions.

Interestingly, we identified the *crvA* mRNA as another key target of the VadR sRNA (Chapter 3, Figs. 2A, 3, 4, S2). CrvA filaments have been reported to assemble in the periplasm, and asymmetrically pattern peptidoglycan insertion, thereby determining the curved shape of *Vibrio* cells (233). In the present work, we confirmed that cell curvature strongly correlated with CrvA levels (Chapter 3, Fig. 4). Furthermore, regulation of *crvA* expression by the VadR sRNA directly correlated with differences in cell curvature (Chapter 3, Fig. 4). CrvA has been reported to mediate insertion of more newly synthesized peptidoglycan to the outer face of the curved cell, thus achieving asymmetry (233). We speculated that this might create a weak spot, since one side of the cell might sustain prolonged damage by treatment with cell wall damaging antibiotics. In agreement with this hypothesis, we found that increased CrvA levels resulted in reduced survival after penicillin G treatment (Chapter 3, Fig. S5B). Furthermore, penicillin G treatment of *vadR* deficient cells, featuring increased cell curvature, resulted in reduced cell survival, while penicillin G treatment of strains over-expressing *vadR*, featuring decreased cell curvature, resulted in increased survival (Chapter 3, Fig. 5C). Further analyses revealed that this phenotype was specifically mediated by base-pairing of VadR to *crvA* mRNA (Chapter 3, Fig. 5C, S5C, D). Together these data suggest, that *vadR* expression is specifically activated in response to cell wall damage and mediates antibiotic resistance by interfering with expression of the periskeletal curvature determinant CrvA. The role of sRNAs in mediating antibiotic resistance has only been recently appreciated (234). For instance, in *S. typhimurium* expression of the sRNA SroA is activated in response to the antibiotic tigecycline, and deletion of *sroA* resulted in increased susceptibility, while overexpression rescued this phenotype, however the mechanism remains elusive (235).

It is interesting to consider why an sRNA is used in the VxrAB stress response to

control biofilm formation and cell shape in response to cell wall damage. The argument that VxrAB could exploit VadR as an indirect negative regulator, as shown for σ^E-dependent sRNAs (139, 202) offers an insufficient explanation, since VxrAB has been reported to act both as an activator and repressor of transcription (222). However, since we observed that VadR has a short half-life of 3min (Chapter 3, Fig. S1C) and achieved fast regulation of a pre-existing mRNA pool (Chapter 3, Figs. 2A, S2A), direct regulation by the VadR sRNA instead of negative regulation by VxrAB might provide improved dynamics to the system (202).

It is also intriguing to consider what physiological role VadR might play during *V. cholerae* infections. In the intestine, *V. cholerae* encounters antimicrobial peptides (AMPs) (122), which have been reported to induce cell wall damage (236). Here, we found that cell wall damage induces *vadR* expression, through VxrAB (Chapter 3, Fig. 5A, B). Indeed, previous reports found that *vxrB* mutants displayed colonization defects (159), suggesting that VxrAB is active and required during host colonization. Biofilm formation plays a critical role in *V. cholerae* infections (237) and we found that VadR down-regulates expression of all components required for the synthesis of the biofilm matrix, including VPS (Chapter 3, Figs. 2A-C, 3). VPS has been reported to bind mucins, as present as a protective coat of epithelial cells in the intestine, and overexpression of *vps* has been associated with reduced colonization, likely due to limited migration through mucus (238). Furthermore, cell curvature is thought to be required for motility in dense hydrogels, as present in the mucus layer (233) and we found that curvature is controlled by VadR (Chapter 3, Fig. 4). The VadR sRNA might play an important role in controlling these processes, which should be addressed in future studies. Although several studies suggest *V. cholerae* to form biofilms in the well-established infant mouse and infant rabbit infection models, the composition and architecture of biofilms formed *in vivo* remains unclear (230, 237, 239). Recently, adherence of *V. cholerae* to epithelial cells has been established *in vitro* and was shown to strongly induce biofilm formation (240), which might provide an initial model system to examine the role of VadR in biofilm formation in conditions mimicking the *in vivo* situation.

5.3 The role of sRNAs in quorum sensing of *V. cholerae*

Bacteria frequently employ quorum sensing to control gene expression profiles and synchronize group behaviors, including virulence factor production and biofilm formation (163). An important attribute of quorum sensing controlled systems is a rapid switch - rather than a progressive change - of gene expression profiles, if a certain threshold of autoinducer molecules is detected. In many cases this switch intimately involves post-transcriptional regulation by sRNAs (178). For example, the QS system in *Staphylococcus aureus* relies on the RNAIII sRNA to inhibit translation of the *rot* mRNA, encoding a transcriptional

repressor of toxin production, and therefore contributes to mediate a switch between virulent and avirulent physiological states (178, 241). In *V. cholerae*, the four homologous sRNAs Qrr1-4 have been reported to create an ultrasensitive switch, controlling the transition from LCD to HCD behaviors, by controlling expression of the LCD and HCD master regulators AphA and HapR, respectively (64, 242). This switch between physiological states and the overall output of the QS response depends on the fate of RNA-duplexes, formed between the Qrr1-4 sRNAs and their QS-related targets (186). For instance, base-pairing of the Qrr3 sRNA with the *aphA* leader has been reported to result in turnover of Qrr3, thereby forming a negative feedback loop to prevent overexpression of *aphA*, when the Qrr3:*aphA* ratio is low (186). Furthermore, while *qrr1-4* expression is activated by phosphorylated LuxO, HapR has been reported to additionally activate the expression of *qrr1-4*, thus establishing a feedback loop to accelerate the switch from HCD to LCD mode (243). Post-transcriptional control of quorum sensing in *V. cholerae* is further expanded by the involvement of the CsrA/B system, in which the three redundant sRNAs CsrBCD and the regulatory protein CsrA control Qrr1-4 expression through LuxO (183). Additionally, *V. cholerae* features a third quorum sensing system, that depends on the autoinducer DPO. DPO binds to the VqmA protein and activates expression of the VqmR sRNA (46, 174).

Quorum sensing in *V. cholerae* seems to preferentially rely on post-transcriptional regulators instead of transcription factors, but it is currently unclear why this is the case. A possible explanation might be that sRNAs have been reported to achieve faster regulation, when compared to transcription factors (244). Indeed, we found that VqmR significantly reduced the mRNA levels of its targets within 15 min of pulse-induction (Chapter 4, Table S1, Supplementary Figure S1A). Furthermore, sRNAs have been reported to reduce leaky gene expression, which might be required to achieve synchronized gene expression throughout a population (245). These features are especially relevant in cases where the number of sRNAs in the cell exceeds the copy number of the regulated mRNA target, since all mRNAs would be silenced (246). Indeed, VqmR has been reported to be expressed in high copy numbers in a cell density dependent manner, increasing from ~70 copies per cell at LCD to ~500 copies per cell at HCD (46). While the exact number of copies per cell for *aphA* mRNA in *V. cholerae* is unknown, Feng *et al.*, reported the copy number of the *hapR* homolog *luxR* in *V. harveyi* (recently, reclassified as *V. campbellii*) to increase from 4.36 copies per cell at LCD to ~44 copies per cell at HCD (186). If we assume similar numbers for the levels of *aphA* mRNA, and take into account that the average (target) mRNA is expressed with between 0.05 to 5 copies per cell (247), VqmR levels likely exceed *aphA* mRNA levels and effectively silences *aphA* translation at the transition to HCD. In the same line of thought, it is interesting to consider why four homologous sRNAs are employed for the AI-2 and CAI-1 quorum sensing systems, while the DPO quorum sensing system relies

on a single sRNA, especially considering that Qrr4 has been reported to be expressed with ~912 copies per cell at LCD, compared to ~56 copies per cell for Qrr2 and Qrr3, and ~14 copies per cell for Qrr1 (186). It would be interesting to compare the copy numbers of all QS-related sRNAs and mRNA targets at the transition from LCD to HCD in future studies to gain a better understanding of the involved dynamics.

While the collective control of *aphA* and QS-regulated gene expression by all three QS systems has been discussed in detail in Chapter 4, an interesting aspect of this regulatory system is how the switch between physiological states would work after a rapid transition from HCD to LCD. In this case, VqmR would be present at high levels, since it has been reported to show high expression levels at HCD, and is very stable with an half-life of more than 30min (46). During the switch from HCD to LCD, the earlier mentioned feedback loop, in which phosphorylated LuxO and HapR activate Qrr1-4 expression, would lead to the presence of high levels of the Qrr1-4 sRNAs, at the same time (243). Therefore, the Qrr1-4 sRNAs would compete with the VqmR sRNA for *aphA* activation or repression, respectively (Chapter 4, Table S1, Figs. 2, 3, (169, 170)). Interestingly, the Qrr1-4 sRNAs have been reported to turn-over following anti-antisense-pairing mediated activation of *aphA* translation (186). In contrast to that we found that the VqmR sRNA repressed *aphA* translation by base-pairing close to the AUG start codon, overlapping the ribsome-binding site (Chapter 4, Supplementary Figs. S5, S3A). This interaction site is in agreement with a mode of inhibiting translation initiation by blocking ribosome access, and indeed toeprinting analyses revealed that VqmR specifically interacts with this site to block 30S ribosomal access (Chapter 4, Supplementary Fig. S3B). While this regulatory mechanism of ribosomal occlusion has been reported to be sufficient to inhibit translation (53), it remains unclear whether base-pairing of VqmR to *aphA* mediates coupled degradation of VqmR, as well (56). It is interesting to consider what the outcome of this competition for regulation of *aphA* would be. Furthermore, it would be intriguing to test if VqmR would delay the switch from HCD to LCD, by limiting the levels of *aphA* transcripts that can be activated by Qrr1-4, or if *aphA* activation by Qrr1-4 or *aphA* repression by VqmR is obtaining superiority in this case. *In vitro* translation assays, using corresponding amounts of activating and repressing sRNAs, might provide an interesting experimental setup to predict the outcome of this competition (80).

5.4 Conclusions and outlook

The overarching goal of the present work was the functional characterization of sRNAs in the cholera pathogen, *V. cholerae*. A particular focus was given to sRNAs that are involved in stress response systems or quorum sensing. However, the majority of sRNAs present in *V. cholerae* remain uncharacterized regarding their mRNA target profiles and physiological

roles (Chapter 5.1). Future studies should address this, for instance by employing high-throughput approaches, e.g. RIL-seq.

Here, we identified the MicV sRNA as a novel member of the σ^E-regulon of *V. cholerae*. In a cellular context MicV acts together with the VrrA sRNA to control OMP synthesis, and thus envelope homeostasis, under envelope stress conditions. We found that both sRNAs engage co-regulated mRNA targets with a conserved seed-region, that is also present in σ^E-dependent sRNAs of other bacteria, albeit overall limited sequence homology. Remaining key questions are mainly concerning sRNA evolution. For instance, it should be clarified whether there might be an ancestral σ^E-dependent sRNA that has been duplicated, and changed its overall sequence composition, keeping only the seed-region intact, or if the conserved seed-region has evolved in a different sRNA scaffold, performing previously unrelated functions.

Furthermore, we found that expression of the *vadR* sRNA is activated by the VxrAB two component system in the presence of cell-wall damaging agents. However, the exact signal bound by the sensor histidine kinase VxrA remains elusive. Future studies should aim to identify the exact signal and elucidate where in a natural environment it could be encountered. We further showed that VadR controls expression of biofilm synthesis in *V. cholerae* and is the first sRNA reported to regulate cell curvature, achieved through the regulation of the curvature determinant CrvA. Regulation of CrvA by VadR affected susceptibility of *V. cholerae* to cell-wall damaging antibiotics, however it remains unclear how curvature and antibiotic resistance are related. Additionally, it is not clear if and how cell curvature is important for biofilm formation and how this could be connected to cell wall damage.

The present work further expanded the known mRNA targets for the VqmR sRNA by five additional targets, including *aphA* - encoding the master regulator of low cell density. VqmR expression is controlled in response to the presence of the autoinducer DPO, and we found that the interplay of three quorum sensing systems is required to achieve a saturated quorum sensing response. It remains unclear how widespread the use of the DPO autoinducer is. It is also interesting to consider how the quorum sensing response would function in presence of other bacteria, for instance in the intestine, or in *V. cholerae*s' aquatic reservoirs.

In summary, we showed sRNAs to play key roles in the physiology of *V. cholerae* under standard laboratory conditions. Future studies should aim to translate these key functions to settings mimicking natural conditions, e.g. in infection models or in natural habitats.

References for Chapters 1 and 5

1. M. Ali, A. R. Nelson, A. L. Lopez, D. A. Sack, Updated global burden of cholera in endemic countries. *PLoS Negl. Trop. Dis.* **9**, 1–13 (2015).

2. M. Bentivoglio, P. Pacini, Filippo Pacini: A determined observer. *Brain Res. Bull.* **38**, 161–165 (1995).

3. T. Shimada, E. Arakawa, K. Itoh, T. Okitsu, A. Matsushima, Y. Asai, S. Yamai, T. Nakazato, G. B. Nair, M. J. Albert, Y. Takeda, Extended serotyping scheme for *Vibrio cholerae*. *Curr. Microbiol.* **28**, 175–178 (1994).

4. A. Mutreja, D. W. Kim, N. R. Thomson, T. R. Connor, J. H. Lee, S. Kariuki, N. J. Croucher, S. Y. Choi, S. R. Harris, M. Lebens, S. K. Niyogi, E. J. Kim, T. Ramamurthy, J. Chun, J. L. N. Wood, J. D. Clemens, C. Czerkinsky, G. B. Nair, J. Holmgren, J. Parkhill, G. Dougan, Evidence for several waves of global transmission in the seventh cholera pandemic. *Nature* **477**, 462–465 (2011).

5. J. Chun, C. J. Grim, N. A. Hasan, J. H. Lee, S. Y. Choi, B. J. Haley, E. Taviani, Y.-S. Jeon, D. W. Kim, J.-H. Lee, T. S. Brettin, D. C. Bruce, J. F. Challacombe, J. C. Detter, C. S. Han, A. C. Munk, O. Chertkov, L. Meincke, E. Saunders, R. A. Walters, A. Huq, G. B. Nair, R. R. Colwell, Comparative genomics reveals mechanism for short-term and long-term clonal transitions in pandemic *Vibrio cholerae*. *Proc. Natl. Acad. Sci. U. S. A.* **106**, 15442–7 (2009).

6. M. John Albert, A. K. Siddique, M. S. Islam, A. S. G. Faruque, M. Ansaruzzaman, S. M. Faruque, R. Bradley Sack, Large outbreak of clinical cholera due to *Vibrio cholerae* non-01 in Bangladesh. *Lancet* **341**, 704 (1993).

7. C. A. Bopp, B. A. Kay, J. G. Wells, “Isolation and Identification of *Vibrio cholerae* O1 from Fecal Specimens” in *Vibrio Cholerae and Cholera*, (American Society of Microbiology, 1994), pp. 3–25.

8. K. H. Thelin, R. K. Taylor, Toxin-coregulated pilus, but not mannose-sensitive hemagglutinin, is required for colonization by *Vibrio cholerae* O1 El Tor biotype and O139 strains. *Infect. Immun.* **64**, 2853–6 (1996).

9. A. Reimer, G. Domselaar, S. Stroika, M. Walker, H. Kent, C. Tarr, D. Talkington, L. Rowe, M. Olsen-Rasmussen, M. Frace, S. Sammons, G. Dahourou, J. Boncy, A. Smith, P. Mabon, A. Petkau, M. Graham, M. Gilmour, P. Gerner-Smidt, Comparative Genomics of *Vibrio cholerae* from Haiti, Asia, and Africa. *Emerg. Infect. Dis.* **17** (2011).

10. S. hun Yoon, C. M. Waters, *Vibrio cholerae*. *Trends Microbiol.* **27**, 806–807 (2019).

11. R. R. Colwell, W. M. Spira, “The Ecology of *Vibrio cholerae*” in *Cholera*, (Springer US, 1992), pp. 107–127.

12. A. Huq, R. R. Colwell, “*Vibrios* in the environment: viable but nonculturable *Vibrio cholerae*” in *Vibrio Cholerae and Cholera*, (American Society of Microbiology, 1994), pp. 117–133.

13. M. Alam, M. Sultana, G. B. Nair, R. B. Sack, D. A. Sack, A. K. Siddique, A. Ali, A. Huq, R. R. Colwell, Toxigenic *Vibrio cholerae* in the aquatic environment of Mathbaria, Bangladesh. *Appl. Environ. Microbiol.* **72**, 2849–55 (2006).

14. M. L. Tamplin, A. L. Gauzens, A. Huq, D. A. Sack, R. R. Colwell, Attachment of *Vibrio cholerae* serogroup O1 to zooplankton and phytoplankton of Bangladesh waters. *Appl. Environ. Microbiol.* **56**, 1977–80 (1990).

15. L. Vezzulli, C. Pruzzo, A. Huq, R. R. Colwell, Environmental reservoirs of *Vibrio cholerae* and their role in cholera. *Environ. Microbiol. Rep.* **2**, 27–33 (2010).

16. D. S. Merrell, S. M. Butler, F. Qadri, N. A. Dolganov, A. Alam, M. B. Cohen, S. B. Calderwood, G. K. Schoolnik, A. Camilli, Host-induced epidemic spread of the cholera bacterium. *Nature* **417**, 642–645 (2002).

17. D. S. Merrell, A. Camilli, The *cadA* gene of *Vibrio cholerae* is induced during infection and plays a role in acid tolerance. *Mol. Microbiol.* **34**, 836–849 (1999).

18. J. Zhu, J. J. Mekalanos, Quorum Sensing-Dependent Biofilms Enhance Colonization in *Vibrio cholerae*. *Dev. Cell* **5**, 647–656 (2003).

19. T. Yamamoto, T. Yokota, Electron microscopic study of *Vibrio cholerae* O1 adherence to the mucus coat and villus surface in the human small intestine. *Infect. Immun.* **56**, 2753–9 (1988).

20. C. Robbe, C. Capon, B. Coddeville, J.-C. Michalski, Structural diversity and specific distribution of O-glycans in normal human mucins along the intestinal tract. *Biochem. J.* **384**, 307–16 (2004).

21. A. J. Silva, K. Pham, J. A. Benitez, Haemagglutinin/protease expression and mucin gel penetration in El Tor biotype *Vibrio cholerae*. *Microbiology* **149**, 1883–1891 (2003).

22. N. K. Ganguly, T. Kaur, Mechanism of action of cholera toxin & other toxins. *Indian J. Med. Res.* **104**, 28–37 (1996).

23. I. Lönnroth, J. Holmgren, Subunit structure of cholera toxin. *J. Gen. Microbiol.* **76**, 417–427 (1973).

24. J. Sánchez, J. Holmgren, Cholera toxin structure, gene regulation and pathophysiological and immunological aspects. *Cell. Mol. Life Sci.* **65**, 1347–1360 (2008).

25. A. T. Nielsen, N. A. Dolganov, G. Otto, M. C. Miller, C. Y. Wu, G. K. Schoolnik, RpoS Controls the *Vibrio cholerae* Mucosal Escape Response. *PLoS Pathog.* **2**, e109 (2006).

26. C. Lutz, M. Erken, P. Noorian, S. Sun, D. McDougald, Environmental reservoirs and mechanisms of persistence of *Vibrio cholerae*. *Front. Microbiol.* **4**, 1–15 (2013).

27. M. M. S. M. Wösten, Eubacterial sigma-factors. *FEMS Microbiol. Rev.* **22**, 127–150 (1998).

28. A. Feklístov, B. D. Sharon, S. A. Darst, C. A. Gross, Bacterial Sigma Factors: A Historical, Structural, and Genomic Perspective. *Annu. Rev. Microbiol.* **68**, 357–376 (2014).

29. S. Frietze, P. J. Farnham, A Handbook of Transcription Factors - Transcription Factor Effector Domains. *A Handb. Transcr. Factors* **52**, 261–277 (2011).

30. E. Balleza, L. N. López-Bojorquez, A. Martínez-Antonio, O. Resendis-Antonio, I. Lozada-Chávez, Y. I. Balderas-Martínez, S. Encarnación, J. Collado-Vides, Regulation by transcription factors in bacteria: Beyond description. *FEMS Microbiol. Rev.* **33**, 133–151 (2009).

31. D. J. Lee, S. D. Minchin, S. J. W. Busby, Activating Transcription in Bacteria. *Annu. Rev. Microbiol.* **66**, 125–152 (2012).

32. K. M. Wassarman, A. Zhang, G. Storz, Small RNAs in *Escherichia coli*. *Trends Microbiol.* **7**, 37–45 (1999).

33. A. J. Westermann, S. A. Gorski, J. Vogel, Dual RNA-seq of pathogen and host. *Nat. Rev. Microbiol.* **10**, 618–630 (2012).

34. E. G. H. Wagner, P. Romby, *Small RNAs in Bacteria and Archaea: Who They Are, What They Do, and How They Do It* (Elsevier Ltd, 2015).

35. E. Loh, F. Righetti, H. Eichner, C. Twittenhoff, F. Narberhaus, RNA Thermometers in Bacterial Pathogens. *Microbiol. Spectr.* **6**, 1–16 (2018).

36. A. Serganov, E. Nudler, A decade of riboswitches. *Cell* **152**, 17–24 (2013).

37. V. J. DiRita, C. Parsot, G. Jander, J. J. Mekalanos, Regulatory cascade controls virulence in *Vibrio cholerae*. *Proc. Natl. Acad. Sci. U. S. A.* **88**, 5403–5407 (1991).

38. G. G. Weber, J. Kortmann, F. Narberhaus, K. E. Klose, RNA thermometer controls temperature-dependent virulence factor expression in *Vibrio cholerae*. *Proc. Natl. Acad. Sci. U. S. A.* **111**, 14241–14246 (2014).

39. S. Brantl, Regulatory mechanisms employed by *cis*-encoded antisense RNAs. *Curr. Opin. Microbiol.* **10**, 102–109 (2007).

40. J. Georg, W. R. Hess, *cis*-Antisense RNA, Another Level of Gene Regulation in Bacteria. *Microbiol. Mol. Biol. Rev.* **75**, 286–300 (2011).

41. D. H. Bechhofer, M. P. Deutscher, Bacterial ribonucleases and their roles in RNA metabolism. *Crit. Rev. Biochem. Mol. Biol.* **54**, 242–300 (2019).

42. J. Tomizawa, T. Itoh, G. Selzer, T. Som, Inhibition of ColE1 RNA primer formation by a plasmid-specified small RNA. *Proc. Natl. Acad. Sci. U. S. A.* **78**, 1421–1425 (1981).

43. S. Brantl, Antisense-RNA regulation and RNA interference. *Biochim. Biophys. Acta - Gene Struct. Expr.* **1575**, 15–25 (2002).

44. L. M. Mustachio, S. Aksit, R. H. Mistry, R. Scheffler, A. Yamada, J. M. Liu, The *Vibrio cholerae* mannitol transporter is regulated posttranscriptionally by the MtlS small regulatory RNA. *J. Bacteriol.* **194**, 598–606 (2012).

45. H. Chang, J. M. Replogle, N. Vather, M. Tsao-Wu, R. Mistry, J. M. Liu, A *cis*-regulatory antisense RNA represses translation in *Vibrio cholerae* through extensive complementarity and proximity to the target locus. *RNA Biol.* **12**, 136–148 (2015).

46. K. Papenfort, K. U. Förstner, J.-P. Cong, C. M. Sharma, B. L. Bassler, Differential RNA-seq of *Vibrio cholerae* identifies the VqmR small RNA as a regulator of biofilm formation. *Proc. Natl. Acad. Sci. U. S. A.* **112**, E766-75 (2015).

47. G. Storz, J. Vogel, K. M. Wassarman, Regulation by Small RNAs in Bacteria: Expanding Frontiers. *Mol. Cell* **43**, 880–891 (2011).

48. E. Holmqvist, P. R. Wright, L. Li, T. Bischler, L. Barquist, R. Reinhardt, R. Backofen, J. Vogel, Global RNA recognition patterns of post-transcriptional regulators Hfq and CsrA revealed by UV crosslinking *in vivo* . *EMBO J.* **35**, 991–1011 (2016).

49. K. Papenfort, M. Bouvier, F. Mika, C. M. Sharma, J. Vogel, Evidence for an autonomous 5' target recognition domain in an Hfq-associated small RNA. *Proc. Natl. Acad. Sci.* **107**, 20435–20440 (2010).

50. A. Hüttenhofer, H. F. Noller, Footprinting mRNA-ribosome complexes with chemical probes. *EMBO J.* **13**, 3892–3901 (1994).

51. D. Beyer, E. Skripkin, J. Wadzack, K. H. Nierhaus, How the ribosome moves along the mRNA during protein synthesis. *J. Biol. Chem.* **269**, 30713–30717 (1994).

52. C. Del Campo, A. Bartholomäus, I. Fedyunin, Z. Ignatova, Secondary Structure across the Bacterial Transcriptome Reveals Versatile Roles in mRNA Regulation and Function. *PLoS Genet.* **11**, 1–23 (2015).

53. T. Morita, Y. Mochizuki, H. Aiba, Translational repression is sufficient for gene silencing by bacterial small noncoding RNAs in the absence of mRNA destruction. *Proc. Natl. Acad. Sci. U. S. A.* **103**, 4858–4863 (2006).

54. A. J. Carpousis, The RNA Degradosome of *Escherichia coli* : An mRNA-Degrading Machine Assembled on RNase E. *Annu. Rev. Microbiol.* **61**, 71–87 (2007).

55. T. Morita, K. Maki, H. Aiba, Erratum: RNase E-based ribonucleoprotein complexes: Mechanical basis of mRNA destabilization mediated by bacterial noncoding RNAs (Genes and Development (2005) 19, (2176-2186)). *Genes Dev.* **20**, 3487 (2006).

56. E. Massé, F. E. Escorcia, S. Gottesman, Coupled degradation of a small regulatory RNA and its mRNA targets in *Escherichia coli*. *Genes Dev.* **17**, 2374–2383 (2003).

57. H. Aiba, Mechanism of RNA silencing by Hfq-binding small RNAs. *Curr. Opin. Microbiol.* **10**, 134–139 (2007).

58. C. L. Beisel, G. Storz, The Base-Pairing RNA Spot 42 Participates in a Multioutput Feedforward Loop to Help Enact Catabolite Repression in *Escherichia coli*. *Mol. Cell* **41**, 286–297 (2011).

59. C. M. Sharma, F. Darfeuille, T. H. Plantinga, J. Vogel, A small RNA regulates multiple ABC transporter mRNAs by targeting C/A-rich elements inside and upstream of ribosome-binding sites. *Genes Dev.* **21**, 2804–2817 (2007).

60. V. Pfeiffer, K. Papenfort, S. Lucchini, J. C. D. Hinton, J. Vogel, Coding sequence targeting by MicC RNA reveals bacterial mRNA silencing downstream of translational initiation. *Nat. Struct. Mol. Biol.* **16**, 840–846 (2009).

61. K. S. Fröhlich, J. Vogel, Activation of gene expression by small RNA. *Curr. Opin. Microbiol.* **12**, 674–682 (2009).

62. K. Papenfort, C. K. Vanderpool, Target activation by regulatory RNAs in bacteria. *FEMS Microbiol. Rev.* **39**, 362–378 (2015).

63. B. K. Hammer, B. L. Bassler, Regulatory small RNAs circumvent the conventional quorum sensing pathway in pandemic *Vibrio cholerae*. *Proc. Natl. Acad. Sci. U. S. A.* **104**, 11145–11149 (2007).

64. D. H. Lenz, K. C. Mok, B. N. Lilley, R. V Kulkarni, N. S. Wingreen, B. L. Bassler, The Small RNA Chaperone Hfq and Multiple Small RNAs Control Quorum Sensing in *Vibrio harveyi* and *Vibrio cholerae*. *Cell* **118**, 69–82 (2004).

65. M. T. Franze De Fernandez, L. Eoyang, J. T. August, Factor fraction required for the synthesis of bacteriophage Qβ-RNA. *Nature* **219**, 588–590 (1968).

66. X. Sun, Predicted structure and phyletic distribution of the RNA-binding protein Hfq. *Nucleic Acids Res.* **30**, 3662–3671 (2002).

67. Y. Chao, J. Vogel, The role of Hfq in bacterial pathogens. *Curr. Opin. Microbiol.* **13**, 24–33 (2010).

68. Y. Ding, B. M. Davis, M. K. Waldor, Hfq is essential for *Vibrio cholerae* virulence and downregulates σE expression. *Mol. Microbiol.* **53**, 345–354 (2004).

69. C. J. Wilusz, J. Wilusz, Eukaryotic Lsm proteins: Lessons from bacteria. *Nat. Struct. Mol. Biol.* **12**, 1031–1036 (2005).

70. C. Kambach, S. Walke, R. Young, J. M. Avis, E. De La Fortelle, V. A. Raker, R. Lührmann, J. Li, K. Nagai, Crystal structures of two Sm protein complexes and their implications for the assembly of the spliceosomal snRNPs. *Cell* **96**, 375–387 (1999).

71. S. Tharun, W. He, A. E. Mayes, P. Lennertz, J. D. Beggs, R. Parker, Yeast Sm-like proteins function in mRNA decapping and decay. *Nature* **404**, 515–518 (2000).

72. M. Albrecht, T. Lengauer, Novel Sm-like proteins with long C-terminal tails and associated methyltransferases. *FEBS Lett.* **569**, 18–26 (2004).

73. J. H. Urban, J. Vogel, Translational control and target recognition by *Escherichia coli* small RNAs in vivo. *Nucleic Acids Res.* **35**, 1018–1037 (2007).

74. J. F. Hopkins, S. Panja, S. A. N. McNeil, S. A. Woodson, Effect of salt and RNA structure on annealing and strand displacement by Hfq. *Nucleic Acids Res.* **37**, 6205–6213 (2009).

75. J. F. Hopkins, S. Panja, S. A. Woodson, Rapid binding and release of Hfq from ternary complexes during RNA annealing. *Nucleic Acids Res.* **39**, 5193–5202 (2011).

76. A. Fender, J. Elf, K. Hampel, B. Zimmermann, E. G. H. Wagner, RNAs actively cycle on the Sm-like protein Hfq, Genes Develop (2010).pdf. *Genes Dev.* **3**, 2621–2626 (2010).

77. T. A. Geissmann, D. Touati, Hfq, a new chaperoning role: Binding to messenger RNA determines access for small RNA regulator. *EMBO J.* **23**, 396–405 (2004).

78. A. Zhang, K. M. Wassarman, J. Ortega, A. C. Steven, G. Storz, The Sm-like Hfq protein increases OxyS RNA interaction with target mRNAs. *Mol. Cell* **9**, 11–22 (2002).

79. C. A. Henderson, H. A. Vincent, A. Casamento, C. M. Stone, J. O. Phillips, P. D. Cary, F. Sobott, D. M. Gowers, J. E. Taylor, A. J. Callaghan, Hfq binding changes the structure of *Escherichia coli* small noncoding RNAs OxyS and RprA, which are involved in the riboregulation of *rpoS*. *RNA* **19**, 1089–1104 (2013).

80. M. Hoekzema, C. Romilly, E. Holmqvist, E. G. H. Wagner, Hfq-dependent mRNA unfolding promotes sRNA-based inhibition of translation . *EMBO J.* **38**, 1–14 (2019).

81. R. G. Brennan, T. M. Link, Hfq structure, function and ligand binding. *Curr. Opin. Microbiol.* **10**, 125–133 (2007).

82. M. A. Schumacher, R. F. Pearson, T. Møller, P. Valentin-Hansen, R. G. Brennan, Structures of the pleiotropic translational regulator Hfq and an Hfq-RNA complex: A bacterial Sm-like protein. *EMBO J.* **21**, 3546–3556 (2002).

83. A. Santiago-Frangos, S. A. Woodson, Hfq chaperone brings speed dating to bacterial sRNA. *Wiley Interdiscip. Rev. RNA* **9** (2018).

84. P. Sobrero, C. Valverde, The bacterial protein Hfq: Much more than a mere RNA-binding factor. *Crit. Rev. Microbiol.* **38**, 276–299 (2012).

85. J. Vogel, B. F. Luisi, Hfq and its constellation of RNA. *Nat. Rev. Microbiol.* **9**, 578–589 (2011).

86. T. B. Updegrove, A. Zhang, G. Storz, Hfq: The flexible RNA matchmaker. *Curr. Opin. Microbiol.* **30**, 133–138 (2016).

87. H. Otaka, H. Ishikawa, T. Morita, H. Aiba, PolyU tail of rho-independent terminator of bacterial small RNAs is essential for Hfq action. *Proc. Natl. Acad. Sci. U. S. A.* **108**, 13059–13064 (2011).

88. H. Ishikawa, H. Otaka, K. Maki, T. Morita, H. Aiba, The functional Hfq-binding module of bacterial sRNAs consists of a double or single hairpin preceded by a U-rich sequence and followed by a 3′ poly(U) tail. *Rna* **18**, 1062–1074 (2012).

89. E. Sauer, O. Weichenrieder, Structural basis for RNA 3′-end recognition by Hfq. *Proc. Natl. Acad. Sci. U. S. A.* **108**, 13065–13070 (2011).

90. Y. Chao, K. Papenfort, R. Reinhardt, C. M. Sharma, J. Vogel, An atlas of Hfq-bound transcripts reveals 3′ UTRs as a genomic reservoir of regulatory small RNAs. *EMBO J.* **31**, 4005–4019 (2012).

91. A. Sittka, S. Lucchini, K. Papenfort, C. M. Sharma, K. Rolle, T. T. Binnewies, J. C. D. Hinton, J. Vogel, Deep sequencing analysis of small noncoding RNA and mRNA targets of the global post-transcriptional regulator, Hfq. *PLoS Genet.* **4** (2008).

92. T. M. Link, P. Valentin-Hansen, R. G. Brennana, Structure of *Escherichia coli* Hfq bound to polyriboadenylate RNA. *Proc. Natl. Acad. Sci. U. S. A.* **106**, 19292–19297 (2009).

93. A. Zhang, D. J. Schu, B. C. Tjaden, G. Storz, S. Gottesman, Mutations in interaction surfaces differentially impact *E. coli* Hfq association with small RNAs and their mRNA targets. *J. Mol. Biol.* **425**, 3678–3697 (2013).

94. D. J. Schu, A. Zhang, S. Gottesman, G. Storz, Alternative Hfq- sRNA interaction modes dictate alternative mRNA recognition . *EMBO J.* **34**, 2557–2573 (2015).

95. P. J. Mikulecky, M. K. Kaw, C. C. Brescia, J. C. Takach, D. D. Sledjeski, A. L. Feig, *Escherichia coli* Hfq has distinct interaction surfaces for DsrA, *rpoS* and poly(A) RNAs. *Nat. Struct. Mol. Biol.* **11**, 1206–1214 (2004).

96. A. Santiago-Frangos, K. Kavita, D. J. Schu, S. Gottesman, S. A. Woodson, C-terminal domain of the RNA chaperone Hfq drives sRNA competition and release of target RNA. *Proc. Natl. Acad. Sci. U. S. A.* **113**, E6089–E6096 (2016).

97. A. Santiago-Frangos, J. R. Jeliazkov, J. J. Gray, S. A. Woodson, Acidic C-terminal domains autoregulate the RNA chaperone Hfq. *Elife* **6**, 1–25 (2017).

98. A. Santiago-Frangos, K. S. Fröhlich, J. R. Jeliazkov, E. M. Małecka, G. Marino, J. J. Gray, B. F. Luisi, S. A. Woodson, S. W. Hardwick, *Caulobacter crescentus* Hfq structure reveals a conserved mechanism of RNA annealing regulation. *Proc. Natl. Acad. Sci. U. S. A.* **166**, 10978–10987 (2019).

99. T. Mizuno, M. Y. Chou, M. Inouye, A unique mechanism regulating gene expression: Translational inhibition by a complementary RNA transcript (micRNA). *Proc. Natl. Acad. Sci. U. S. A.* **81**, 1966–1970 (1984).

100. L. Argaman, R. Hershberg, J. Vogel, G. Bejerano, E. G. H. Wagner, H. Margalit, S. Altuvia, Novel small RNA-encoding genes in the intergenic regions of *Escherichia coli*. *Curr. Biol.* **11**, 941–950 (2001).

101. J. Livny, M. K. Waldor, Identification of small RNAs in diverse bacterial species. *Curr. Opin. Microbiol.* **10**, 96–101 (2007).

102. S. Altuvia, Identification of bacterial small non-coding RNAs: experimental approaches. *Curr. Opin. Microbiol.* **10**, 257–261 (2007).

103. K. M. Wassarman, F. Repoila, C. Rosenow, G. Storz, S. Gottesman, Identification of novel small RNAs using comparative genomics and microarrays. *Genes Dev.* **15**, 1637–1651 (2001).

104. C. Steglich, M. E. Futschik, D. Lindell, B. Voss, S. W. Chisholm, W. R. Hess, The challenge of regulation in a minimal photoautotroph: Non-coding RNAs in *Prochlorococcus*. *PLoS Genet.* **4** (2008).

105. A. Toledo-Arana, O. Dussurget, G. Nikitas, N. Sesto, H. Guet-Revillet, D. Balestrino, E. Loh, J. Gripenland, T. Tiensuu, K. Vaitkevicius, M. Barthelemy, M. Vergassola, M. A. Nahori, G. Soubigou, B. Régnault, J. Y. Coppée, M. Lecuit, J. Johansson, P. Cossart, The *Listeria* transcriptional landscape from saprophytism to virulence. *Nature* **459**, 950–956 (2009).

106. A. Sittka, C. M. Sharma, K. Rolle, J. Vogel, Deep sequencing of *Salmonella* RNA associated with heterologous Hfq proteins in vivo reveals small RNAs as a major target class and identifies RNA processing phenotypes. *RNA Biol.* **6**, 57–66 (2009).

107. T. Bischler, H. S. Tan, K. Nieselt, C. M. Sharma, Differential RNA-seq (dRNA-seq) for annotation of transcriptional start sites and small RNAs in *Helicobacter pylori*. *Methods* **86**, 89–101 (2015).

108. C. M. Sharma, S. Hoffmann, F. Darfeuille, J. Reignier, S. Findeiß, A. Sittka, S. Chabas, K. Reiche, J. Hackermüller, R. Reinhardt, P. F. Stadler, J. Vogel, The primary transcriptome of the major human pathogen *Helicobacter pylori*. *Nature* **464**, 250–255 (2010).

109. C. M. Sharma, J. Vogel, Differential RNA-seq: The approach behind and the biological insight gained. *Curr. Opin. Microbiol.* **19**, 97–105 (2014).

110. J. Vogel, E. G. H. Wagner, Target identification of small noncoding RNAs in bacteria. *Curr. Opin. Microbiol.* **10**, 262–270 (2007).

111. C. M. Sharma, J. Vogel, Experimental approaches for the discovery and characterization of regulatory small RNA. *Curr. Opin. Microbiol.* **12**, 536–546 (2009).

112. P. R. Wright, A. S. Richter, K. Papenfort, M. Mann, J. Vogel, W. R. Hess, R. Backofen, J. Georg, Comparative genomics boosts target prediction for bacterial small RNAs. *Proc. Natl. Acad. Sci.* **110**, E3487–E3496 (2013).

113. P. R. Wright, J. Georg, M. Mann, D. A. Sorescu, A. S. Richter, S. Lott, R. Kleinkauf, W. R. Hess, R. Backofen, CopraRNA and IntaRNA: predicting small RNA targets, networks and interaction domains. *Nucleic Acids Res.* **42**, W119-23 (2014).

114. A. Pain, A. Ott, H. Amine, T. Rochat, P. Bouloc, D. Gautheret, An assessment of bacterial small RNA target prediction programs. *RNA Biol.* **12**, 509–513 (2015).

115. K. Papenfort, V. Pfeiffer, F. Mika, S. Lucchini, J. C. D. Hinton, J. Vogel, SigmaE-dependent small RNAs of *Salmonella* respond to membrane stress by accelerating global omp mRNA decay. *Mol. Microbiol.* **62**, 1674–88 (2006).

116. A. Helwak, G. Kudla, T. Dudnakova, D. Tollervey, Mapping the human miRNA interactome by CLASH reveals frequent noncanonical binding. *Cell* **153**, 654–665 (2013).

117. S. Grosswendt, A. Filipchyk, M. Manzano, F. Klironomos, M. Schilling, M. Herzog, E. Gottwein, N. Rajewsky, Unambiguous Identification of miRNA: Target site interactions by different types of ligation reactions. *Mol. Cell* **54**, 1042–1054 (2014).

118. M. J. Moore, T. K. H. Scheel, J. M. Luna, C. Y. Park, J. J. Fak, E. Nishiuchi, C. M. Rice, R. B. Darnell, MiRNA-target chimeras reveal miRNA 3′-end pairing as a major determinant of Argonaute target specificity. *Nat. Commun.* **6** (2015).

119. J. Hör, S. A. Gorski, J. Vogel, Bacterial RNA Biology on a Genome Scale. *Mol. Cell* **70**, 785–799 (2018).

120. S. Melamed, A. Peer, R. Faigenbaum-Romm, Y. E. Gatt, N. Reiss, A. Bar, Y. Altuvia, L. Argaman, H. Margalit, Global Mapping of Small RNA-Target Interactions in Bacteria. *Mol. Cell* **63**, 884–897 (2016).

121. S. Melamed, R. Faigenbaum-Romm, A. Peer, N. Reiss, O. Shechter, A. Bar, Y. Altuvia, L. Argaman, H. Margalit, Mapping the small RNA interactome in bacteria using RIL-seq. *Nat. Protoc.* **13**, 1–33 (2018).

122. J. G. Conner, J. K. Teschler, C. J. Jones, F. H. Yildiz, Staying Alive: *Vibrio cholerae*'s Cycle of Environmental Survival, Transmission, and Dissemination. *Virulence Mech. Bact. Pathog. Fifth Ed.*, 593–633 (2016).

123. H. Nikaido, Outer membrane. In: Neidhardt F C, Curtiss III R, Ingraham J L, Lin E C C, Low K B Jr, Magasanik B, Reznikoff W S, Riley M, Schaechter M, Umbarger H E, editors. *Escherichia coli* and *Salmonella*: cellular and molecular biology. 2nd ed. Washington, D.C: Amer. *Microbiol. Mol. Biol. Rev.* **67**, 29–47 (1996).

124. X. Z. Li, P. Plésiat, H. Nikaido, The challenge of efflux-mediated antibiotic resistance in Gram-negative bacteria. *Clin. Microbiol. Rev.* **28**, 337–418 (2015).

125. T. J. Silhavy, D. Kahne, S. Walker, The Bacterial Cell Envelope. *Cold Spring Harb Perspect Biol* **2**, 1–16 (2010).

126. M. Grabowicz, T. J. Silhavy, Envelope Stress Responses: An Interconnected Safety Net. *Trends Biochem. Sci.* **42**, 232–242 (2017).

127. A. M. Mitchell, T. J. Silhavy, Envelope stress responses: balancing damage repair and toxicity. *Nat. Rev. Microbiol.* **17**, 417–428 (2019).

128. K. S. Fröhlich, S. Gottesman, Small Regulatory RNAs in the Enterobacterial Response to Envelope Damage and Oxidative Stress. *Regul. with RNA Bact. Archaea*, 213–228 (2018).

129. S. E. Ades, L. E. Connolly, B. M. Alba, C. A. Gross, The *Escherichia coli* σ(E)-dependent extracytoplasmic stress response is controlled by the regulated proteolysis of an anti-σ factor. *Genes Dev.* **13**, 2449–2461 (1999).

130. E. A. Campbell, J. L. Tupy, T. M. Gruber, S. Wang, M. M. Sharp, C. A. Gross, S. A. Darst, Crystal structure of *Escherichia coli* σE with the cytoplasmic domain of its anti-σ RseA. *Mol. Cell* **11**, 1067–1078 (2003).

131. N. P. Walsh, B. M. Alba, B. Bose, C. A. Gross, R. T. Sauer, OMP peptide signals initiate the envelope-stress response by activating DegS protease via relief of inhibition mediated by its PDZ domain. *Cell* **113**, 61–71 (2003).

132. R. Chaba, B. M. Alba, M. S. Guo, J. Sohn, N. Ahuja, R. T. Sauer, C. A. Gross, Signal integration by DegS and RseB governs the σE- mediated envelope stress response in *Escherichia coli*. *Proc. Natl. Acad. Sci. U. S. A.* **108**, 2106–2111 (2011).

133. S. Lima, M. S. Guo, R. Chaba, C. A. Gross, R. T. Sauer, Dual molecular signals mediate the bacterial response to outer-membrane stress. *Science (80-.).* **340**, 837–841 (2013).

134. Y. Akiyama, K. Kanehara, K. Ito, RseP (YaeL), an *Escherichia coli* RIP protease, cleaves transmembrane sequences. *EMBO J.* **23**, 4434–4442 (2004).

135. K. Akiyama, S. Mizuno, Y. Hizukuri, H. Mori, T. Nogi, Y. Akiyama, Roles of the membrane-reentrant β-hairpin-like loop of RseP protease in selective substrate cleavage. *Elife* **4** (2015).

136. J. M. Flynn, I. Levchenko, R. T. Sauer, T. A. Baker, Modulating substrate choice: The SspB adaptor delivers a regulator of the extracytoplasmic-stress response to the AAA+ protease ClpXP for degradation. *Genes Dev.* **18**, 2292–2301 (2004).

137. V. A. Rhodius, W. C. Suh, G. Nonaka, J. West, C. A. Gross, Conserved and variable functions of the sigmaE stress response in related genomes. *PLoS Biol.* **4**, e2 (2006).

138. K. I. Udekwu, F. Darfeuille, J. Vogel, J. Reimegård, E. Holmqvist, E. G. H. Wagner, Hfq-dependent regulation of OmpA synthesis is mediated by an antisense RNA. *Genes Dev.* **19**, 2355–2366 (2005).

139. M. S. Guo, T. B. Updegrove, E. B. Gogol, S. A. Shabalina, C. A. Gross, G. Storz, MicL, a new σE-dependent sRNA, combats envelope stress by repressing synthesis of Lpp, the major outer membrane lipoprotein. *Genes Dev.* **28**, 1620–1634 (2014).

140. E. B. Gogol, V. A. Rhodius, K. Papenfort, J. Vogel, C. A. Gross, Small RNAs endow a transcriptional activator with essential repressor functions for single-tier control of a global stress regulon. *Proc. Natl. Acad. Sci. U. S. A.* **108**, 12875–12880 (2011).

141. J. Vogel, K. Papenfort, Small non-coding RNAs and the bacterial outer membrane. *Curr Opin Microbiol* **9**, 605–611 (2006).

142. T. Song, F. Mika, B. Lindmark, Z. Liu, S. Schild, A. Bishop, J. Zhu, A. Camilli, J. Johansson, J. Vogel, S. N. Wai, A new *Vibrio cholerae* sRNA modulates colonization and affects release of outer membrane vesicles. *Mol. Microbiol.* **70**, 100–11 (2008).

143. T. Song, S. N. Wai, A novel sRNA that modulates virulence and environmental fitness of *Vibrio cholerae*. *RNA Biol.* **6**, 254–258 (2009).

144. T. Song, D. Sabharwal, S. N. Wai, VrrA Mediates Hfq-Dependent Regulation of OmpT Synthesis in *Vibrio cholerae*. *J. Mol. Biol.* **400**, 682–688 (2010).

145. D. Sabharwal, T. Song, K. Papenfort, S. N. Wai, The VrrA sRNA controls a stationary phase survival factor *vrp* of *Vibrio cholerae*. *RNA Biol.* **12**, 186–196 (2015).

146. T. Song, D. Sabharwal, J. M. Gurung, A. T. Cheng, A. E. Sjöström, F. H. Yildiz, B. E. Uhlin, S. N. Wai, *Vibrio cholerae* Utilizes Direct sRNA Regulation in Expression of a Biofilm Matrix Protein. *PLoS One* **9**, e101280 (2014).

147. N. Peschek, M. Hoyos, R. Herzog, K. U. Förstner, K. Papenfort, A conserved RNA seed-pairing domain directs small RNA-mediated stress resistance in enterobacteria. *EMBO J.* (2019) https:/doi.org/10.15252/embj.2019101650.

148. N. Majdalani, S. Gottesman, THE RCS PHOSPHORELAY: A Complex Signal Transduction System. *Annu. Rev. Microbiol.* **59**, 379–405 (2005).

149. M. E. Laubacher, S. E. Ades, The Rcs phosphorelay is a cell envelope stress response activated by peptidoglycan stress and contributes to intrinsic antibiotic resistance. *J. Bacteriol.* **190**, 2065–2074 (2008).

150. L. Ferrières, S. N. Aslam, R. M. Cooper, D. J. Clarke, The *yjbEFGH* locus in *Escherichia coli* K-12 is an operon encoding proteins involved in exopolysaccharide production. *Microbiology* **153**, 1070–1080 (2007).

151. M. Wehland, F. Bernhard, The RcsAB box. Characterization of a new operator essential for the regulation of exopolysaccharide biosynthesis in enteric bacteria. *J. Biol. Chem.* **275**, 7013–7020 (2000).

152. A. Francez-Charlot, B. Laugel, A. Van Gemert, N. Dubarry, F. Wiorowski, M. P. Castanié-Cornet, C. Gutierrez, K. Cam, RcsCDB His-Asp phosphorelay system negatively regulates the *flhDC* operon in *Escherichia coli*. *Mol. Microbiol.* **49**, 823–832 (2003).

153. N. Majdalani, D. Hernandez, S. Gottesman, Regulation and mode of action of the second small RNA activator of RpoS translation, RprA. *Mol. Microbiol.* **46**, 813–826 (2002).

154. N. Majdalani, S. Chen, J. Murrow, K. St. John, S. Gottesman, Regulation of RpoS by a novel small RNA: The characterization of RprA. *Mol. Microbiol.* **39**, 1382–1394 (2001).

155. J. M. Navarro Llorens, A. Tormo, E. Martínez-García, Stationary phase in Gram-negative bacteria. *FEMS Microbiol. Rev.* **34**, 476–495 (2010).

156. D. K. Ranjit, K. D. Young, The RCS stress response and accessory envelope proteins are required for *de novo* generation of cell shape in *Escherichia coli*. *J. Bacteriol.* **195**, 2452–2462 (2013).

157. T. Dörr, B. M. Davis, M. K. Waldor, Endopeptidase-Mediated Beta Lactam Tolerance. *PLoS Pathog.* **11**, 1–16 (2015).

158. T. Dörr, L. Alvarez, F. Delgado, B. M. Davis, F. Cava, M. K. Waldor, A cell wall damage response mediated by a sensor kinase/response regulator pair enables beta-lactam tolerance. *Proc. Natl. Acad. Sci. U. S. A.* **113**, 404–409 (2016).

159. A. T. Cheng, K. M. Ottemann, F. H. Yildiz, *Vibrio cholerae* Response Regulator VxrB Controls Colonization and Regulates the Type VI Secretion System. *PLOS Pathog.* **11**, e1004933 (2015).

160. J. K. Teschler, A. T. Cheng, F. H. Yildiz, The Two-Component Signal Transduction System VxrAB Positively Regulates *Vibrio cholerae* Biofilm Formation. *J. Bacteriol.* **199**, 1–16 (2017).

161. S. Gottesman, G. Storz, Bacterial small RNA regulators: Versatile roles and rapidly evolving variations. *Cold Spring Harb. Perspect. Biol.* **3** (2011).

162. B. L. Bassler, R. Losick, Bacterially Speaking. *Cell* **125**, 237–246 (2006).

163. K. Papenfort, B. L. Bassler, Quorum sensing signal–response systems in Gram-negative bacteria. *Nat. Rev. Microbiol.* **14**, 576–588 (2016).

164. C. M. Waters, W. Lu, J. D. Rabinowitz, B. L. Bassler, Quorum sensing controls biofilm formation in *Vibrio cholerae* through modulation of cyclic di-GMP levels and repression of *vpsT*. *J. Bacteriol.* **190**, 2527–2536 (2008).

165. J. Zhu, M. B. Miller, R. E. Vance, M. Dziejman, B. L. Bassler, J. J. Mekalanos, Quorum-sensing regulators control virulence gene expression in *Vibrio cholerae*. *Proc. Natl. Acad. Sci. U. S. A.* **99**, 3129–3134 (2002).

166. R. C. Kelly, M. E. Bolitho, D. A. Higgins, W. Lu, W. L. Ng, P. D. Jeffrey, J. D. Rabinowitz, M. F. Semmelhack, F. M. Hughson, B. L. Bassler, The *Vibrio cholerae* quorum-sensing autoinducer CAI-1: Analysis of the biosynthetic enzyme CqsA. *Nat. Chem. Biol.* **5**, 891–895 (2009).

167. X. Chen, S. Schauder, N. Potier, A. Van Dorsselaer, I. Pelczer, B. L. Bassler, F. M. Hughson, Structural identification of a bacterial quorum-sensing signal containing boron. *Nature* **415**, 545–549 (2002).

168. Y. Shao, L. Feng, S. T. Rutherford, K. Papenfort, B. L. Bassler, Functional determinants of the quorum-sensing non-coding RNAs and their roles in target regulation. *EMBO J.* **32**, 2158–2171 (2013).

169. Y. Shao, B. L. Bassler, Quorum-sensing non-coding small RNAs use unique pairing regions to differentially control mRNA targets. *Mol. Microbiol.* **83**, 599–611 (2012).

170. S. T. Rutherford, J. C. Van Kessel, Y. Shao, B. L. Bassler, AphA and LuxR/HapR reciprocally control quorum sensing in *Vibrios*. *Genes Dev.* **25**, 397–408 (2011).

171. J. C. Van Kessel, S. T. Rutherford, Y. Shao, A. F. Utria, B. L. Bassler, Individual and combined roles of the master regulators Apha and Luxr in control of the *Vibrio harveyi* quorum-sensing regulon. *J. Bacteriol.* **195**, 436–443 (2013).

172. M. G. Jobling, R. K. Holmes, Characterization of *hapR* , a positive regulator of the *Vibrio cholerae* HA/protease gene *hap* , and its identification as a functional homologue of the *Vibrio harveyi luxR* gene. *Mol. Microbiol.* **26**, 1023–1034 (1997).

173. W.-L. Ng, B. L. Bassler, Bacterial Quorum-Sensing Network Architectures. *Annu. Rev. Genet.* **43**, 197–222 (2009).

174. K. Papenfort, J. E. Silpe, K. R. Schramma, J.-P. Cong, M. R. Seyedsayamdost, B. L. Bassler, A *Vibrio cholerae* autoinducer–receptor pair that controls biofilm formation. *Nat. Chem. Biol.* **13**, 551–557 (2017).

175. C. Casper-Lindley, F. H. Yildiz, VpsT Is A Transcriptional Regulator Required for Expression of *vps* Biosynthesis Genes and the Development of Rugose Colonial Morphology in *Vibrio cholerae* O1 El Tor. *J. Bacteriol.* **186**, 1574–1578 (2004).

176. Z. Wang, M. Gerstein, M. Snyder, RNA-Seq: A revolutionary tool for transcriptomics. *Nat. Rev. Genet.* **10**, 57–63 (2009).

177. R. Herzog, N. Peschek, K. S. Fröhlich, K. Schumacher, K. Papenfort, Three autoinducer molecules act in concert to control virulence gene expression in *Vibrio cholerae*. *Nucleic Acids Res.* **47**, 3171–3183 (2019).

178. K. Papenfort, J. Vogel, Regulatory RNA in bacterial pathogens. *Cell Host Microbe* **8**, 116–127 (2010).

179. T. B. Updegrove, S. A. Shabalina, G. Storz, How do base-pairing small RNAs evolve? *FEMS Microbiol. Rev.* **39**, 379–391 (2015).

180. C. C. Caswell, A. Oglesby-Sherrouse, E. R. Murphy, Sibling rivalry: Related bacterial small RNAs and their redundant and non-redundant roles. *Front. Cell. Infect. Microbiol.* **4** (2014).

181. A. R. Mey, S. A. Craig, S. M. Payne, Characterization of *Vibrio cholerae* RyhB: The RyhB regulon and role of RyhB in biofilm formation. *Infect. Immun.* **73**, 5706–5719 (2005).

182. J. M. Liu, J. Livny, M. S. Lawrence, M. D. Kimball, M. K. Waldor, A. Camilli, Experimental discovery of sRNAs in *Vibrio cholerae* by direct cloning, 5S/ tRNA depletion and parallel sequencing. *Nucleic Acids Res.* **37**, 1–10 (2009).

183. D. H. Lenz, M. B. Miller, J. Zhu, R. V. Kulkarni, B. L. Bassler, CsrA and three redundant small RNAs regulate quorum sensing in *Vibrio cholerae*. *Mol. Microbiol.* **58**, 1186–1202 (2005).

184. H. A. Butz, A. R. Mey, A. L. Ciosek, S. M. Payne, *Vibrio cholerae* CsrA directly regulates *varA* to increase expression of the three nonredundant Csr small RNAs. *MBio* **10**, 1–15 (2019).

185. X. Zhao, B. J. Koestler, C. M. Waters, B. K. Hammer, Post-transcriptional activation of a diguanylate cyclase by quorum sensing small RNAs promotes biofilm formation in *Vibrio cholerae*. *Mol. Microbiol.* **89**, 989–1002 (2013).

186. L. Feng, S. T. Rutherford, K. Papenfort, J. D. Bagert, J. C. Van Kessel, D. A. Tirrell, N. S. Wingreen, B. L. Bassler, A Qrr noncoding RNA deploys four different regulatory mechanisms to optimize quorum-sensing dynamics. *Cell* **160**, 228–240 (2015).

187. A. L. Richard, J. H. Withey, S. Beyhan, F. Yildiz, V. J. Dirita, The *Vibrio cholerae* virulence regulatory cascade controls glucose uptake through activation of TarA, a small regulatory RNA. *Mol. Microbiol.* **78**, 1171–1181 (2010).

188. E. S. Bradley, K. Bodi, A. M. Ismail, A. Camilli, A genome-wide approach to discovery of small RNAs involved in regulation of virulence in *Vibrio cholerae*. *PLoS Pathog.* **7** (2011).

189. S. Yamamoto, H. Izumiya, J. Mitobe, M. Morita, E. Arakawa, M. Ohnishi, H. Watanabe, Identification of a chitin-induced small RNA that regulates translation of the *tfoX* gene, encoding a positive regulator of natural competence in *Vibrio cholerae*. *J. Bacteriol.* **193**, 1953–1965 (2011).

190. K. L. Meibom, M. Blokesch, N. A. Dolganov, C. Y. Wu, G. K. Schoolnik, Microbiology: Chitin induces natural competence in *Vibrio cholerae*. *Science (80-.).* **310**, 1824–1827 (2005).

191. J. W. Veening, M. Blokesch, Interbacterial predation as a strategy for DNA acquisition in naturally competent bacteria. *Nat. Rev. Microbiol.* **15**, 621–629 (2017).

192. B. M. Davis, M. K. Waldor, RNase E-dependent processing stabilizes MicX, a *Vibrio cholerae* sRNA. *Mol. Microbiol.* **65**, 373–385 (2007).

193. T. G. Dong, J. J. Mekalanos, Characterization of the RpoN regulon reveals differential regulation of T6SS and new flagellar operons in *Vibrio cholerae* O37 strain V52. *Nucleic Acids Res.* **40**, 7766–7775 (2012).

194. S. C. Pulvermacher, L. T. Stauffer, G. V. Stauffer, The role of the small regulatory RNA GcvB in GcvB/mRNA posttranscriptional regulation of *oppA* and *dppA* in *Escherichia coli*. *FEMS Microbiol. Lett.* **281**, 42–50 (2008).

195. G. T. Hansen, R. Ahmad, E. Hjerde, C. G. Fenton, N. P. Willassen, P. Haugen, Expression profiling reveals Spot 42 small RNA as a key regulator in the central metabolism of *Aliivibrio salmonicida*. *BMC Genomics* **13** (2012).

196. B. M. Davis, M. Quinones, J. Pratt, Y. Ding, M. K. Waldor, Characterization of the small untranslated RNA RyhB and its regulon in *Vibrio cholerae*. *J. Bacteriol.* **187**, 4005–4014 (2005).

197. M. Bouvier, C. M. Sharma, F. Mika, K. H. Nierhaus, J. Vogel, Small RNA Binding to 5′ mRNA Coding Region Inhibits Translational Initiation. *Mol. Cell* **32**, 827–837 (2008).

198. Y. Chao, L. Li, D. Girodat, K. U. Förstner, N. Said, C. Corcoran, M. Śmiga, K. Papenfort, R. Reinhardt, H. J. Wieden, B. F. Luisi, J. Vogel, *In Vivo* Cleavage Map Illuminates the Central Role of RNase E in Coding and Non-coding RNA Pathways. *Mol. Cell* **65**, 39–51 (2017).

199. T. Morita, H. Aiba, Mechanism and physiological significance of autoregulation of the *Escherichia coli hfq* gene. *RNA* **25**, 264–276 (2019).

200. G. Rowley, M. Spector, J. Kormanec, M. Roberts, Pushing the envelope: extracytoplasmic stress responses in bacterial pathogens. *Nat. Rev. Microbiol.* **4**, 383–394 (2006).

201. V. K. Mutalik, G. Nonaka, S. E. Ades, V. A. Rhodius, C. A. Gross, Promoter strength properties of the complete sigmaE regulon of *Escherichia coli* and *Salmonella enterica*. *J. Bacteriol.* **191**, 7279–7287 (2009).

202. A. Brosse, M. Guillier, Bacterial Small RNAs in Mixed Regulatory Networks. *Microbiol. Spectr.* **6** (2018).

203. A. A. Rasmussen, M. Eriksen, K. Gilany, C. Udesen, T. Franch, C. Petersen, P. Valentin-Hansen, Regulation of *ompA* mRNA stability: The role of a small regulatory RNA in growth phase-dependent control. *Mol. Microbiol.* **58**, 1421–1429 (2005).

204. D. L. Leyton, M. J. Belousoff, Lithgow Trevor, The ß-Barrel Assembly Machinery Complex. *Methods Mol. Biol.* **1329**, 1–16 (2015).

205. J. C. Malinverni, J. Werner, S. Kim, J. G. Sklar, D. Kahne, R. Misra, T. J. Silhavy, YfiO stabilizes the YaeT complex and is essential for outer membrane protein assembly in *Escherichia coli*. *Mol. Microbiol.* **61**, 151–164 (2006).

206. V. Douchin, C. Bohn, P. Bouloc, Down-regulation of porins by a small RNA bypasses the essentiality of the regulated intramembrane proteolysis protease RseP in *Escherichia coli*. *J. Biol. Chem.* **281**, 12253–12259 (2006).

207. M. Guillier, S. Gottesman, G. Storz, Modulating the outer membrane with small RNAs. *Genes Dev.* **20**, 2338–2348 (2006).

208. K. Papenfort, D. Podkaminski, J. C. D. Hinton, J. Vogel, The ancestral SgrS RNA discriminates horizontally acquired *Salmonella* mRNAs through a single G-U wobble pair. *Proc. Natl. Acad. Sci. U. S. A.* **109** (2012).

209. K. Papenfort, N. Said, T. Welsink, S. Lucchini, J. C. D. Hinton, J. Vogel, Specific and pleiotropic patterns of mRNA regulation by ArcZ, a conserved, Hfq-dependent small RNA. *Mol. Microbiol.* **74**, 139–158 (2009).

210. H. Nikaido, E. Y. Rosenberg, Porin channels in *Escherichia coli*: Studies with liposomes reconstituted from purified proteins. *J. Bacteriol.* **153**, 241–252 (1983).

211. J. T. Kelley, C. D. Parker, Identification and preliminary characterization of *Vibrio cholerae* outer membrane proteins. *J. Bacteriol.* **145**, 1018–1024 (1981).

212. M. Pathania, S. Acosta-Gutierrez, S. P. Bhamidimarri, A. Baslé, M. Winterhalter, M. Ceccarelli, B. van den Berg, Unusual Constriction Zones in the Major Porins OmpU and OmpT from *Vibrio cholerae*. *Structure* **26**, 708-721.e4 (2018).

213. S. A. Gorski, J. Vogel, J. A. Doudna, RNA-based recognition and targeting: Sowing the seeds of specificity. *Nat. Rev. Mol. Cell Biol.* **18**, 215–228 (2017).

214. J. Mecsas, P. E. Rouviere, J. W. Erickson, T. J. Donohue, C. A. Gross, The activity of σ(E), an *Escherichia coli* heat-inducible σ-factor, is modulated by expression of outer membrane proteins. *Genes Dev.* **7**, 2618–2628 (1993).

215. B. M. Davis, M. K. Waldor, High-throughput sequencing reveals suppressors of *Vibrio cholerae rpoE* mutations: one fewer porin is enough. *Nucleic Acids Res.* **37**, 5757–5767 (2009).

216. D. Provenzano, D. A. Schuhmacher, J. L. Barker, K. E. Klose, The virulence regulatory protein ToxR mediates enhanced bile resistance in *Vibrio cholerae* and other pathogenic *Vibrio* species. *Infect. Immun.* **68**, 1491–1497 (2000).

217. D. Provenzano, K. E. Klose, Altered expression of the ToxR-regulated porins OmpU and OmpT diminishes *Vibrio cholerae* bile resistance, virulence factor expression, and intestinal colonization. *Proc. Natl. Acad. Sci. U. S. A.* **97**, 10220–10224 (2000).

218. J. A. Wibbenmeyer, D. Provenzano, C. F. Landry, K. E. Klose, A. H. Delcour, *Vibrio cholerae* OmpU and OmpT porins are differentially affected by bile. *Infect. Immun.* **70**, 121–126 (2002).

219. D. feng Zhang, J. zhou Ye, H. hou Dai, X. min Lin, H. Li, X. xian Peng, Identification of ethanol tolerant outer membrane proteome reveals OmpC-dependent mechanism in a manner of EnvZ/OmpR regulation in *Escherichia coli*. *J. Proteomics* **179**, 92–99 (2018).

220. E. J. Capra, M. T. Laub, Evolution of Two-Component Signal Transduction Systems. *Annu. Rev. Microbiol.* **66**, 325–347 (2012).

221. T. Krell, J. Lacal, A. Busch, H. Silva-Jiménez, M.-E. Guazzaroni, J. L. Ramos, Bacterial Sensor Kinases: Diversity in the Recognition of Environmental Signals. *Annu. Rev. Microbiol.* **64**, 539–559 (2010).

222. J.-H. Shin, D. Choe, B. Ransegnola, H.-R. Hong, I. Onyekwere, B.-K. Cho, T. Doerr, A multifaceted cellular damage repair and prevention pathway promotes high level tolerance to β-lactam antibiotics. *bioRxiv*, 777375 (2019).

223. L. Li, Q. Wang, H. Zhang, M. Yang, M. I. Khan, X. Zhou, Sensor histidine kinase is a β-lactam receptor and induces resistance to β-lactam antibiotics. *Proc. Natl. Acad. Sci. U. S. A.* **113**, 1648–53 (2016).

224. K. J. Forsberg, A. Reyes, B. Wang, E. M. Selleck, M. O. A. Sommer, G. Dantas, The shared antibiotic resistome of soil bacteria and human pathogens. *Science (80-.).* **337**, 1107–1111 (2012).

225. H. Shi, B. P. Bratton, Z. Gitai, K. C. Huang, How to Build a Bacterial Cell: MreB as the Foreman of *E. coli* Construction. *Cell* **172**, 1294–1305 (2018).

226. T. Cross, B. Ransegnola, J.-H. Shin, A. Weaver, K. Fauntleroy, M. S. VanNieuwenhze, L. F. Westblade, T. Dörr, Spheroplast-Mediated Carbapenem Tolerance in Gram-Negative Pathogens. *Antimicrob. Agents Chemother.* **63** (2019).

227. P. Srivastava, G. Demarre, T. S. Karpova, J. McNally, D. K. Chattoraj, Changes in nucleoid morphology and origin localization upon inhibition or alteration of the actin homolog, MreB, of *Vibrio cholerae*. *J. Bacteriol.* **189**, 7450–7463 (2007).

228. C. Jacobs, J. M. Frère, S. Normark, Cytosolic intermediates for cell wall biosynthesis and degradation control inducible β-lactam resistance in Gram-negative bacteria. *Cell* **88**, 823–832 (1997).

229. M. Yang, E. M. Frey, Z. Liu, R. Bishar, J. Zhu, The virulence transcriptional activator AphA enhances biofilm formation by *Vibrio cholerae* by activating expression of the biofilm regulator VpsT. *Infect. Immun.* **78**, 697–703 (2010).

230. J. C. N. Fong, K. A. Syed, K. E. Klose, F. H. Yildiz, Role of *Vibrio* polysaccharide (*vps*) genes in VPS production, biofilm formation and *Vibrio cholerae* pathogenesis. *Microbiology* **156**, 2757–2769 (2010).

231. C. D. Nadell, B. L. Bassler, A fitness trade-off between local competition and dispersal in *Vibrio cholerae* biofilms. *Proc. Natl. Acad. Sci. U. S. A.* **108**, 14181–14185 (2011).

232. J. K. Teschler, D. Zamorano-Sánchez, A. S. Utada, C. J. A. Warner, G. C. L. Wong, R. G. Linington, F. H. Yildiz, Living in the matrix: Assembly and control of *Vibrio cholerae* biofilms. *Nat. Rev. Microbiol.* **13**, 255–268 (2015).

233. T. M. Bartlett, B. P. Bratton, A. Duvshani, A. Miguel, Y. Sheng, N. R. Martin, J. P. Nguyen, A. Persat, S. M. Desmarais, M. S. VanNieuwenhze, K. C. Huang, J. Zhu, J. W. Shaevitz, Z. Gitai, A Periplasmic Polymer Curves *Vibrio cholerae* and Promotes Pathogenesis. *Cell* **168**, 172-185.e15 (2017).

234. P. Dersch, M. A. Khan, S. Mühlen, B. Görke, Roles of regulatory RNAs for antibiotic resistance in bacteria and their potential value as novel drug targets. *Front. Microbiol.* **8** (2017).

235. J. Yu, T. Schneiders, Tigecycline challenge triggers sRNA production in *Salmonella enterica* serovar Typhimurium. *BMC Microbiol.* **12**, 195 (2012).

236. L. T. Nguyen, E. F. Haney, H. J. Vogel, The expanding scope of antimicrobial peptide structures and their modes of action. *Trends Biotechnol.* **29**, 464–472 (2011).

237. A. J. Silva, J. A. Benitez, *Vibrio cholerae* Biofilms and Cholera Pathogenesis. *PLoS Negl. Trop. Dis.* **10**, 1–25 (2016).

238. Z. Liu, Y. Wang, S. Liu, Y. Sheng, K. G. Rueggeberg, H. Wang, J. Li, F. X. Gu, Z. Zhong, B. Kan, J. Zhu, *Vibrio cholerae* represses polysaccharide synthesis to promote motility in mucosa. *Infect. Immun.* **83**, 1114–1121 (2015).

239. Y. A. Millet, D. Alvarez, S. Ringgaard, U. H. von Andrian, B. M. Davis, M. K. Waldor, Insights into *Vibrio cholerae* Intestinal Colonization from Monitoring Fluorescently Labeled Bacteria. *PLoS Pathog.* **10** (2014).

240. C. Sengupta, O. Mukherjee, R. Chowdhury, Adherence to intestinal cells promotes biofilm formation in *Vibrio cholerae*. *J. Infect. Dis.* **214**, 1571–1578 (2016).

241. S. Boisset, T. Geissmann, E. Huntzinger, P. Fechter, N. Bendridi, M. Possedko, C. Chevalier, A. C. Helfer, Y. Benito, A. Jacquier, C. Gaspin, F. Vandenesch, P. Romby, *Staphylococcus aureus* RNAIII coordinately represses the synthesis of virulence factors and the transcription regulator Rot by an antisense mechanism. *Genes Dev.* **21**, 1353–1366 (2007).

242. S. L. Svenningsen, K. C. Tu, B. L. Bassler, Gene dosage compensation calibrates four regulatory RNAs to control *Vibrio cholerae* quorum sensing. *EMBO J.* **28**, 429–439 (2009).

243. S. L. Svenningsen, C. M. Waters, B. L. Bassler, A negative feedback loop involving small RNAs accelerates *Vibrio cholerae*'s transition out of quorum-sensing mode. *Genes Dev.* **22**, 226–238 (2008).

244. Y. Shimoni, G. Friedlander, G. Hetzroni, G. Niv, S. Altuvia, O. Biham, H. Margalit, Regulation of gene expression by small non-coding RNAs: a quantitative view. *Mol. Syst. Biol.* **3**, 138 (2007).

245. T. Long, K. C. Tu, Y. Wang, P. Mehta, N. P. Ong, B. L. Bassler, N. S. Wingreen, Quantifying the Integration of Quorum-Sensing Signals with Single-Cell Resolution. *PLoS Biol.* **7**, e1000068 (2009).

246. C. L. Beisel, G. Storz, Base pairing small RNAs and their roles in global regulatory networks. *FEMS Microbiol. Rev.* **34**, 866–882 (2010).

247. Y. Taniguchi, P. J. Choi, G. W. Li, H. Chen, M. Babu, J. Hearn, A. Emili, X. Sunney Xie, Quantifying *E. coli* proteome and transcriptome with single-molecule sensitivity in single cells. *Science (80-.).* **329**, 533–538 (2010).

Supplemental information - Chapter 3

RNA-mediated control of cell shape modulates antibiotic resistance in *Vibrio cholerae*

Roman Herzog[1,2*], Nikolai Peschek[1,2*], Praveen K. Singh[3], Kathrin S. Fröhlich[1,2], Luise Schröger[1,2], Fabian Meyer[1,4], Marc Bramkamp[1,4], Knut Drescher[3,5], and Kai Papenfort[1,2,6#]

[1] Friedrich Schiller University, Institute of Microbiology, 07745 Jena, Germany

[2] Faculty of Biology I, Ludwig-Maximilians-University of Munich, 82152 Martinsried, Germany

[3] Max Planck Institute for Terrestrial Microbiology, 35043 Marburg, Germany

[4] Institute for General Microbiology, Christian-Albrechts-University, Kiel, Germany,

[5] Department of Physics, Philipps-Universität Marburg, 35032 Marburg, Germany

[6] Microverse Cluster, Friedrich Schiller University Jena, 07743 Jena, Germany.

* These authors contributed equally

Corresponding author:

Kai Papenfort

E-mail: kai.papenfort@uni-jena.de

Phone: +49-3641-939-5753

This supplement contains:

Supplementary Materials and Methods

Supplemental References

Figures S1-5

Tables S1-4

TABLE OF CONTENTS

Supplementary Materials and Methods

Plasmid construction

All plasmids and DNA oligonucleotides used in this study are listed in Table S3 and Table S4, respectively. If not stated otherwise, all insert fragments were amplified from genomic DNA of *V. cholerae* C6706. The backbone for the overexpression plasmids pNP-001/003-006/008-010/013 was linearized with KPO-0092/1023 using pEVS143 as a PCR template. For the amplifications of the inserted sRNAs, the following combinations of oligonucleotides were used: KPO-1003/1004 (pNP-001), KPO-1024/1025 (pNP-003), KPO-1005/1006 (pNP-004), KPO-1015/1016 (pNP-005), KPO-1021/1022 (pNP-006), KPO-1009/1010 (pNP-008), KPO-1219/1220 (pNP-009), KPO-1001/1002 (pNP-010), and KPO-1017/1018 (pNP-013). Subsequently, linearized vector and sRNA inserts were treated with XbaI restriction enzyme and fused by ligation. The construction of overexpression plasmids pLS-014-020, pRH-005, and pSG-001/002 was achieved by Gibson assembly. pEVS143 backbone was linearized using KPO-0092/1397 (pLS-014-020) or KPO-0092/1023 (pRH-005, pSG-001/002). sRNA insert sequences were amplified using KPO-5835/5836 (pLS-014), KPO-5837/5838 (pLS-015), KPO-5841/5842 (pLS-016), KPO-5843/5844 (pLS-017), KPO-5845/5846 (pLS-018), KPO-5847/5848 (pLS-019), KPO-5849/5850 (pLS-020), KPO-1226/1227 (pRH-005), KPO-1858/1859 (pSG-001), and KPO-1860/1861 (pSG-002). Further, Gibson assembly was used to generate the inducible overexpression plasmids pMD-097, pNP-019, and pNP-123-127. For these plasmids, pMD-004 served as backbone and was linearized using KPO-0196/1397 (pMD-097 and pNP-019) or KPO-0196/1488 (pNP-123-127). Amplification of insert genes were achieved with oligonucleotide combinations KPO-2554/2555 (pMD-097), KPO-1400/1401 (pNP-019), KPO-4852/4918 (pNP-123), KPO-4852/4919 (pNP-125), KPO-4852/4920 (pNP-126), and KPO-4852/4921 (pNP-127). Plasmid pNP-124 was assembled from two insert fragments, which were amplified with oligonucleotides KPO-4852/4853 and KPO-4854/4855, respectively. Plasmids pEE-007 and pLS-026-028 were generated by oligonucleotide-directed mutagenesis of pNP-005 (pEE-007) and pAE-002 (pLS-026-028), using KPO-4098/4099 (pEE-007), KPO-5981/5982 (pLS-026), KPO-5983/5984 (pLS-027), and KPO-5985/5986 (pLS-028). The promoter region of *vadR* was amplified using KPO-1906/1907 and KPO-4410/4411 for plasmids pAE-002 and pNP-122, respectively. To generate pAE-002, the obtained fragment and the pCMW-1C vector were digested with SphI and SalI enzymes and fused by ligation. Likewise, pNP-122 was obtained by ligation after treating insert and pBBR1-MCS5-lacZ equally with restriction enzymes SpeI and SalI. 5' UTRs and initial coding sequences for the construction of the translational reporter plasmids pNP-064/070-073, pRG-011-013 and pRH-090/092 were amplified using KPO-1720/1721 (pNP-064),

KPO-2067/2068 (pNP-070), KPO-2069/2070 (pNP-071), KPO-2071/2072 (pNP-072), KPO-2065/2066 (pNP-073), KPO-3735/3736 (pNP-113), KPO-3739/3740 (pNP-114), KPO-3737/3738 (pNP-115), KPO-2383/2384 (pRG-011), KPO-2385/2386 (pRG-012), KPO-2389/2390 (pRG-013), KPO-5534/5535 (pRH-090), and KPO-5538/5539 (pRH-092). Restriction digests of the amplified fragments and the pXG10-SF vector were conducted using NsiI and NheI enzymes. Inserts and vectors were combined by ligation. Plasmid pMH-039 was generated by Gibson assembly, using KPO-1702/1703 to linearize the pXG10-SF vector and KPO-1801/2803 to amplify the insert fragment, respectively. To build the suicide plasmid pNP-133, flanking regions of the *vadR* locus were amplified using KPO-1294/1295 and KPO-1296/1297. The two fragments were combined by overlap PCR with KPO-1298/1299. Restriction digest of the obtained insert fragment and of the pKAS32 vector using KpnI and ArvII enzymes and subsequent ligation, yielded the functional plasmid. To build plasmid pRH-093, pNP-133 was linearized with KPO-5550/5551. The required insert was amplified from pNP-117 using KPO-5548/5549. Gibson assembly of both parts resulted in pRH-093. Plasmids pNP-128/132/134/135 and pRH-099 were obtained by Gibson assembly, using a pKAS32 vector, which was linearized with KPO-0267/0268. The single insert fragment of pNP-128 was amplified with KPO-5456/5457. The flanking regions of the *crvA* gene and the *vxrABCDE* operon were amplified using the two oligonucleotide combinations KPO-5450/5451, KPO-5452/5453 (pNP-134) and KPO-4621/4622, KPO-4625/4626 (pNP-135), respectively. To introduce a *crvA-3xFLAG* construct onto the chromosome of *V. cholerae*, plasmid pNP-132 was designed. The corresponding flanking regions were amplified using KPO-5442/5443 and KPO-5446/5447. Oligonucleotides KPO-5444/5445 were used to amplify the 3xFLAG epitope from template plasmid pRH-030. The *araC*-P_{BAD} insert of pRH-099 was amplified from pMD-004 using KPO-4529/0196. Flanking regions of the *crvAB* promoter were amplified using oligos KPO-6013/6014 and KPO-6015/6016, respectively.

All mutations for compensatory base pair exchanges were introduced by oligonucleotide-directed mutagenesis using the oligonucleotides listed in Table S4, and the respective parental plasmids as a template.

Construction of *V. cholerae* mutant strains

All strains used in this study is are listed in Table S2. *V. cholerae* C6706 was used as the wild-type strain in this study. *V. cholerae* mutant strains were generated as described previously[2]. Conjugal transfer was used to introduce plasmids into *V. cholerae* from *E. coli* S17λpir donor strains. Transconjugants were selected using appropriate antibiotics, and 50 U/ml polymyxin B was used to select against *E. coli* donor strains.

Transcript stability experiments

Stability of VadR was determined as described previously[3]. Briefly, biological triplicates of V. cholerae wild-type (KPS-0014) and Δ*hfq* (KPS-0054) strains were grown to OD600 = 0.2 and transcription was terminated by addition of 250 µg/ml rifampicin. Transcript levels were probed and quantified using Northern blot analysis.

Quantitative real-time PCR

Total RNA was isolated using the SV Total RNA Isolation System (Promega), according to the manufacturer's instructions. qRT-PCR was performed using the Luna Universal One-Step RT-qPCR Kit (New England BioLabs) and the MyiQ™ Single-Color Real-Time PCR Detection System (Bio-Rad). *recA* was used as a reference gene.

Analysis of VxrB-HIS ChIP-seq data

The raw data of the VxrB-HIS ChIP experiment conducted by Shin et al.[1] was obtained from Gene Expression Omnibus (GEO) under the accession number GSE135009. The read files were imported into CLC Genomics Workbench v11 (Qiagen) and trimmed for quality using default parameters. Reads were mapped to the *V. cholerae* reference genome (NCBI accession numbers: NC_002505.1 and NC_002506.1) using the "RNA-Seq Analysis" tool with default parameters.

RNA *in vitro* analysis

A DNA template carrying the T7 promoter for *in vitro* synthesis of RNA was prepared by PCR using oligonucleotides KPO-5083 and KPO-5084. 200 ng of template DNA were *in vitro* transcribed using the AmpliScribe T7-Flash transcription kit (Epicentre) following the manufacturer's recommendations. RNA size and integrity were verified on denaturing polyacrylamide gels. For 5' end labelling, 20 pmol of RNA were dephosphorylated using 10 units of calf alkaline phosphatase (NEB), followed by P:C:I extraction and ethanol precipitation of RNA. Dephosphorylated RNA was incubated with [^{32}P]-γATP (20 µCi) and 1 unit of polynucleotide kinase (NEB) for 1h at 37°C. Unincorporated nucleotides were removed using Microspin G-50 Columns (GE Healtcare). Labelled RNA was loaded on a 6%/7M urea gel, cut from the gel, eluted overnight at 4°C in RNA elution buffer (0.1 M sodium acetate, 0.1% SDS, 10 mM EDTA), and recovered by P:C:I extraction.

RNA structure probing was carried out as described previously (PMID 24141880) with few modifications. In brief, for 0.4 pmol 5′-end-labelled VadR sRNA was denatured, quickly chilled on ice and supplemented with 1x structure buffer (0.01 M Tris [pH 7], 0.1 M KCl, 0.01 M $MgCl_2$) and 1 µg yeast RNA. Samples were incubated at 37°C, and treated with

RNase T1 (0.1 U; Ambion no. AM2283) for 60,120 and 180 sec, or with lead(II) acetate (final concentration, 5 mM; Sigma no. 316512) for 15, 30 and 90 sec.

Reactions were stopped by the addition of 2 vol. stop/precipitation buffer (1M guanidinium thiocyanate, 0.167% N-lauryl-sarcosine, 10 mM DTT, 83% 2-propanol). RNA was precipitated for 2 h at -20°C, and collected by centrifugation (30 min, 4°C, 13.000 rpm). Samples were dissolved in GLII loading buffer, and separated on 10% polyacrylamide sequencing gels.

Supplemental References

1. Shin, J.-H. et al. A multifaceted cellular damage repair and prevention pathway promotes high level tolerance to β-lactam antibiotics. 777375 (2019).
2. Papenfort, K. et al. A Vibrio cholerae autoinducer-receptor pair that controls biofilm formation. *Nat Chem Biol* **13**, 551-557 (2017).
3. Papenfort, K., Forstner, K.U., Cong, J.P., Sharma, C.M. & Bassler, B.L. Differential RNA-seq of Vibrio cholerae identifies the VqmR small RNA as a regulator of biofilm formation. *Proc Natl Acad Sci U S A* **112**, E766-75 (2015).
4. Thelin, K.H. & Taylor, R.K. Toxin-coregulated pilus, but not mannose-sensitive hemagglutinin, is required for colonization by Vibrio cholerae O1 El Tor biotype and O139 strains. *Infect Immun* **64**, 2853-6 (1996).
5. Svenningsen, S.L., Tu, K.C. & Bassler, B.L. Gene dosage compensation calibrates four regulatory RNAs to control Vibrio cholerae quorum sensing. *EMBO J* **28**, 429-39 (2009).
6. Datsenko, K.A. & Wanner, B.L. One-step inactivation of chromosomal genes in Escherichia coli K-12 using PCR products. *Proc Natl Acad Sci U S A* **97**, 6640-5 (2000).
7. de Lorenzo, V. & Timmis, K.N. Analysis and construction of stable phenotypes in gram-negative bacteria with Tn5- and Tn10-derived minitransposons. *Methods Enzymol* **235**, 386-405 (1994).
8. Fried, L., Lassak, J. & Jung, K. A comprehensive toolbox for the rapid construction of lacZ fusion reporters. *J Microbiol Methods* **91**, 537-43 (2012).
9. Herzog, R., Peschek, N., Frohlich, K.S., Schumacher, K. & Papenfort, K. Three autoinducer molecules act in concert to control virulence gene expression in Vibrio cholerae. *Nucleic Acids Res* **47**, 3171-3183 (2019).
10. Waters, C.M. & Bassler, B.L. The Vibrio harveyi quorum-sensing system uses shared regulatory components to discriminate between multiple autoinducers. *Genes Dev* **20**, 2754-67 (2006).
11. Nadell, C.D., Drescher, K., Wingreen, N.S. & Bassler, B.L. Extracellular matrix structure governs invasion resistance in bacterial biofilms. *ISME J* **9**, 1700-9 (2015).
12. Yan, J., Sharo, A.G., Stone, H.A., Wingreen, N.S. & Bassler, B.L. Vibrio cholerae biofilm growth program and architecture revealed by single-cell live imaging. *Proc Natl Acad Sci U S A* **113**, E5337-43 (2016).
13. Skorupski, K. & Taylor, R.K. Positive selection vectors for allelic exchange. *Gene* **169**, 47-52 (1996).
14. Corcoran, C.P. et al. Superfolder GFP reporters validate diverse new mRNA targets of the classic porin regulator, MicF RNA. *Mol Microbiol* **84**, 428-45 (2012).
15. Donnell, Z. Regulation of cqsA and cqsS in Vibrio cholerae. (Princeton, NJ : Princeton University, 2015).

Figure S1

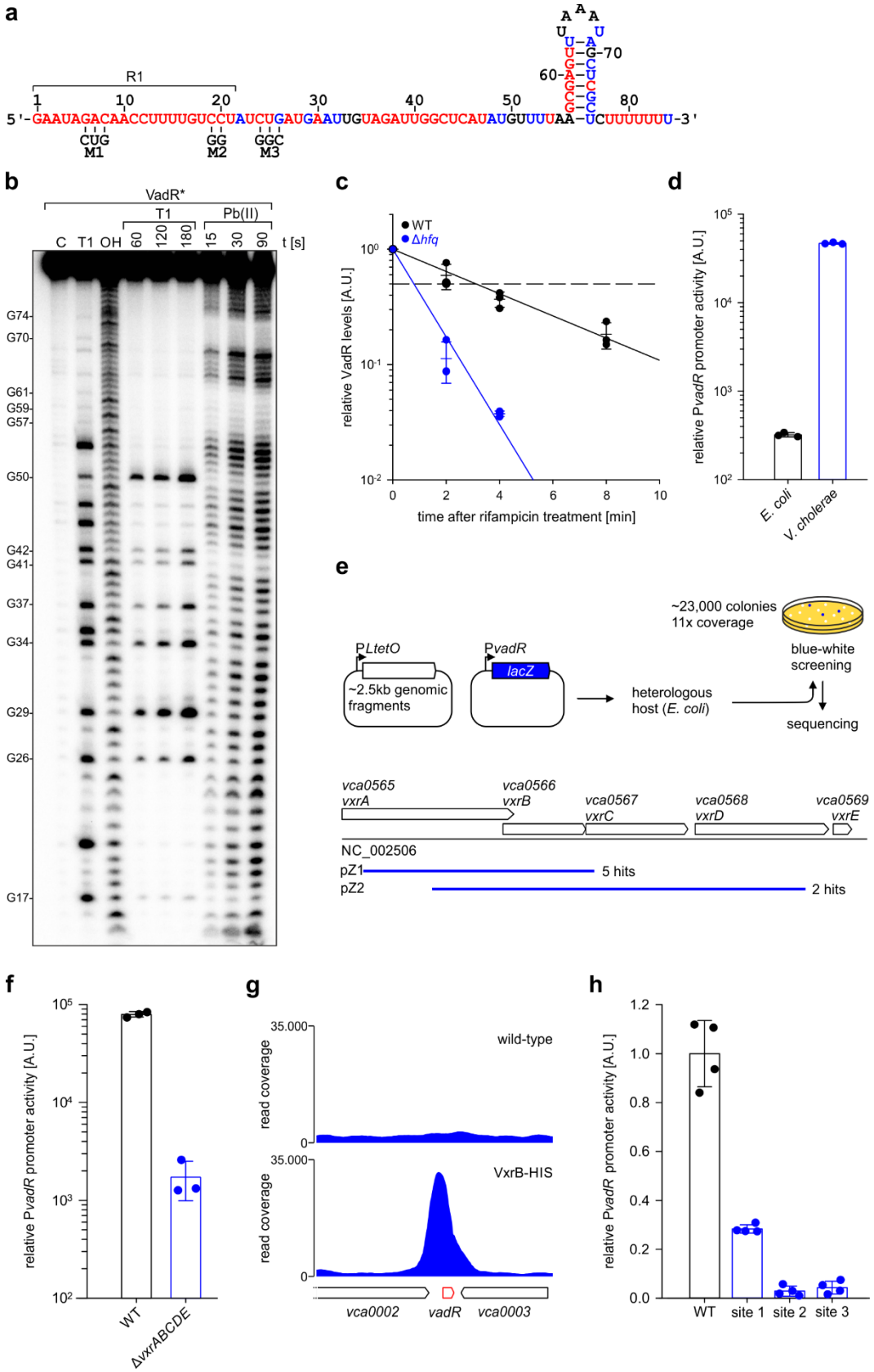
a
R1
5'-GAAUAGACAACCUUUUGUCCUAUCUGAUGAAUUGUAGAUUGGCUCAUAUGUUUUAA-UCUUUUUU-3'
CUG M1
GG M2
GGC M3
b
VadR*
T1
Pb(II)
C T1 OH 60 120 180 15 30 90 t [s]
G74
G70
G61
G59
G57
G50
G42
G41
G37
G34
G29
G26
G17
c
WT
Δhfq
relative VadR levels [A.U.]
time after rifampicin treatment [min]
d
relative PvadR promoter activity [A.U.]
E. coli
V. cholerae
e
~23,000 colonies
11x coverage
blue-white screening
PLtetO
PvadR
lacZ
~2.5kb genomic fragments
heterologous host (E. coli)
sequencing
vca0565 vxrA
vca0566 vxrB
vca0567 vxrC
vca0568 vxrD
vca0569 vxrE
NC_002506
pZ1
5 hits
pZ2
2 hits
f
relative PvadR promoter activity [A.U.]
WT
ΔvxrABCDE
g
wild-type
VxrB-HIS
read coverage
35.000
0
vca0002
vadR
vca0003
h
relative PvadR promoter activity [A.U.]
WT
site 1
site 2
site 3

Figure S1: Structure and transcriptional control of the VadR sRNA

(a) The secondary structure of the VadR sRNA predicted by structure probing experiments (b).
(b) Secondary structure probing of the VadR sRNA. VadR was synthesized *in vitro* and labelled with ^{32}P. Enzymatic treatment was performed using RNase T1, or lead-acetate (Pb(II)). The untreated control is labelled with C, denatured ladders for RNase T1 and alkaline ladder are provided and labelled with T1 and OH, respectively. Guanin residues are labelled on the left side.
(c) Rifampicin treatment to determine half-life of the VadR sRNA, in wild-type or *hfq* mutant strains. The dashes represent the mean pf biological replicates ± SD, $n = 3$.
(d) VadR promoter activities in *E. coli* and *V. cholerae* cultures grown for 16h in LB were determined using a fluorescent transcriptional reporter. Data are the mean of biological replicates ± SD, $n = 3$.
(e) Upper part: Experimental outline to identify transcription factors affecting *vadR* transcription. Lower part: Identified fragments that yielded blue colonies.
(f) *V. cholerae* wild-type and *vxrABCDE* mutant strains were grown to $OD_{600} = 0.5$ and VadR promoter activities were measured. Bars show the mean of biological replicates ± SD, $n = 3$.
(g) ChIP-seq data from *V. cholerae* wild-type and *vxrB-HIS* strains, which were treated with Penicillin G for 3h[1]. Data was re-analyzed and read coverages for the *vadR* genomic locus were plotted.
(h) Three putative VxrB binding sites in the promoter region of *vadR* were deleted. The resulting strains and *V. cholerae* wild-type were cultivated to $OD_{600} = 1.0$ and assayed for *vadR* promoter activities using a fluorescent transcriptional reporter. Bars represent the mean of biological replicates ± SD, $n = 4$. The mean of wild-type cells was set to 1.

Figure S2

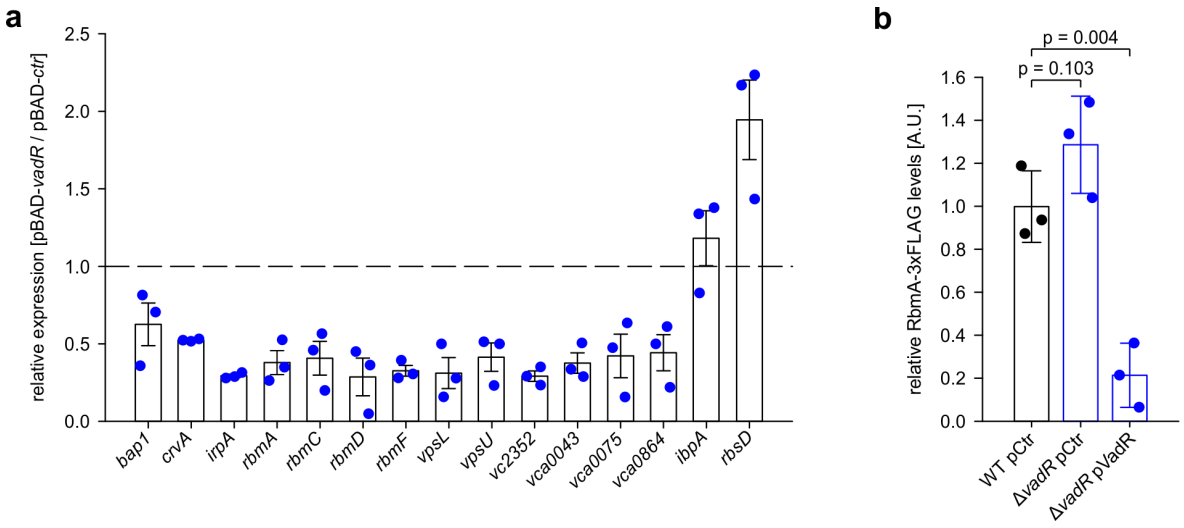

Figure S2: RNA-seq target validation and VadR-mediated regulation of RbmA
(a) qRT-PCR analysis after short period VadR expression. Expression was calculated relative to an empty vector control (pBAD-ctr). Bars represent mean of biological replicates ± SE, *n* = 3.
(b) Western blot analysis of RbmA-3xFLAG levels in *V. cholerae* wild-type and *vadR* mutant strains carrying either an empty control plasmid (pCtr) or a constitutive *vadR* overexpression plasmid. Cells were grown at 30 °C without agitation. Whole cell protein fractions were harvested at OD_{600} = 0.4. Bars indicate mean of biological replicates ± SD, *n* = 3. Statistical significance was determined using one-way ANOVA and post-hoc Holm-Sidak test.

Figure S3

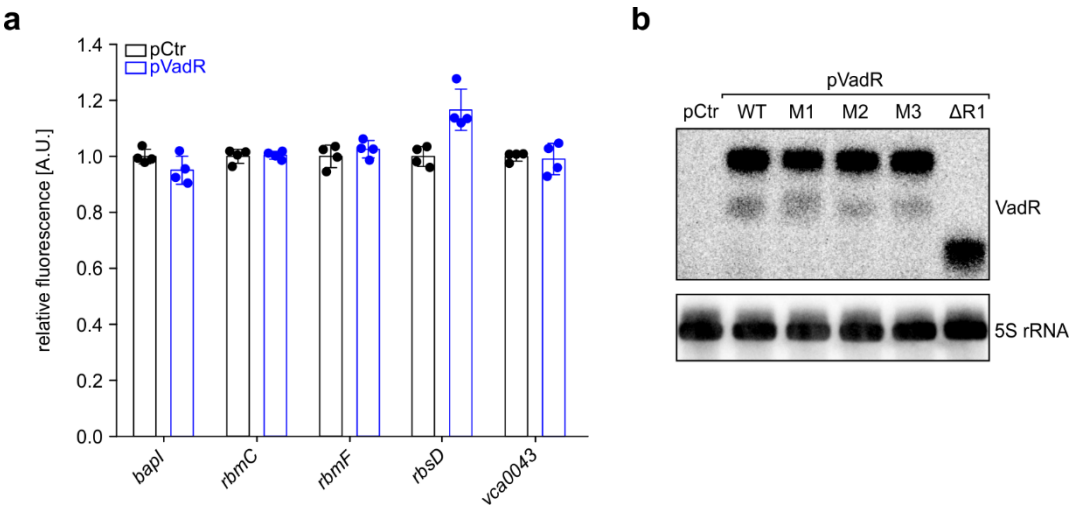

Figure S3: Indirectly regulated genes by VadR and expression of VadR variants
(a) Genes which are not post-transcriptionally regulated by VadR. Fluorescence intensities of *E. coli* strains carrying the gene-specific reporter and the control plasmid (pCtr) were set to 1. Bars show mean of biological replicates ± SD, $n = 4$.
(b) Northern blot analysis confirms similar expression levels of all plasmid-borne VadR variants used in this study. RNA was obtained from *E. coli* cells at $OD_{600} = 1.0$, which were overexpressing the indicated *vadR* variants.

Figure S4

a

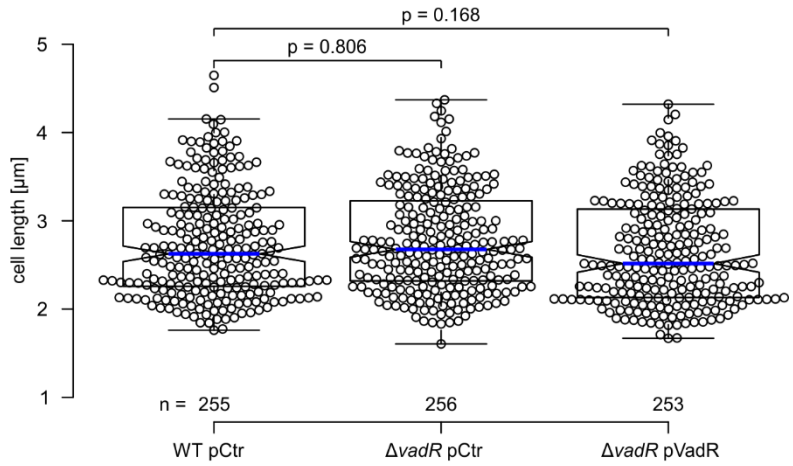

b

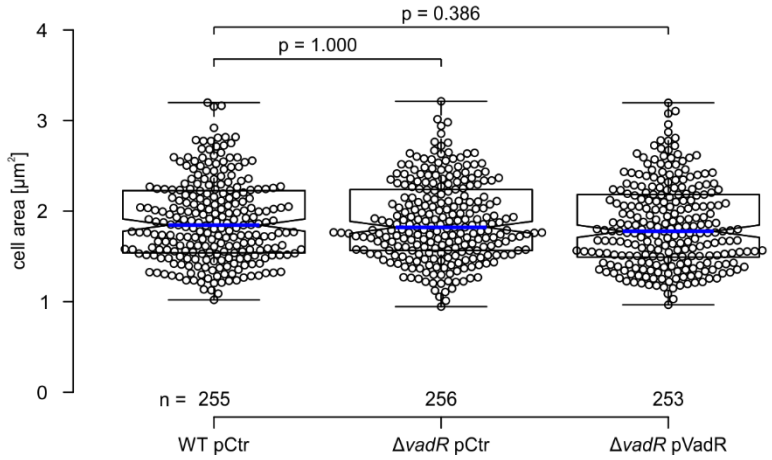

Figure S4: VadR does not affect the length and area of *V. cholerae* cells
(a-b) Analysis of cell length (a) and cell area (b) in –Cef samples of Fig. 4b. A blue line indicates the median, boxes represent 25th and 75th percentiles, whiskers represent 5th and 95th percentiles and notches indicate 95% confidence intervals for each median. *n* of each set is listed above the x-axis. Statistical significance was determined using Kruskal-Wallis test and post-hoc Dunn's test.

Figure S5

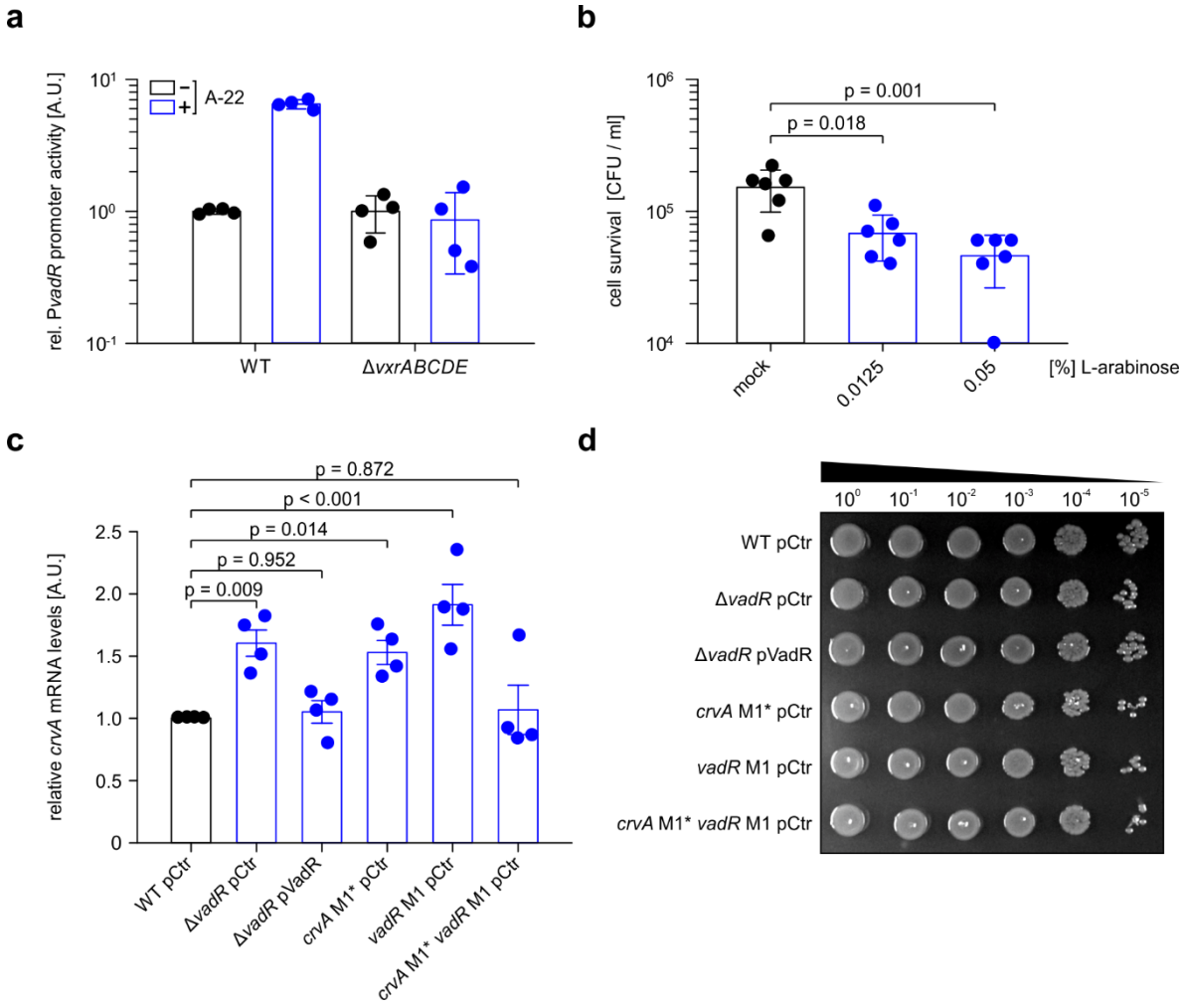

Figure S5: The VadR promoter responds to A22 treatment and *V. cholerae* depends on a tight regulation of *crvA* to increase Penicillin G tolerance.

(a) *V. cholerae* wild-type and *vxrABCDE* mutant strains were grown to OD_{600} = 0.2. Cultures were split and one set was treated with A-22 (10 µg/ml final conc.), while the other set received the same volume of water as mock treatment. VadR promoter activities in both sets were measured after 3h using a fluorescent transcriptional reporter. Promoter activities of mock-treated strains were set to 1. Bars represent mean of biological replicates ± SD, *n* = 4.

(b) Expression of the *crvAB* operon was regulated by replacing its native promoter with a P_{BAD} promoter and by using different L-arabinose concentrations for induction. Cells were treated with Penicillin G for 3h and colony forming units (CFUs) were counted. Bars show mean of biological replicates ± SD, *n* = 6. Statistical significance was determined using one-way ANOVA and post-hoc Holm-Sidak test.

(c) The indicated *V. cholerea* strains (x-axis) were grown to OD_{600} = 0.2 and treated with Penicillin G for 30min. Total RNA was isolated and analyzed for *crvA* expression by qRT-PCR. Bars represent mean of biological replicates ± SE, *n* = 4, relative to *V. cholerae* wild-type. Statistical significance was determined using one-way ANOVA and post-hoc Holm-Sidak test.

(d) The indicated *V. cholerea* strains (y-axis) were grown to OD_{600} = 0.4 + 3h and assayed for CFUs by spotting serial dilutions on agar plates.

Table S1 Genes differentially regulated by *vadR* pulse expression

ID	Gene	Description[#]	Fold change*
vc0932	*rbmE*	uncharacterized protein	-4.70
vc0934	*vpsL*	capsular polysaccharide biosynthesis glycosyltransferase	-4.61
vc0933	*rbmF*	uncharacterized protein	-4.57
vc0928	*rbmA*	rugosity and biofilm structure modulator A	-3.58
vc0935	*vpsM*	polysaccharide biosynthesis protein	-3.48
vc0936	*vpsN*	polysaccharide biosynthesis/export protein	-3.23
vc0917	*vpsA*	UDP-N-acetylglucosamine 2-epimerase	-3.19
vc0919	*vpsC*	serine O-acetyltransferase	-3.03
vc0918	*vpsB*	UDP-N-acetyl-D-mannosaminuronic acid dehydrogenase	-2.92
vc0916	*vpsU*	tyrosine-protein phosphatase	-2.83
vc0931	*rbmD*	hypothetical protein	-2.71
vca0043		hypothetical protein	-2.55
vca0864		methyl-accepting chemotaxis protein	-2.53
vc0920	*vpsD*	polysaccharide biosynthesis protein	-2.47
vc1888	*bap1*	extracellular matrix protein	-2.38
vc0937	*vpsO*	polysaccharide biosynthesis transport protein	-2.38
vc1264	*irpA*	iron-regulated protein A	-2.34
vc0938	*vpsP*	polysaccharide biosynthesis protein	-2.14
vc2352		concentrative nucleoside transporter, CNT familiy	-1.97
vca0075		hypothetical protein	-1.89
vca1075	*crvA*	hypothetical protein	-1.81
vc0930	*rbmC*	rugosity and biofilm structure modulator C	-1.79
vca0044		pseudogene	-1.77
vca0074		diguanylate cyclase	-1.77
vc0018	*ibpA*	molecular chaperone IbpA	-1.76
vca0129	*rbsC*	ribose transport system permease protein	1.81
vca0128	*rbsA*	ribose transport system ATP-binding protein	1.96
vca0127	*rbsD*	D-ribose pyranase	2.22

[#]Description is based on the annotation at KEGG (https://www.genome.jp/kegg)

*Fold change is based on transcriptomic analysis of pBAD-derived *vadR* expression using RNA-seq. Genes with a fold-change of at least 1.75-fold in either condition and a FDR adjusted p-value ≤ 0.001 were considered to be differentially expressed.

Table S2 Bacterial strains used in this study

Strain	Relevant markers/ genotype	Reference/ source
V. cholerae		
KPS-0014	Wild-type C6706	[4]
KPS-0053	Δ*hapR* C6706	[3]
KPS-0054	Δ*hfq* C6706	[5]
KPVC-10126	Δ*vadR* C6706	This study
KPVC-12430	Δ*vxrABCDE* C6706	This study
KPVC-12817	Δ*crvA* C6706	This study
KPVC-12912	*crvA* M1* C6706	This study
KPVC-12913	*crvA::crvA-3xFLAG* C6706	This study
KPVC-12914	Δ*vadR crvA::crvA-3xFLAG* C6706	This study
KPVC-13214	*vadR* M1 C6706	This study
KPVC-13215	*vadR* M1 *crvA* M1* C6706	This study
KPVC-13223	*rbmA::rbmA-3xFLAG, rbmC::rbmC-3xFLAG, bapI::bapI-3xFLAG* C6706	This study
KPVC-13384	P_{crvAB}*::araC*-P_{BAD} C6706	This study
KPVC-13439	Δ*hapR* Δ*rbmA* C6706	This study
E. coli		
BW25113	*lacI*$^{+}$ *rrnB*$_{T14}$ *ΔlacZ*$_{WJ16}$ *hsdR514 ΔaraBAD*$_{AH33}$ *ΔrhaBAD*$_{LD78}$ *rph-1 Δ(araB–D)567 Δ(rhaD–B)568 ΔlacZ4787(::rrnB-3) hsdR514 rph-1*	[6]
TOP10	*mcr*AΔ*(mrr-hsd*RMS-*mcr*BC) Φ80*lac*ZΔM15Δ*lac*X74*deo*R*rec*A1 *ara*D139Δ*(ara-leu)*7697 *gal*U *gal*K *rps*L *end*A1 *nup*G	Invitrogen
S17λpir	Δ*lacU*169 (Φ*lacZ*ΔM15), *recA*1, *endA*1, *hsdR*17, *thi*-1, *gyrA*96, *relA*1, *λpir*	[7]

Table S3 Plasmids used in this study

Plasmid trivial name	Plasmid stock name-	Relevant fragment	Comment	Origin, marker	Reference
pBBR1MCS5-5-lacZ		*lacZ*	Promoterless plasmid for transcriptional reporters	pBBR1, Gent^R	[8]
P*vadR-mKate2*	pAE-002	P*vadR-mKate2*	*vadR* transcriptional reporter plasmid	p15A, Cm^R	This study
pCMW-1C	pCMW-1C	Cm^R cassette	Promoterless plasmid for transcriptional reporters	p15A, Cm^R	[9]
pCtr	pCMW-1K	Kan^R cassette	Control plasmid	p15A, Kan^R	[10]
pKAS32-Δ*rbmA*	pCN-007	up-/downstream flanks of *rbmA*	suicide plasmid for *rbmA* knockout	R6K, Amp^R	[11]
pKAS32-*rbmA-3xFLAG*	pCN-018	3xFLAG	*rbmA-3xFLAG* allelic replacement	R6K, Amp^R	[11]
pKAS32-*rbmC-3xFLAG*	pCN-019	3xFLAG	*rbmC-3xFLAG* allelic replacement	R6K, Amp^R	[11]
pKAS32-*bapI-3xFLAG*	pCN-020	3xFLAG	*bap1-3xFLAG* allelic replacement	R6K, Amp^R	[12]
pVadRΔR1	pEE-007	*vadR* Δ*R1*	*vadR* Δ*R1* expression plasmid	p15A, Kan^R	This study
pEVS143	pEVS143	Ptac promoter	Constitutive over-expression plasmid	p15A, Kan^R	[3]
pKAS32	pKAS32		suicide plasmid for allelic exchange	R6K, Amp^R	[13]
pVcr025	pLS-014	*vcr025*	*vcr025* expression plasmid	p15A, Kan^R	This study
pVcr062	pLS-015	*vcr062*	*vcr062* expression plasmid	p15A, Kan^R	This study
pVcr058	pLS-016	*vcr058*	*vcr058* expression plasmid	p15A, Kan^R	This study
pVcr071	pLS-017	*vcr071*	*vcr071* expression plasmid	p15A, Kan^R	This study
pVcr067	pLS-018	*vcr067*	*vcr067* expression plasmid	p15A, Kan^R	This study
pVcr094	pLS-019	*vcr094*	*vcr094* expression plasmid	p15A, Kan^R	This study
pVcr099	pLS-020	*vcr099*	*vcr099* expression plasmid	p15A, Kan^R	This study
pΔ*site1-mKate2*	pLS-026	P*vadR*Δ*site1-mKate2*	*vadR* transcriptional reporter plasmid	p15A, Cm^R	This study
pΔ*site2-mKate2*	pLS-027	P*vadR*Δ*site2-mKate2*	*vadR* transcriptional reporter plasmid	p15A, Cm^R	This study
pΔ*site3-mKate2*	pLS-028	P*vadR*Δ*site3-mKate2*	*vadR* transcriptional reporter plasmid	p15A, Cm^R	This study
pBAD	pMD-004		Control plasmid	p15A, Kan^R	[9]
pVcr084	pMD-097	*vcr084*	*vcr084* expression plasmid	p15A, Kan^R	This study

p*vca0864-gfp*	pMH-039	*vca0864-gfp*	Translational reporter *vca0864-gfp*	pSC101*, Cm^R	This study
pVcr002	pNP-001	*vcr002*	*vcr002* expression plasmid	p15A, Kan^R	This study
pVcr036	pNP-003	*vcr036*	*vcr036* expression plasmid	p15A, Kan^R	This study
pVcr043	pNP-004	*vcr043*	*vcr043* expression plasmid	p15A, Kan^R	This study
pVadR	pNP-005	*vadR*	*vadR* expression plasmid	p15A, Kan^R	This study
pVcr079	pNP-006	*vcr079*	*vcr079* expression plasmid	p15A, Kan^R	This study
pVcr034	pNP-008	*vcr034*	*vcr034* expression plasmid	p15A, Kan^R	This study
pVcr082	pNP-009	*vcr082*	*vcr082* expression plasmid	p15A, Kan^R	This study
pVcr092	pNP-010	*vcr092*	*vcr092* expression plasmid	p15A, Kan^R	This study
pVcr045	pNP-013	*vcr045*	*vcr045* expression plasmid	p15A, Kan^R	This study
pBAD-*vadR*	pNP-019	P_{BAD}-*vadR*	Inducible *vadR* expression plasmid	p15A, Kan^R	This study
p*rbmC-gfp*	pNP-064	*rbmC-gfp*	Translational reporter *rbmC-gfp*	pSC101*, Cm^R	This study
p*vpsU-gfp*	pNP-070	*vpsU-gfp*	Translational reporter *vpsQ-gfp*	pSC101*, Cm^R	This study
p*rbmA-gfp*	pNP-071	*rbmA-gfp*	Translational reporter *rbmA-gfp*	pSC101*, Cm^R	This study
p*rbmD-gfp*	pNP-072	*rbmD-gfp*	Translational reporter *rbmD-gfp*	pSC101*, Cm^R	This study
p*vpsL-gfp*	pNP-073	*vpsL-gfp*	Translational reporter *vpsL-gfp*	pSC101*, Cm^R	This study
p*irpA-gfp*	pNP-113	*irpA-gfp*	Translational reporter *irpA-gfp*	pSC101*, Cm^R	This study
p*vc2352-gfp*	pNP-114	*vc2352-gfp*	Translational reporter *vc2352-gfp*	pSC101*, Cm^R	This study
p*vca0043-gfp*	pNP-115	*vca0043-gfp*	Translational reporter *vca0043-gfp*	pSC101*, Cm^R	This study
p*crvA M1*-gfp*	pNP-116	*crvA M1*-gfp*	Translational reporter *crvA* M1-*gfp*	pSC101*, Cm^R	This study
pVadR M1	pNP-117	*vadR* M1	*vadR* M1 expression plasmid	p15A, Kan^R	This study
pVadR M3	pNP-118	*vadR* M3	*vadR* M3 expression plasmid	p15A, Kan^R	This study
p*vpsU M2*-gfp*	pNP-119	*vpsU M2*-gfp*	Translational reporter *vpsU* M2-*gfp*	pSC101*, Cm^R	This study
p*rbmA M1*-gfp*	pNP-120	*rbmA M1*-gfp*	Translational reporter *rbmA* M1-*gfp*	pSC101*, Cm^R	This study
p*vpsL M3*-gfp*	pNP-121	*vpsL M3*-gfp*	Translational reporter *vpsL* M3-*gfp*	pSC101*, Cm^R	This study

P*vadR-lacZ*	pNP-122	P*vadR-lacZ*	*vadR* transcriptional reporter plasmid	pBBR1, $Gent^R$	This study
pBAD-*vxrA*	pNP-123	*vxrA*	Inducible *vxrA* expression plasmid	p15A, Kan^R	This study
pBAD-*vxrAB*	pNP-124	*vxrAB*	Inducible *vxrAB* expression plasmid	p15A, Kan^R	This study
pBAD-*vxrABC*	pNP-125	*vxrABC*	Inducible *vxrABC* expression plasmid	p15A, Kan^R	This study
pBAD-*vxrABCD*	pNP-126	*vxrABCD*	Inducible *vxrABCD* expression plasmid	p15A, Kan^R	This study
pBAD-*vxrABCDE*	pNP-127	*vxrABCDE*	Inducible *vxrABCDE* expression plasmid	p15A, Kan^R	This study
pKAS32-Δ*crvA*	pNP-128	*crvA* region	*crvA* region	R6K, Amp^R	This study
pKAS32-*crvA* M1*	pNP-129	*crvA* M1*	*crvA* M1* allelic replacement	R6K, Amp^R	This study
pKAS32-*crvA-3xFLAG*	pNP-132	*crvA-3xFLAG*	*crvA-3xFLAG* allelic replacement	R6K, Amp^R	This study
pKAS32-Δ*vadR*	pNP-133	up-/downstream flanks *vadR*	suicide plasmid for *vadR* knockout	R6K, Amp^R	This study
pKAS32-Δ*crvA*	pNP-134	up-/downstream flanks *crvA*	suicide plasmid for *crvA* knockout	R6K, Amp^R	This study
pKAS32-Δ*vxrABCDE*	pNP-135	up-/downstream flanks *vxrABCDE*	suicide plasmid for *vxrABCDE* knockout	R6K, Amp^R	This study
pVadR M2	pNP-168	*vadR* M2	*vadR* M2 expression plasmid	p15A, Kan^R	This study
p*bap1-gfp*	pRG-011	*bap1-gfp*	Translational reporter *bap1-gfp*	pSC101*, Cm^R	This study
p*crvA-gfp*	pRG-012	*crvA-gfp*	Translational reporter *crvA-gfp*	pSC101*, Cm^R	This study
p*rbmF-gfp*	pRG-013	*rbmF-gfp*	Translational reporter *rbmEF-gfp*	pSC101*, Cm^R	This study
pVcr098	pRH-005	*vcr098*	*vcr098* expression plasmid	p15A, Kan^R	This study
pKAS32-*aphA-3xFLAG*	pRH-030	3xFLAG	*aphA-3xFLAG* allelic replacement	R6K, Amp^R	[13]
p*vca0075-gfp*	pRH-090	*vca0075-gfp*	Translational reporter *vca0075-gfp*	pSC101*, Cm^R	This study
p*rbsD-gfp*	pRH-092	*rbsD-gfp*	Translational reporter *rbsD-gfp*	pSC101*, Cm^R	This study
pKAS32- *vadR* M1	pRH-093	*vadR* M1	*vadR* M1 allelic replacement	R6K, Amp^R	This study
pKAS32- *araC*-P_{BAD}	pRH-099	*araC*-P_{BAD}, flanking regions of P_{crvAB}	*araC*-P_{BAD} allelic replacement	R6K, Amp^R	This study
pVcr017	pSG-001	*vcr017*	*vcr017* expression plasmid	p15A, Kan^R	This study
pVcr080	pSG-002	*vcr080*	*vcr080* expression plasmid	p15A, Kan^R	This study
pXG10-SF	pXG10SF	'*lacZ::gfp*	template plasmid for translational reporters	pSC101*, Cm^R	[14]

pCMW-1C-mKate2	pYH-010	mKate2	Promoterless plasmid for transcriptional reporters	P15A, Cm^R	[6]
pZ1	pZ1	*vcrAB* fragment 1	*vxrAB* fragment 1 expression plasmid	p15A, Cm^R	This study
pZ2	pZ2	*vcrAB* fragment 2	*vxrAB* fragment 2 expression plasmid	p15A, Cm^R	This study
pZach	pZND132	*V.ch.* genomic fragments	Genomic fragment expression plasmid	p15A, Cm^R	[15]

Table S4 DNA oligonucleotides used in this study

Sequences are given in 5' → 3' direction; 5' P denotes a 5' monophosphate

ID	Sequence	Description
KPO-0092	CCACACATTATACGAGCCGA	pNP-001/003-006/008-010/013, pSG001/002, pLS014-020, pRH-005
KPO-0196	GGAGAAACAGTAGAGAGTTGCG	pNP-019/123-127, pMD-097, pRH-099
KPO-0243	TTCGTTTCACTTCTGAGTTCGG	5S-rRNA probe
KPO-0267	TAATAGGCCTAGGATGCATATG	pNP-128/132/133/134/135, pRH-099
KPO-0268	CGTTAACAACCGGTACCTCTA	pNP-128/132/133/134/135, pRH-099
KPO-0331	GAGCCAATCTACAATTCATCAGA	VadR probe
KPO-1001	P-TCACAGAACCGCTGTGACCA	pNP-010
KPO-1002	GTTTTTTCTAGATTGACTACTTCATTCGCCAC	pNP-010
KPO-1003	P-GCAAACACATTGGTAAGATATTAG	pNP-001
KPO-1004	GTTTTTTCTAGATATAACCTGTTCAGAATGTGCT	pNP-001
KPO-1005	P-GTCATCTCGTTAGTCATTACGA	pNP-004
KPO-1006	GTTTTTTCTAGACACTGACAAACCGGTGTTGG	pNP-004
KPO-1009	P-ACTTACTTGGATAAATATGCATTG	pNP-008
KPO-1010	GTTTTTTCTAGAGTATTGTTTGTCTGTCATAAAGTT	pNP-008
KPO-1015	P-AATAGACAACCTTTTGTCCTATC	pNP-005
KPO-1016	GTTTTTTCTAGAATAGAAAGCACTGAGTCAGGA	pNP-005
KPO-1017	P-TTGCCCGCAAGCCACGGC	pNP-013
KPO-1018	GTTTTTTCTAGAAGGCGATTGGTCGTGTTGTT	pNP-013
KPO-1021	P-GTTTGAACCCCGGCGGCT	pNP-006
KPO-1022	GTTTTTTCTAGAAAACCGACTCCTTGCAAGAA	pNP-006
KPO-1023	GTTTTTTCTAGAGGATCCGGTGATTGATTGAG	pNP-001/003-006/008-010/013, pSG001/002, pRH-005
KPO-1024	P-ACCCAAAGGGTAGAGCAAAC	pNP-003
KPO-1025	GTTTTTTCTAGAGAAAACGAAGTAATCTTCACCTT	pNP-003
KPO-1219	P-AGCTTCGCTAGCGAAGAG	pNP-009
KPO-1220	GTTTTTTCTAGAGAATGTTGCGATCAAGTTCG	pNP-009
KPO-1226	TCGTATAATGTGTGGGTAAGGTTAGTGAGAACATTTCT	pRH-005
KPO-1227	ACCGGATCCTCTAGAAGTTTCAAATTTCGTGGACAGC	pRH-005
KPO-1294	GTACATTTTGGTGTGGGAGC	pNP-133
KPO-1295	GCACTGAGTCAGGATTTTGCGTATCGGCGGTTATTCGGTTC	pNP-133
KPO-1296	GCAAAATCCTGACTCAGTGC	pNP-133
KPO-1297	CAAACCCAGCTCTTTAGCTTC	pNP-133
KPO-1298	GTTTTTGGTACCGACGCGAGATTATTTCTTCC	pNP-133
KPO-1299	GTTTTTCCTAGGGATAGTCAGGCCGCTTTCG	pNP-133
KPO-1397	GATCCGGTGATTGATTGAGC	pNP-019, pMD-097, pLS014-020
KPO-1400	CGCAACTCTCTACTGTTTCTCCGAATAGACAACCTTTTGTCCTATC	pNP-019
KPO-1401	GCTCAATCAATCACCGGATCATAGAAAGCACTGAGTCAGGA	pNP-019
KPO-1488	TTTTTTCTAGATTAAATCAGAACGCAG	pNP-123-127
KPO-1702	ATGCATGTGCTCAGTATCTCTATC	pMH-039

KPO-1703	GCTAGCGGATCCGCTGG	pMH-039
KPO-1720	GAGATACTGAGCACATGCATAGGTTGTTATTAGCAATCCGCGATAC	pNP-064
KPO-1721	GAGCCAGCGGATCCGCTAGCCAACGACAAAAGACCGACAGCAAG	pNP-064
KPO-1801	CTGTCACCAATTACGCTGGTTTTTCCTTTTTATTAAC	pMH-039
KPO-1858	TCGGCTCGTATAATGTGTGGGCTAGCGAAAACTATAATCATAAAC	pSG-001
KPO-1859	CTCAATCAATCACCGGATCCGCTTTGATTGAGCAGACGTTG	pSG-001
KPO-1860	TCGGCTCGTATAATGTGTGGGCAAGTCAGTGGTGTTGG	pSG-002
KPO-1861	CTCAATCAATCACCGGATCCGTACTGTCAATATCGACCAC	pSG-002
KPO-1906	GTTTTTGCATGCGCTGCGTGTTGAAAACGATG	pAE-002
KPO-1907	GTTTTTGTCGACCTATTCGTGAAGCAGTGTATC	pAE-002
KPO-2065	GTTTTTATGCATAGATATTTCTATTGATAAAGATGTAGTCTT	pNP-073
KPO-2066	GTTTTTGCTAGCGCTATCAATTAATCGGTAGAAAAATTTAC	pNP-073
KPO-2067	GTTTTTATGCATACTCTGATAATGAGTAGATTGCG	pNP-070
KPO-2068	GTTTTTGCTAGCCTCTGCCATTGGCGAACGA	pNP-070
KPO-2069	GTTTTTATGCATTTAGCCAATGCAATTGTCTTAGATTTG	pNP-071
KPO-2070	GTTTTTGCTAGCATAAGAAGCCGTTGAAAATAACAATGC	pNP-071
KPO-2071	GTTTTTATGCATATGGCATGGCGGAGCAAGTTG	pNP-072
KPO-2072	GTTTTTGCTAGCACTGCCAAGAGGGATTGGTAAC	pNP-072
KPO-2378	GGTAACCCAGAAACTACCACTG	*recA* qRT-PCR
KPO-2379	CACCACTTCTTCGCCTTCTT	*recA* qRT-PCR
KPO-2383	GTTTTTATGCATGCTCTCAGCATATCGTTATTG	pRG-011
KPO-2384	GTTTTTGCTAGCGAATGCGGTGCTTTGAGTC	pRG-011
KPO-2385	GTTTTTATGCATGCTTAGATCTAAAGTTCAAAAAATCAG	pRG-012
KPO-2386	GTTTTTGCTAGCCGATGCAGATACCCATAAAGG	pRG-012
KPO-2389	GTTTTTATGCATAAAGAAATAATATGTATCGTTTATCG	pRG-013
KPO-2390	GTTTTTGCTAGCATTCATGCTAGGAAAAAATGCAATC	pRG-013
KPO-2554	CGCAACTCTCTACTGTTTCTCCTATTACAACAAGAGAGGCTC	pMD-097
KPO-2555	GCTCAATCAATCACCGGATCCAGACGCTACATCAAACTG	pMD-097
KPO-2803	GAGCCAGCGGATCCGCTAGCGACCACCCAACGCAGCAATC	pMH-039
KPO-3613	CTTGATTGGTTGGCGTGTATTG	*vpsL-O* qRT-PCR
KPO-3614	CTTGCCCTTGAGTAGTCATACC	*vpsL-O* qRT-PCR
KPO3615	CTTGTGGCGCACTTTCAATC	*rbmEF* qRT-PCR
KPO3616	GTGGATGACCAACGAGTACAA	*rbmEF* qRT-PCR
KPO-3617	GCTCTTACTGATGGTCGTATGT	*rbmA* qRT-PCR
KPO-3618	CTGCAACGACTTGAAGAGAAAC	*rbmA* qRT-PCR
KPO-3621	TAGTGCTGGCACGCTAAAG	*vpsQA-K* qRT-PCR
KPO-3622	TTGAGTCACTTGCTGGACTG	*vpsQA-K* qRT-PCR
KPO-3623	CTTGGTTGCCGCGTTATTG	*rbmD* qRT-PCR
KPO-3624	GCATAGAAGGCCTGACAGATAC	*rbmD* qRT-PCR
KPO-3625	GAGCTGCAAGGTAAGGGATAC	*vca0043-44* qRT-PCR
KPO-3626	AACTACAGACGGGCACAATC	*vca0043-44* qRT-PCR
KPO-3627	CAGTCCCTATCCGAGCATATTG	*vca0864* qRT-PCR
KPO-3628	GGTAAGCTCCTCTAACCGATAAC	*vca0864* qRT-PCR
KPO-3629	CCGTCTCTTACTGGTTCTTTGG	*bapI* qRT-PCR
KPO-3630	GTGTCACAGGAACGGCATAA	*bapI* qRT-PCR
KPO-3631	CGATCTTGAGTGGATGGAGAAG	*irpA* qRT-PCR
KPO-3632	ATAGCGAGCCCATACCAAAC	*irpA* qRT-PCR
KPO-3633	GCGTGAAAGTAGCGTGTTAGA	*crvA* qRT-PCR
KPO-3634	TTCTGCTTCGTCAGGTATTGG	*crvA* qRT-PCR

KPO-3635	CTGAGCTGTTTGCGGTAATG	*vc2352* qRT-PCR
KPO-3636	CCGCTACCAAGTATTCGATCT	*vc2352* qRT-PCR
KPO-3637	GGCATCGAACATCACGATACA	*vca0074-75* qRT-PCR
KPO-3638	CCATGGCAGTTCAGTGGTAAA	*vca0074-75* qRT-PCR
KPO-3641	TCGGCCATACCGATGAAATC	*rbsDACB* qRT-PCR
KPO-3642	AGTCAGCGCGAGATCAATAC	*rbsDACB* qRT-PCR
KPO-3643	GGTTCTGAGCTATGGAGCTATG	*rbmC* qRT-PCR
KPO-3644	ATCTCAACGATTCCGTCACC	*rbmC* qRT-PCR
KPO-3735	GTTTTTATGCATGAAATAACAAATGATAATAATTTGCAATTC	pNP-113
KPO-3736	GTTTTTGCTAGCCGCTGATGTAGTGAGCGTC	pNP-113
KPO-3737	GTTTTTATGCATAGCGAGTCACCAACTAATTTG	pNP-115
KPO-3738	GTTTTTGCTAGCTTCCAAAGCCACGCGATAAC	pNP-115
KPO-3739	GTTTTTATGCATGCTTAATCGCTCCATTTTGTAAC	pNP-114
KPO-3740	GTTTTTGCTAGCCAGTAGAACTGCGATTCCTAG	pNP-114
KPO-4098	TCGGCTCGTATAATGTGTGGATCTGATGAATTGTAGATTGGCT	pEE-007
KPO-4099	AATAGACAACCTTTTGTCCTATCTGATGAATTGATATGTTTTAAGC	pEE-007
KPO-4250	GAATACTGAACCTTTTGTCCTATCTG	pNP-117
KPO-4251	GTTCAGTATTCCCACACATTATACG	pNP-117
KPO-4252	GTTTCAGTTTCCCACTTTATGTGG	pNP-116
KPO-4253	GGAAACTGAAACTTTTGACAGCTTTG	pNP-116
KPO-4410	GTTTTTTACTAGTGCTGCGTGTTGAAAACGATG	pNP-122
KPO-4411	GTTTTTTGTCGACCTATTCGTGAAGCAGTGTATC	pNP-122
KPO-4529	TATAAGATCATAAAAGACCCTTCATTTATG	pRH-099
KPO-4621	AGAGGTACCGGTTGTTAACGCATCATCAAGTCCACACCACT	pNP-135
KPO-4622	TATCCGGTAAAGAGATATTCGAG	pNP-135
KPO-4625	GAATATCTCTTTACCGGATACACCAAACCTGCTAAAAACACG	pNP-135
KPO-4626	TATGCATCCTAGGCCTATTACGATACCGGTGAAGCTAATGA	pNP-135
KPO-4846	GATTGGCTTTGACCGTCTACT	*ibpA* qRT-PCR
KPO-4847	GCTCGATATTGTATGGAGGGTATC	*iboA* qRT-PCR
KPO-4852	CAACTCTCTACTGTTTCTCCGGATAATGCGTTATAGTTTTTGC	pNP-123-127
KPO-4853	TCAACGAGAAGCAGTGTCTG	pNP-124
KPO-4854	CAGACACTGCTTCTCGTTGAAGATGATAAAAACCTCGCTGAC	pNP-124
KPO-4855	CTGATTTAATCTAGAAAAAATGATCACGCTTTCATTTTGTAAC	pNP-124
KPO-4918	CTGATTTAATCTAGAAAAAATCAACGAGAAGCAGTGTCTG	pNP-123
KPO-4919	CTGATTTAATCTAGAAAAAACTATAGCGGCATATTGTCCAA	pNP-125
KPO-4920	CTGATTTAATCTAGAAAAAAGAGCCACACTATAAAGAGATG	pNP-126
KPO-4921	CTGATTTAATCTAGAAAAAAGAAAAATTGGCTACGATTATTACC	pNP-127
KPO-5083	GTTTTTTTTAATACGACTCACTATAGGAATAGACAACCTTTTGTCCT	In-vitro VadR
KPO-5084	AAAAAAAGAGCGAGCTATTTAAAC	In-vitro VadR
KPO-5442	AGAGGTACCGGTTGTTAACGGCTTAGATCTAAAGTTCAAAAAATCAG	pNP-132
KPO-5443	GCTGTCTTTGTTTGGTCTGAG	pNP-132
KPO-5444	TCAGACCAAACAAAGACAGCGACTACAAAGACCATGACGGTG	pNP-132
KPO-5445	ATCGTTGGATTTTTGTGCGGTTACTATTTATCGTCATCTTTGTAGTC	pNP-132
KPO-5446	CCGCACAAAAATCCAACGATTTC	pNP-132
KPO-5447	TATGCATCCTAGGCCTATTAGCAGCAATACTTCAACCGGAG	pNP-132
KPO-5450	AGAGGTACCGGTTGTTAACGGAGCTCAATAAGCGAGGAATTC	pNP-134
KPO-5451	GAAATATGCAAGCTGAGTTTTCC	pNP-134
KPO-5452	AAACTCAGCTTGCATATTTCGTCGGAATTCACAAACCTGTC	pNP-134
KPO-5453	TATGCATCCTAGGCCTATTAGAATGGTCTGATCGGAGGTG	pNP-134

KPO-5456	AGAGGTACCGGTTGTTAACGGAACGTACTTTGATTGGAAAAACC	pNP-128
KPO-5457	TATGCATCCTAGGCCTATTACTTCTTTCGATACGGTGACTTG	pNP-128
KPO-5458	GTTTCAGTTTCCCACTTTATGTGGCTAAAC	pNP-129
KPO-5459	GAAACTGAAACTTTTGACAGCTTTGTAGATAG	pNP-129
KPO-5534	GTTTTTATGCATCAAATAATGATGATTAGCCGTCAA G	pRH-090
KPO-5535	GTTTTTGCTAGCGTTCGATGCCAAAGCGAGAG	pRH-090
KPO-5538	GTTTTTATGCATGTAAACTATTATGTCATCGAAACG	pRH-092
KPO-5539	GTTTTTGCTAGCCACCAAGTAAGAGAGTTCAGAG	pRH-092
KPO-5548	CCGCCGATACACTGCTTCACGAATACTGAACCTTTTGTCCTATC	pRH-093
KPO-5549	GATTTTGCCAAATCGTAGGCAAAAAAAGAGCGAGCTATTTAAACTC	pRH-093
KPO-5550	TTCAGTATTCGTGAAGCAGTGTATCGGCGGTTATTCGGTTC	pRH-093
KPO-5551	CTTTTTTTGCCTACGATTTGGCAAAATCCTGACTCAGTGC	pRH-093
KPO-5552	GAGCGAGCTATTTAAACTCGC	VadR 3' probe
KPO-5692	GTTCAGTAACTTTAAAGGATCTATCATG	pNP-120
KPO-5693	GTTACTGAACCATTTGTTTTTACAACTG	pNP-120
KPO-5696	GTTACCGTATGAAGGTTAAAGGTTTATCAG	pNP-119
KPO-5697	CATACGGTAACTACGCACATGATTTAATATTG	pNP-119
KPO-5698	CAAGGTTTTGTCCTATCTGATGAATTG	pNP-168
KPO-5699	CAAAACCTTGTCTATTCCCACACATTA	pNP-168
KPO-5700	GTGGTATCTGATGAATTGTAGATTGG	pNP-118
KPO-5701	GATACCACAAAAGGTTGTCTATTCC	pNP-118
KPO-5743	GAACCAAAAAAGCAGAATACGCATTAC	pNP-121
KPO-5744	CTTTTTTGGTTCATCACTAGACGCTC	pNP-121
KPO-5835	TCGGCTCGTATAATGTGTGGGCGGGTAAAACGCAACTAATC	pLS014
KPO-5836	GCTCAATCAATCACCGGATCCCACCATTTTATGCTCTAGAAATG	pLS014
KPO-5837	TCGGCTCGTATAATGTGTGGGAGAGGTACATAAGAGTTCAAG	pLS-015
KPO-5838	GCTCAATCAATCACCGGATCCGATGTTTTAGGGATATAAAAATAG	pLS-015
KPO-5841	TCGGCTCGTATAATGTGTGGATATATTTCCCAAAGTGGGAAATAG	pLS-016
KPO-5842	GCTCAATCAATCACCGGATCGGAATTGATATGATGAAGACAGAAA	pLS-016
KPO-5843	TCGGCTCGTATAATGTGTGGAGAATCGTTGCTAATCCTGCG	pLS-017
KPO-5844	GCTCAATCAATCACCGGATCCAATGCTCAGTCGTTTGGGTAT	pLS-017
KPO-5845	TCGGCTCGTATAATGTGTGGCCCGAACAGTCTATTTTGCTATTC	pLS-018
KPO-5846	GCTCAATCAATCACCGGATCCCAATCACATAGTCTGCCTATGC	pLS-018
KPO-5847	TCGGCTCGTATAATGTGTGGAATTTGATTATTCTGAATAACCATTAC	pLS-019
KPO-5848	GCTCAATCAATCACCGGATCGTGACTTGCAACTCCGAGT	pLS-019
KPO-5849	TCGGCTCGTATAATGTGTGGGAACTCAGTAGAATCGCTTAGG	pLS-020
KPO-5850	GCTCAATCAATCACCGGATCGCACCATTTTACCGTGGTTTAG	pLS-020
KPO-5981	GTTTTGTTAAACCTGACAACAGTCTGAC	pLS-026
KPO-5982	GTTTAACAAAACCAACGCCCAGCC	pLS-026
KPO-5983	AAACCAACAGTCTGACATTGAACCGAATAAC	pLS-027
KPO-5984	CTGTTGGTTTAAGTCACAAAACCAACGC	pLS-027
KPO-5985	CAGTCATTGAACCGAATAACCGCCG	pLS-028
KPO-5986	TCAATGACTGTTGTCAGGTTTAAGTCAC	pLS-028
KPO-6013	CAACTCTCTACTGTTTCTCC GCTTAGATCTAAAGTTCAAAAAATC	pRH-099
KPO-6014	TATGCATCCTAGGCCTATTA GTTCGCCCACTGTTTATCTTG	pRH-099
KPO-6015	GGGTCTTTTATGATCTTATA CGTTTTGAAGCAATTTGAGATACC	pRH-099
KPO-6016	AGAGGTACCGGTTGTTAACG GTAGTCACTAGGGTTTTGTCATC	pRH-099

Acknowledgements

At the end of this thesis, I want to take the opportunity to thank all the people that made this work possible.

First and foremost, I want to thank Prof. Dr. Kai Papenfort for introducing me to the exciting world of post-transcriptional gene regulation in bacteria. I also want to thank him for always encouraging me to present my work on many national and international conferences.

I would like to express my sincere gratitude to all members of my thesis committee, especially Prof. Dr. Kirsten Jung, who not only served as a second examiner of this thesis, but also ensured I could use my office in Munich to write this thesis in a calm environment. I also thank all members of my thesis advisory committee: Prof. Dr. Ralf Heermann, Dr. Arne Weiberg, and Dr. Kathrin Fröhlich, for their encouraging support and countless ideas and suggestions.

I also want to thank all collaborators and research students for the great teamwork. Especially, Dr. Praveen Singh, who ran countless biofilm experiments for Chapter 3 of this work, and whose company I enjoyed at several conferences.

Further, I want to thank all members of the Papenfort lab for the nice working atmosphere and cooperative environment. My special thanks go to my friends Roman Herzog and Andreas Starick, I will dearly miss our archery and stone-throwing competitions during coffee breaks and wish you all the best for the future.

Last but not least, I want to thank my family and especially, Sabine and Leonie, without your love and support, none of this would have been possible.

Curriculum Vitae

Removed for protection of privacy.

Aus Datenschutzgründen entfernt.